11-2012

Journal of Cave and Karst Studies, Volume 74, No. 3, December 2012, Table of Contents

National Speleological Society

Journal of Cave and Karst Studies

Volume 74 Number 3 December 2012

Article 235
Electrical Resistivity Imaging of Cave Div Aska Jama, Slovenia
Mihevc Andrej and Stepisnik Uros

Article 243
A Survey of the Algal Flora of Anthropogenic Caves of Campi Flegrei (Naples, Italy)
Archeological District
Paloa Cennamo, Chiara Marzano, Claudia Ciniglia, Gabriele Pinto, Piergiulio Cappelletti, Palolo Caputo, and Antonino Pollio

Article 251
Assessment of Spatial Properties of Karst Areas on a Regional Scale using GIS and Statistics –
The Case of Slovenia
Marko Komac and Janko Urbanc

Article 262
Lizards and Snakes (Lepidosauria, Squamata) from the Late Quaternary of the State of Ceará in Northeastern Brazil
Annie Schmaltz Hsiou, Paulo Victor De Oliveira, Celso Lira Ximenes, and Maria Somália Sales Viana

Article 271
Diet of the Newt, *Triturus Carnifex* (Laurenti, 1768), in the Flooded Karst Sinkhole Pozzo Del Merro, Central Italy
Antonio Romano, Sebastiano Salvidio, Roberto Palozzi, and Velerio Sbordoni

Article 278
Human Urine in Lechuguilla Cave: The Microbiological Impact and Potential for Bioremediation
Michael D. Johnston, Brittany A. Muench, Eric D. Banks, and Hazel A. Barton

Article 292
A Method to Determine Cover-Collapse Frequency in the Western Pennyroyal Karst of Kentucky
James C. Currens, Randall L. Paylor, E. Glynn Beck, and Bart Davidson

Journal of Cave and Karst Studies

Volume 74 Number 3 December 2012

JOURNAL OF CAVE AND KARST STUDIES

December 2012
Volume 74, Number 3
ISSN 1090-6924
A Publication of the National Speleological Society

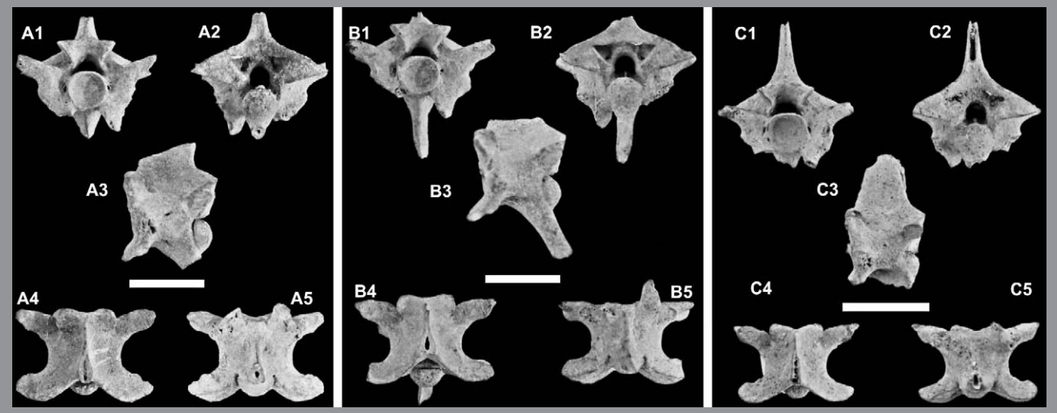

DEDICATED TO THE ADVANCEMENT OF SCIENCE, EDUCATION, AND EXPLORATION

Published By
The National Speleological Society

The *Journal of Cave and Karst Studies* (ISSN 1090-6924, CPM Number #40065056) is a multi-disciplinary, refereed journal published three times a year by the National Speleological Society, 2813 Cave Avenue, Huntsville, Alabama 35810-4431 USA; Phone (256) 852-1300; Fax (256) 851-9241, email: nss@caves.org; World Wide Web: http://www.caves.org/pub/journal/.
Check the *Journal* website for subscripion rates. Back issues and cumulative indices are available from the NSS office.

POSTMASTER: send address changes to the *Journal of Cave and Karst Studies*, 2813 Cave Avenue, Huntsville, Alabama 35810-4431 USA.

The *Journal of Cave and Karst Studies* is covered by the following ISI Thomson Services Science Citation Index Expanded, ISI Alerting Services, and Current Contents/Physical, Chemical, and Earth Sciences.

Front cover: Vertebrae of *Crotalus durissus* collected from a cave in northeastern Brazil. See Hsiou et al. in this issue.

GUIDE TO AUTHORS

The *Journal of Cave and Karst Studies* is a multidisciplinary journal devoted to cave and karst research. The *Journal* is seeking original, unpublished manuscripts concerning the scientific study of caves or other karst features. Authors do not need to be members of the National Speleological Society, but preference is given to manuscripts of importance to North American speleology.

LANGUAGES: The *Journal of Cave and Karst Studies* uses American-style English as its standard language and spelling style, with the exception of allowing a second abstract in another language when room allows. In the case of proper names, the *Journal* tries to accommodate other spellings and punctuation styles. In cases where the Editor-in-Chief finds it appropriate to use non-English words outside of proper names (generally where no equivalent English word exists), the *Journal* italicizes them. However, the common abbreviations i.e., e.g., et al., and etc. should appear in roman text. Authors are encouraged to write for our combined professional and amateur readerships.

CONTENT: Each paper will contain a title with the authors' names and addresses, an abstract, and the text of the paper, including a summary or conclusions section. Acknowledgments and references follow the text.

ABSTRACTS: An abstract stating the essential points and results must accompany all articles. An abstract is a summary, not a promise of what topics are covered in the paper.

STYLE: The *Journal* consults The Chicago Manual of Style on most general style issues.

REFERENCES: In the text, references to previously published work should be followed by the relevant author's name and date (and page number, when appropriate) in parentheses. All cited references are alphabetical at the end of the manuscript with senior author's last name first, followed by date of publication, title, publisher, volume, and page numbers. Geological Society of America format should be used (see http://www.geosociety.org/pubs/geoguid5.htm). Please do not abbreviate periodical titles. Web references are acceptable when deemed appropriate. The references should follow the style of: Author (or publisher), year, Webpage title: Publisher (if a specific author is available), full URL (e.g., http://www.usgs.gov/citguide.html) and date when the web site was accessed in brackets; for example [accessed July 16, 2002]. If there are specific authors given, use their name and list the responsible organization as publisher. Because of the ephemeral nature of websites, please provide the specific date. Citations within the text should read: (Author, Year).

SUBMISSION: Effective February 2011, all manuscripts are to be submitted via Peertrack, a web-based system for online submission. The web address is http://www.edmgr.com/jcks. Instructions are provided at that address. At your first visit, you will be prompted to establish a login and password, after which you will enter information about your manuscript (e.g., authors and addresses, manuscript title, abstract, etc.). You will then enter your manuscript, tables, and figure files separately or all together as part of the manuscript. Manuscript files can be uploaded as DOC, WPD, RTF, TXT, or LaTeX. A DOC template with additional manuscript specifications may be downloaded. (Note: LaTeX files should not use any unusual style files; a LaTeX template and BiBTeX file for the *Journal* may be downloaded or obtained from the Editor-in-Chief.) Table files can be uploaded as DOC, WPD, RTF, TXT, or LaTeX files, and figure files can be uploaded as TIFF, EPS, AI, or CDR files. Alternatively, authors may submit manuscripts as PDF or HTML files, but if the manuscript is accepted for publication, the manuscript will need to be submitted as one of the accepted file types listed above. Manuscripts must be typed, double spaced, and single-sided. Manuscripts should be no longer than 6,000 words plus tables and figures, but exceptions are permitted on a case-by-case basis. Authors of accepted papers exceeding this limit may have to pay a current page charge for the extra pages unless decided otherwise by the Editor-in-Chief. Extensive supporting data will be placed on the *Journal*'s website with a paper copy placed in the NSS archives and library. The data that are used within a paper must be made available. Authors may be required to provide supporting data in a fundamental format, such as ASCII for text data or comma-delimited ASCII for tabular data.

DISCUSSIONS: Critical discussions of papers previously published in the *Journal* are welcome. Authors will be given an opportunity to reply. Discussions and replies must be limited to a maximum of 1000 words and discussions will be subject to review before publication. Discussions must be within 6 months after the original article appears.

MEASUREMENTS: All measurements will be in Systeme Internationale (metric) except when quoting historical references. Other units will be allowed where necessary if placed in parentheses and following the SI units.

FIGURES: Figures and lettering must be neat and legible. Figure captions should be on a separate sheet of paper and not within the figure. Figures should be numbered in sequence and referred to in the text by inserting (Fig. x). Most figures will be reduced, hence the lettering should be large. Photographs must be sharp and high contrast. Color will generally only be printed at author's expense.

TABLES: See http://www.caves.org/pub/journal/PDF/Tables.pdf to get guidelines for table layout.

COPYRIGHT AND AUTHOR'S RESPONSIBILITIES: It is the author's responsibility to clear any copyright or acknowledgement matters concerning text, tables, or figures used. Authors should also ensure adequate attention to sensitive or legal issues such as land owner and land manager concerns or policies.

PROCESS: All submitted manuscripts are sent out to at least two experts in the field. Reviewed manuscripts are then returned to the author for consideration of the referees' remarks and revision, where appropriate. Revised manuscripts are returned to the appropriate Associate Editor who then recommends acceptance or rejection. The Editor-in-Chief makes final decisions regarding publication. Upon acceptance, the senior author will be sent one set of PDF proofs for review. Examine the current issue for more information about the format used.

ELECTRONIC FILES: The *Journal* is printed at high resolution. Illustrations must be a minimum of 300 dpi for acceptance.

M. Andrej and S. Uroš – Electrical resistivity imaging of cave Divaška jama, Slovenia. *Journal of Cave and Karst Studies,* v. 74, no. 3, p. 235–242. DOI: 10.4311/2010ES0138R1

ELECTRICAL RESISTIVITY IMAGING OF CAVE DIVAŠKA JAMA, SLOVENIA

MIHEVC ANDREJ[1] AND STEPIŠNIK UROŠ[2]

Abstract: Electrical resistivity imaging is a widely used tool in geophysical surveys for investigation of various subsurface structures. To assess its applicability for subsurface karst, electrical resistivity imaging was conducted in the southeastern part of the karst plateau above Divaška jama and its sediment-filled denuded continuation on the surface. Cave passages that are not filled with sediment were not detected with electrical resistivity imaging, because the electrical resistivity difference between voids and highly resistive carbonate bedrock is small. On the other hand, denuded caves and cave sections that are filled with loamy material can be clearly distinguished from less resistive carbonate bedrock.

INTRODUCTION

The study area is situated in a southeastern part of the Kras plateau called the Divača karst and on the northwestern side of the Divača karst above the caves Divaška jama and Trhlovca and their denuded continuation towards the east. This manuscript discusses the application of electrical resistivity imaging on the surface above known passages in Divaška jama, its presumed subsurface continuation, and its denuded continuation on the rim and slope of collapse doline Gorenjski Radvanj. The main purpose of the paper is to test the applicability of electrical resistivity imaging to the investigation of subsurface structures where there are small resistivity differences.

The Kras is a limestone plateau situated above the Trieste Bay in the northern Adriatic Sea. Stretching in the Dinaric (northwest-southeast) direction, it is 40 km long, 14 km wide, and covers about 440 km^2. It is morphologically quite distinct from the surrounding regions. Lower flysch regions and the Adriatic Sea bound it on the southwest and the northeast, and to the northwest it is surrounded by the fluvial sediments of the River Soča (Isonzo) plain. Towards the southeast, the border of the Kras is well-defined by the non-carbonate flysch Brkini Hills and the River Reka valley.

The Divača karst is situated in the southeastern part of the Kras plateau between the hinterland of the River Reka ponor and the town of Divača (Fig. 1). The bedrock in the area comprises thickly-bedded Cretaceous limestone, dipping approximately 20 degrees towards the south, and is bounded to the south and north by Paleogene thin-bedded limestone. On the edge of the area, the River Reka sinks into Škocjanske jame at the elevation of 317 m a.s.l. The terminal sump of this 5800 m long cave is at 190 m a.s.l. Beyond about 900 m of unexplored passages, the underground river flows through 12,750 m long Kačna jama. The surface of the Divača karst, at approximately 430 m, is largely flat, with numerous solution dolines, collapse dolines, and denuded caves. Solution dolines are 50 to 100 m in diameter and are about 10 m deep. Their density can be higher than two hundred dolines per km^2. The volumes vary between some thousands to several tens of thousands of cubic meters (Mihevc, 1997). On the surface, there are also twenty-seven large collapse dolines with a total volume of more than 41×10^6 m^3. Their mean depth is about 45 m, and their mean diameter is 135 m. On the planated surface, it is possible to recognize several denuded caves that are mostly unroofed sections of horizontal or sub-horizontal epiphreatic cave passages. The largest section is about 30 m wide and can be recognized over a distance of about 600 m (Mihevc, 1997).

The study area (Fig. 2) is situated on the edge of a doline in the northwest part of the Divača karst. The surface is mostly flat at an elevation of about 460 m, and is interrupted by several dolines with diameters up to 100 m and about 15 m deep. The eastern part of the surface gradually dips into the elongated depression of a denuded cave that in its eastern part continues into the Divaški Radvanj collapse doline. Two large caves are known in this area. The biggest is Divaška jama, which runs approximately southwest-northeast at an elevation between 350 and 410 m. The other large cave, Trhlovca, is located southwest of Divaška jama.

Divaška jama is developed in bedded limestone of Senonian age (Jurkovšek et al., 1996). Limestone beds in the cave dip toward the southwest in the northeastern part of the cave and toward the south in the southwestern part (Gospodarič, 1985). The cave is a roughly 700 m long relict of an originally larger cave system of epiphreatic and partially phreatic origin. The main part of the cave consists of a large passage up to 20 m high and 15 m wide. The cave is filled with at least 30 m of lithologically varied sediments and speleothems of different ages. The most extensive sediment in the cave is thick, laminated flood loam. The loam filled up most of the cave, but was later partially eroded away in lower parts by percolating water. Both ends of the cave are choked with allogenic sediments and flowstone. The only known

[1] Karst research institute ZRC SAZU, Titov trg 2, SI-6230 Postojna, Slovenia, mihevc@zrc-sazu.si
[2] University of Ljubljana, Department of Geography, Aškerčeva 2, SI-1000 Ljubljana, Slovenia, urosstepisnik@hotmail.com

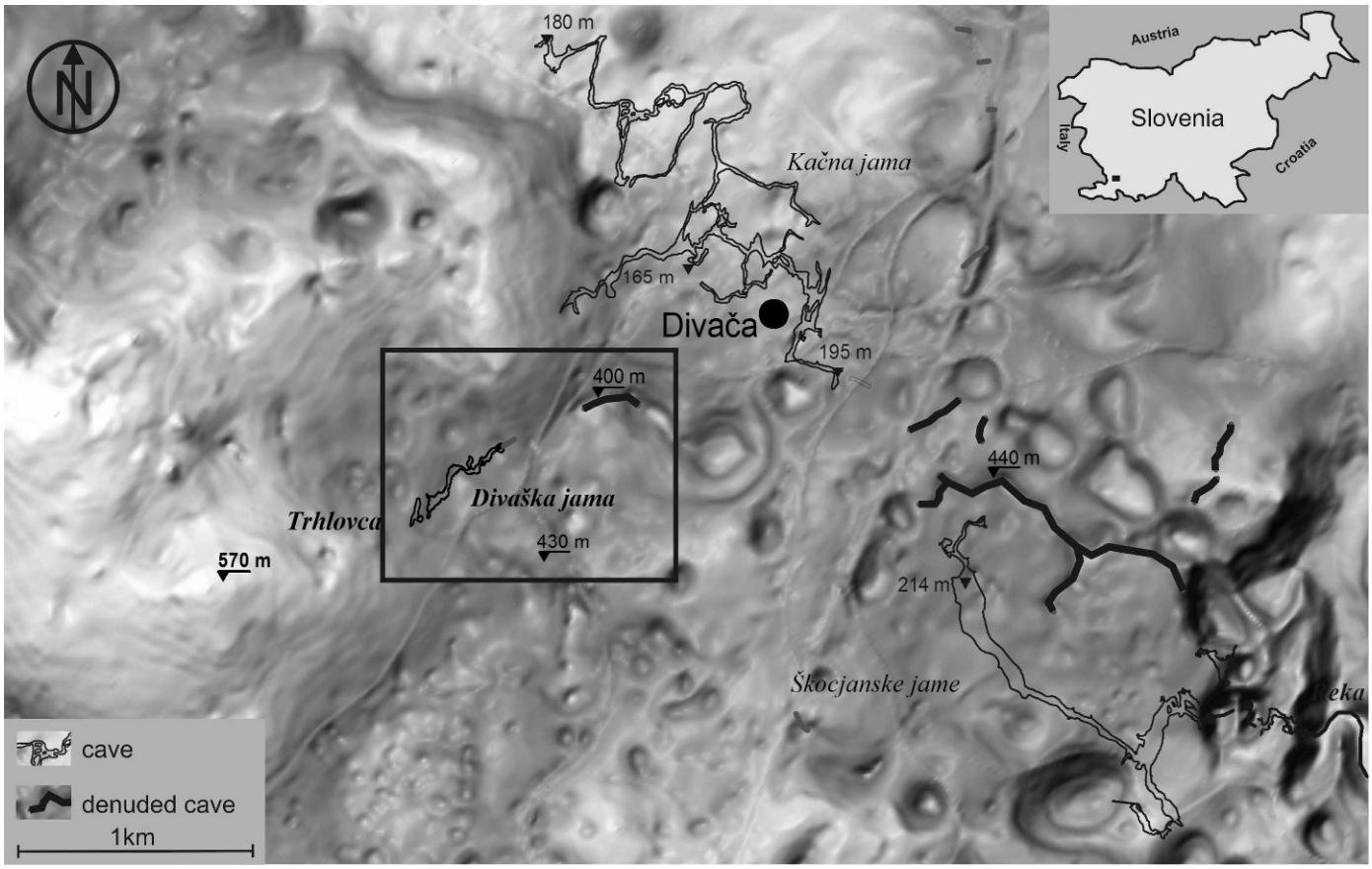

Figure 1. Location of the study area.

subsurface continuation of the Divaška jama is Trhlovca, although they are not directly connected. Trhlovca is 142 m long and 22 m deep. The entrance to this cave is below vertical walls at the side of a doline. The doline probably represents the unroofed continuation of the cave, as the passage that connects the main passage with the surface is a phreatic channel intercepted by the surface. The southwestern end of Divaška jama is about 40 m below the end of this doline. Trhlovca is developed in bedded, southerly dipping limestone of the Sežana formation (Jurkovšek et al., 1996). The main part of the cave is a meandering canyon approximately 15 m high, about 3 m wide, and 60 m long running north-south at an elevation of 404 to 419 m. Scallops and undulating notches are developed on walls, indicating evolution in phreatic and partially in paragenetic conditions. This passage was completely filled with clastic fluvial sediments. The cave became accessible after the sediments were washed out (Zupan Hajna et al., 2008).

In the east of the study area are two collapse dolines, Divaški Radvanj and Gorenjski Radvanj, which is the actual eastern limit of the study area. The slopes of Gorenjski Radvanj are mostly balanced. Lower parts of the slopes are covered with loamy material. On the western slopes there are two erosion gullies filled with sediment consisting of clay, silt and sand, and flowstone.

METHODS

Although electrical resistivity imaging has been successfully utilized for characterizing the subsurface for many years, it has certain limitations. The method is labor intensive, interpretation of the data is time consuming, and the results are based on subjective interpretation (Roman, 1952; Zhou et al., 2002). The development of computer controlled multi-electrode systems and resistivity modeling software have allowed more cost-effective resistivity surveys and better interpretation of the subsurface (Locke and Barker, 1996). These surveys are usually referred to as electrical resistivity imaging (ERI) or electrical resistivity tomography (ERT) (Zhou et al., 2002). These methods allow data to be collected and processed quickly, so that ERI surveys become a valuable tool in subsurface investigations (Zhou et al., 2000).

ERI surveys are typically conducted to determine the resistivity of subsurface features and can be used to determine the location of various geologic and soil strata, bedrock fractures, faults, and voids. Fundamental to all resistivity methods is the concept that current is injected into the ground, and the voltages induced by this current can be measured. These potentials or differences of potential, ratios of potential differences, or some other parameter that is

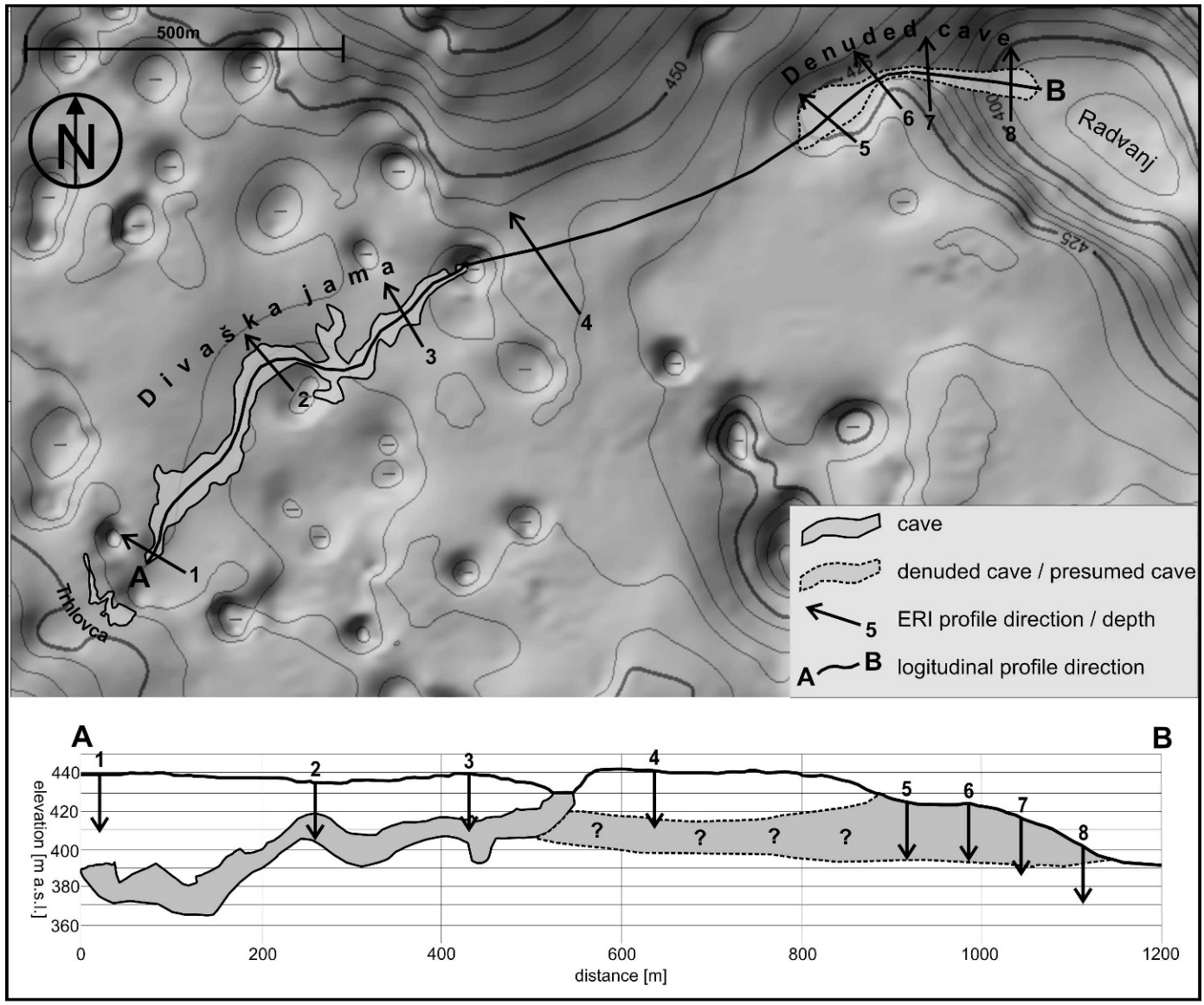

Figure 2. Top: Detailed map of the study area showing the electrical resistivity imaging lines over the cave (1–3), its presumed filled continuation (4), and the unroofed cave at the sinkhole (5–8). Bottom: Profile sketch along the curve A–B in the top part, with depths of the electrical resistivity imaging profiles that were calculated.

directly related to these variables are the most commonly measured effect of the injected current. The principal differences among various methods of electrical resistivity lie in the number and spacing of the current and potential electrodes, the variable calculated, and the manner of presenting the results (Zhou et al., 2000).

Generally, carbonate rock has a significantly higher resistivity than loamy material, because of its considerably smaller primary porosity and fewer interconnected pore spaces. Its resistivity value is about 1000 ohm-m (Telford et al., 1990). Loamy materials can hold more moisture and have higher concentrations of ions to conduct electricity; therefore, their resistivity values are below 250 ohm-m (Telford et al., 1990). The high contrast in resistivity values between carbonate rock and loamy material favors the use of electrical resistivity to determine the boundary between bedrock and overburden or loamy sediment (Zhou et al., 2000).

A frequently occurring problem with electrical resistivity imaging is deciding which electrode configuration will respond best to the material changes in karst features. Each type of array has distinctive advantages and disadvantages in terms of sensitivity to material variations, depth from which information may be obtained, and signal strength. The most common arrays are the dipole-dipole array, the Wenner array, and the Schlumberger array. The dipole-dipole array gives good horizontal resolution, while the Wenner and Schlumberger arrays are more intended for

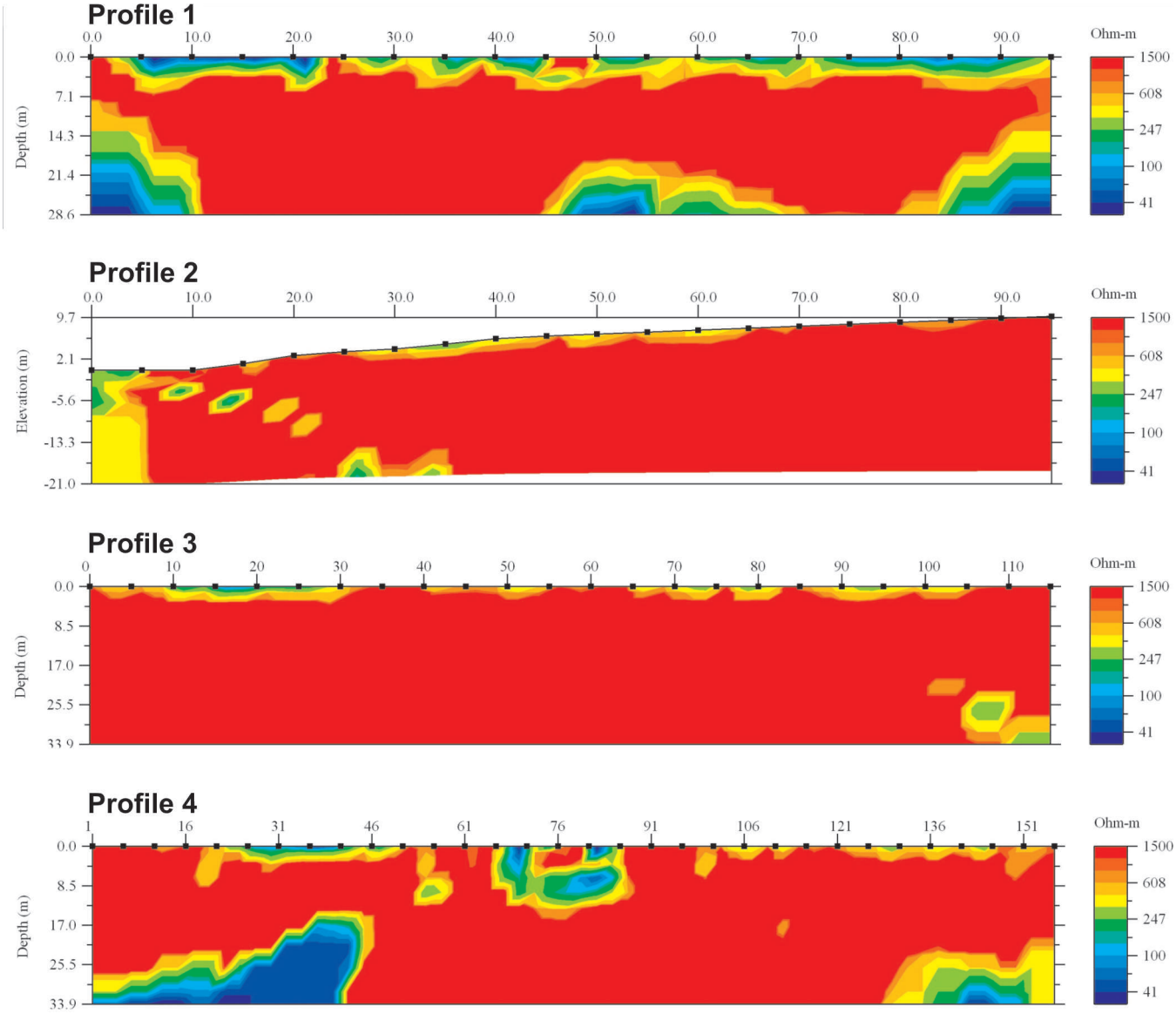

Figure 3. ERI profiles 1–4, scale 0 to 1500 ohm-m.

vertical resolution. In the application to karst surveys, the dipole-dipole array has provided highest precision of ground changes sensitivity and has the greatest sensitivity to vertical resistivity boundaries (Zhou et al., 2002).

Electrical resistivity data were collected along eight different lines above Divaška jama, its presumed continuation, and the denuded section on the slope of the collapse doline (Fig. 2). The SuperSting R1/IP earth resistivity meter developed by Advanced Geosciences, Inc. was used for data collection. The survey was conducted with a dipole-dipole array with 5 m electrode spacing. In most cases, twenty electrodes were used simultaneously, with alternation of two current and two potential electrodes. For longer profiles, a roll-along survey was used. The data were processed to generate two-dimensional resistivity models using Earthimager 2D resistivity inversion software developed by Advanced Geosciences, Inc. This combination of equipment and software have been shown to be appropriate for providing a robust visualization of the epikarst structure and the subsurface structure of collapse dolines (Stepišnik and Mihevc, 2008; Stepišnik, 2008). The root-mean-square error quantifies the difference between the measured resistivity values and those calculated from the true resistivity model. A small RMS value indicates small differences. The minimum RMS error in the survey was 2.59%, and the maximum error was 8.2%.

Previous applications of this method in various karst features in the Slovenian karst revealed that the resistivity value for carbonate rock exceeds 1000 ohm-m. For soil and weathered bedrock, the resistivity values are between approximately 200 and 1000 ohm-m. Loamy material has resistivity values lower than 150 ohm-m (Stepišnik, 2007;

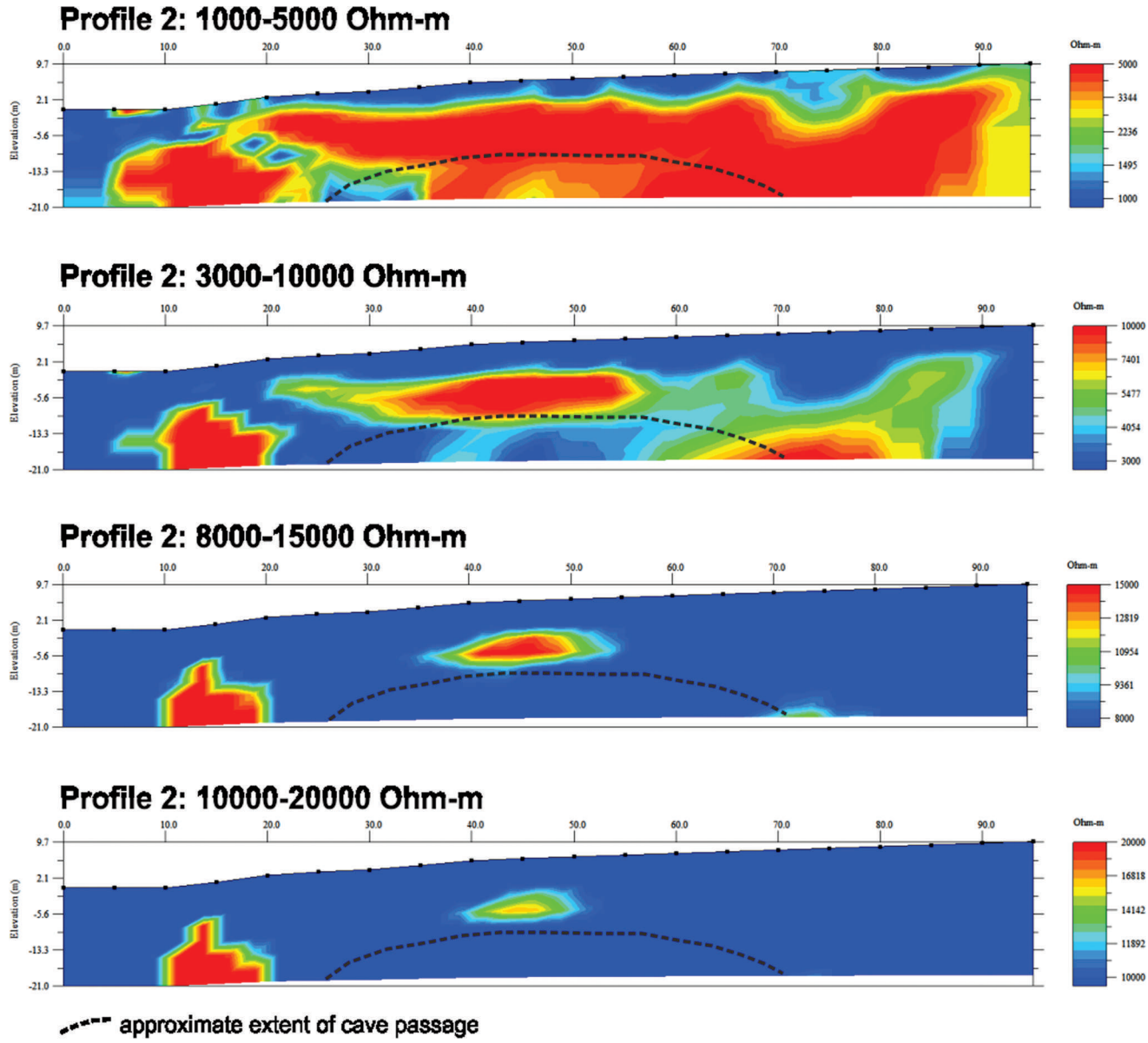

Figure 4. ERI profile 2 computed with additional higher scales of resistivity values.

Stepišnik and Mihevc, 2008; Stepišnik, 2008). However, threshold resistivity values that would discriminate between voids and carbonate bedrock have not yet been determined. Since voids should have infinite resistivity, the analysis was repeated at different ranges of resistivity to check if subsurface openings can be detected.

The ERI profiles across Divaška jama (profiles 1, 2 and 3) exhibit relatively uniform subsurface structure, which is a result of the high electrical resistivity of limestone bedrock, as well as cave voids (Fig. 3). Line 1 was situated on the surface above the southeastern end of the Divaška jama, oriented 290°. Even though the surface is gently inclined towards the north, the inclination is uniform, and so for the purpose of the analysis, the topography of the profile is presented as flat (Fig. 3). In this profile, bedrock with resistivity value more than 1000 ohm-m is covered by thin layers of less resistive soil, mechanically weathered rock, or loamy material with resistivity about 500 ohm-m. In the central part of the profile, at the depth of about 25 m there is a clearly distinguished area with electrical resistivity lower than 500 ohm-m, which might be a high-level extension of Divaška jama towards Trhlovca that is completely choked with loamy sediment. Known passages of Divaška jama are positioned about 50 m below the surface and were not detected in the ERI profile, as the maximum depth in this profile was 28 m.

Line 2 was situated above the central part of Divaška jama that lies approximately 15 m below the surface. The surface is on the northwestern slope of a doline in the direction of 300°. In this profile, bedrock with resistivity value more than

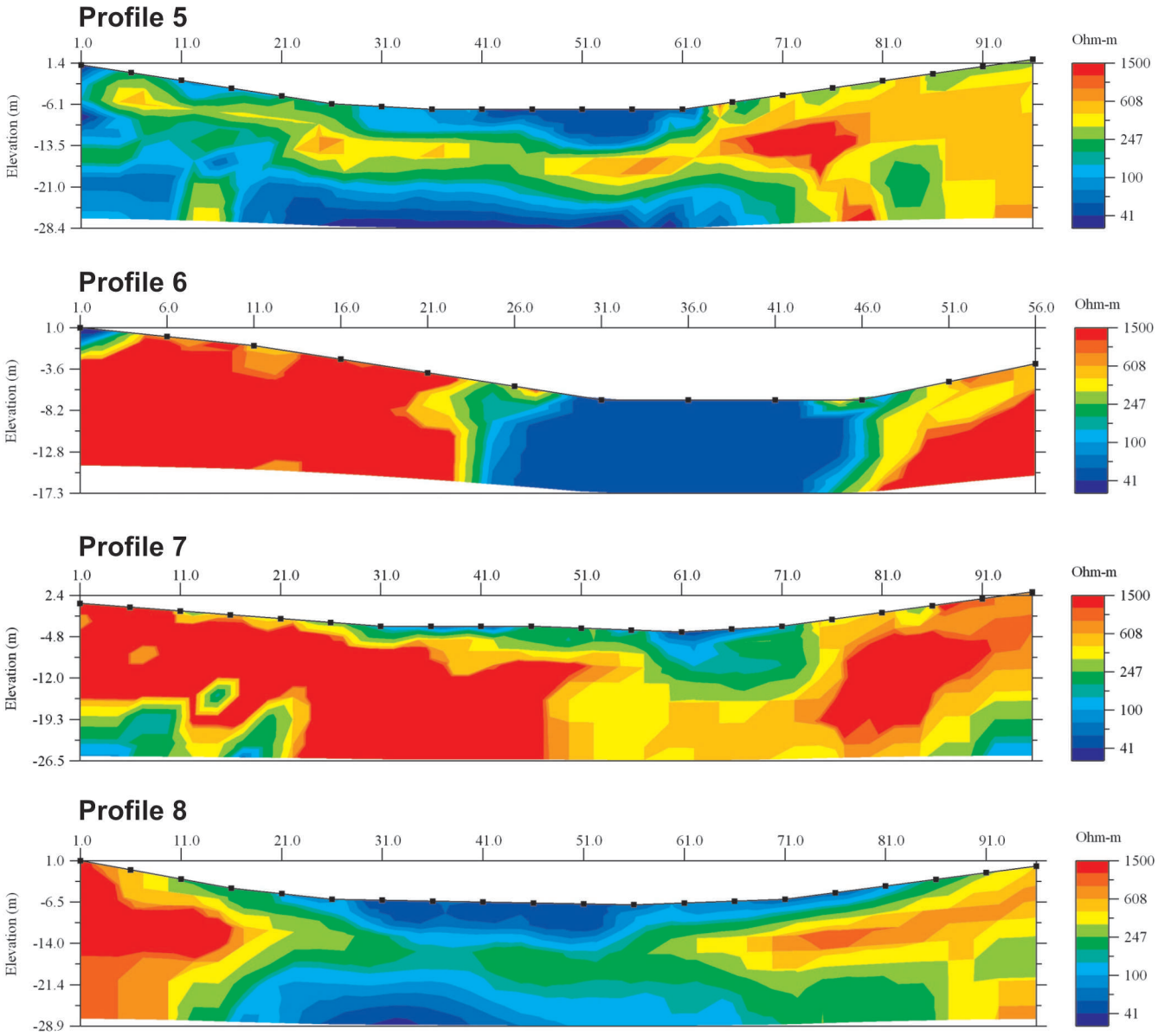

Figure 5. ERI profiles 5–8, scale 0 to 1500 ohm-m.

1000 ohm-m is covered by thin layers of less resistive soil, mechanically weathered rock, or loamy material with resistivity about 500 ohm-m. In the central part of the profile, at the depth of about 15 m, a cave passage in Divaška jama is present. It should be seen on the profile, as resistivity values should be extremely high. However, resistivity values of the whole section of the profile appear like those of the surrounding bedrock. Different ranges of resistivity values were used in an attempt to find a resistivity threshold between the cave passage and the surrounding bedrock (Fig. 4). None of the applied ranges, differing by an order of magnitude, allowed us detect the actual cave chamber. At higher resistivity values, some anomalies were detected that might be tensional fractures above the cave (15000 and 20000 ohm-m), but they are not at the depth of the cave.

Line 3 was situated near the northeastern end of Divaška jama, which here lies approximately 22 m below the surface. The line ran across a flat karst surface covered with grikes, in the direction of 305°. In this profile, bedrock with resistivity value more than 1000 ohm-m is covered by thin layers of less resistive soil, mechanically weathered rock, or loamy material with resistivity about 500 ohm-m. Passages in Divaška jama lie in the central part of the profile, but they were not detected by use of ERI because they have the same apparent resistivity values as the surrounding bedrock.

Profile 4 is situated on a flat karst surface beyond the northeastern end of Divaška jama, over its presumed subsurface continuation toward denuded cave next to the Gorenjski Radvanj collapse doline (Fig. 4). In this area, no

accessible cave is known. Direction of the profile is 300°. In this profile, too, bedrock with resistivity value more than 1000 ohm-m is partially covered by thin layers of less resistive soil, mechanically weathered rock, or loamy material with resistivity about 500 ohm-m. In the central part of the profile, from the surface to the depth of about 10 m, there is evidence of a small subsurface structure with resistivity values less than 500 ohm-m. Most likely the structure is part of an epikarst void filled with loamy material or soil. Here too, distinct grikes are present on the surface. In the southeastern section of the profile at depths greater than 17 m, a subsurface structure with a diameter of about 30 m is evident. With resistivity values less than 500 ohm-m, the structure is apparently a cave passage completely filled with loamy material. This presumably is a continuation of Divaška jama.

Lines 5 through 8 ran across the unroofed cave section completely filled with loamy material and flowstone (Fig. 5). Results of ERI exhibit a clear difference between cave fill and bedrock. Line 5, in the direction of 290°, was placed over the southwestern section of the denuded cave trench. Its profile exhibits some bedrock with resistivity value around 1000 ohm-m in the southeastern section. It is covered with a thin layer of electrically less resistive soil, mechanically weathered rock, or loamy material with resistivity value about 500 ohm-m. All other parts of the profile exhibit some resistivity values lower than 150 ohm-m that indicates loamy material and flowstone fill material in a denuded cave. Material with resistivity values around 500 ohm-m located in the central and northwestern sections of the profile at a depth between 10 and 15 m is probably weathered bedrock that accumulated there due to slope processes inside the denuded cave.

Line 6 was situated on the denuded cave northeast of line 5, on the rim of the collapse doline. The line was run at 290°, perpendicular to the direction of the denuded cave. In the resulting profile, bedrock with resistivity value more than 1000 ohm-m is present on both slopes of the trench. It is partially covered with thin layers of electrically less resistive soil, mechanically weathered rock, or loamy material with resistivity value about 500 ohm-m. The central part of the profile shows over 15 m of loamy material and flowstone fragments with resistivity values below 150 ohm-m.

Line 7, run at 350°, was placed on the western slope of the collapsed doline close to the denuded cave. Bedrock, with resistivity values more than 1000 ohm-m, is present along the whole profile. A low-resistivity area (below 150 ohm-m) in the central part of the profile, where the surface is covered with loam and flowstone particles, is up to 10 m thick.

Line 8 was situated on the floor of the western part of the collapse doline just under the slope where the denuded cave is disintegrating. Both ends of the profile show the presence of bedrock, with resistivity values higher than 1000 ohm-m, on the slopes of the collapse doline. In the upper part of central section of the profile, material with resistivity values lower than 150 ohm-m appears up to a depth of 5 m. This is most likely loamy outwash of the denuded cave fill from the slope. Below the outwash, at depths between 5 to 15 m, the profile shows resistivity values from 150 to 500 ohm-m that most likely represent weathered bedrock accumulated as scree at the foot of the slope. Below, there is again the material that exhibits resistivity values lower than 150 ohm-m, suggesting loamy fill in the doline (Stepišnik, 2008).

Conclusions

Electrical resistivity imaging data were collected for eight lines over caves Divaška jama and Trhlovca and across their denuded continuation on the slope of the collapse doline Gorenjski Radvanj.

The ERI profiles across Divaška jama (profiles 1, 2 and 3) exhibit relatively uniform subsurface structure that is a result of the high electrical resistivity of limestone bedrock and cave voids. Although the cave passages are relatively close to the surface, they were not detected with the application of ERI, even at the highest resistivity values that should show the difference between bedrock and void.

Profile 4, across the presumed underground continuation of Divaška jama in the direction of the unroofed cave shows some differences in subsurface electrical resistivity that may indicate the existence of cave conduits completely filled with less resistive loamy material. The unroofed section of the cave is completely filled with loamy material and flowstone. ERI profiles 4, 5, 6, and 7 exhibit a clear difference between allogenic cave fill and bedrock. In the upper section above the slopes of the collapse doline, where the denuded cave is up to 20 m wide, the loamy fill is 15 m thick. On the slopes, the thickness of loamy fill diminishes, probably because it has been washed into the doline. The ERI profile in the lower section of the slope exhibits up to 25 m of loamy material fill.

Application of the ERI method has proved appropriate for detailed investigation of subsurface structures with large differences in electrical resistivity. Parts of denuded caves and cave passages that are filled with loamy material can be clearly distinguished from less resistive carbonate bedrock. In the measured ERI profiles, resistivity values of soil- and sediment-filled features are lower than 150 ohm-m and weathered bedrock is around 500 ohm-m, while bedrock exhibits values higher than 1000 ohm-m.

On the other hand, underground parts of the caves with huge chambers were not detected in this survey by ERI method, as resistivity differences between voids and the highly resistive carbonate bedrock are insignificant. In calculated profiles with high maximum resistivity (Fig. 4), limestone bedrock exhibits resistivity values approximately between 5000 and 10000 ohm-m. Previous applications of ERI over cave passages gave resistivity values of limestone bedrock up to 5000 ohm-m, while voids have higher values

(e.g., Barbadello et al., 2002; Brown et al., 2011). In this case, the problem of not detecting the voids seems to be a consequence of the very high electrical resistivity of this type of limestone.

REFERENCES

Barbadello, L., Bratus, A., Yabar, D.N., Paganini, P., and Palmieri, F., 2002, Integrated geophysical methods to define hypogenous karstic features: Atti del Museo Civico di Storia Naturale di Trieste, v. 40, p. 15–21.

Brown, W.A., Stafford, K.W., Shaw-Faulkner, M., and Grubbs, A., 2011, A comperative integrated geophysical study of Horseshoe Chimney Cave, Colorado Bend State Park, Texas: International Journal of Speleology, v. 40, no. 1, p. 9–16.

Gospodarič, R., 1985, O speleogenezi Divaške jame in Trhlovce: Acta Carsologica, v. 13, p. 5–34.

Jurkovšek, B., Toman, M., Ogorelec, B., Šribar, L., Drobne, K., Poljak, M., and Šribar, L., 1996, Formacijska geološka karta južnega dela Tržaško – komenske planate 1:50.000: kredne in paleogenske karbonatne kamnine, Ljubljana, Inštitut za geologijo, geotehniko in geofiziko, 143 p.

Mihevc, A., 1997, Dolines, their morphology and origin, case study: dolines from the Kras, west Slovenia (the Škocjan karst), *in* James, J., and Forti, P., eds., Fourth International Conference on Geomorphology, Karst Geomorphology (Geografia Fisica e Dinamica Quaternaria, Supplement 3, part 3), p. 69–74.

Roman, I., 1952, Resistivity reconnaissance, *in* Symposium on Surface and Subsurface Reconnaissance, Philadelphia, American Society for Testing Materials, Special Technical Publication 122, p. 171–226.

Stepišnik, U., 2007, Loamy sediment fills in collapse dolines near the Ljubljanica River springs, Dinaric Karst, Slovenia: Cave and Karst Science, v. 33, p. 105–110.

Stepišnik, U., 2008, The application of electrical resistivity imaging in collapse doline floors: Divača karst, Slovenia: Studia Geomorphologica Carpatho-Balcanica, v. 42, p. 41–56.

Stepišnik, U., and Mihevc, A., 2008, Investigation of structure of various surface karst formations in limestone and dolomite bedrock with application of the electrical resistivity imaging: Acta Carsologica, v. 37, no. 1, p. 133–140.

Telford, W.M., Geldart, L.P., and Sheriff, R.E., 1990, Applied Geophysics (2. edition): New York, Cambridge University Press, 790 p.

Zhou, W., Beck, B.F., and Adams, A.L., 2002, Effective electrode array in mapping karst hazards in electrical resistivity tomography: Environmental Geology, v. 42, p. 922–928. doi:10.1007/s00254-002-0594-z.

Zhou, W., Beck, B.F., and Stephenson, J.B., 2000, Reliability of dipole-dipole electrical resistivity tomography for defining depth to bedrock in covered karst terrains: Environmental Geology, v. 39, p. 760–766. doi:10.1007/s002540050491.

Zupan Hajna, N., Mihevc, A., Pruner, P., and Bosák, P., 2008, Paleomagnetism and magnetostratigraphy of karst sediments in Slovenia, Ljubljana, Založba ZRC, Carsologica Series, 266 p.

P. Cennamo, C. Marzano, C. Ciniglia, G. Pinto, P. Cappelletti, P. Caputo, and A. Pollio – A survey of the algal flora of anthropogenic caves of Campi Flegrei (Naples, Italy) archeological district. *Journal of Cave and Karst Studies,* v. 74, no. 3, p. 243–250. DOI: 10.4311/2011JCKS0194

A SURVEY OF THE ALGAL FLORA OF ANTHROPOGENIC CAVES OF CAMPI FLEGREI (NAPLES, ITALY) ARCHEOLOGICAL DISTRICT

Paola Cennamo[1*], Chiara Marzano[2], Claudia Ciniglia[3], Gabriele Pinto[2], Piergiulio Cappelletti[4], Paolo Caputo[2], and Antonino Pollio[2]

Abstract: Campi Flegrei is a large volcanic area situated northwest of Naples, Italy. Two archeological sites, the Sybil's Cave and the Piscina Mirabilis, are artificial caves dug in the yellow tuff and used during antiquity for various purposes. This paper describes for the first time the algal biodiversity of these caves and determines whether environmental factors such as light intensity and humidity are influential in species distribution. A total of twenty-two algal species were identified by molecular methods (18S rDNA); the largest group was Cyanobacteria (eleven species), followed by algae Chlorophyta (six), Rhodophyta (two) and Bacillariophyta (two). Cluster analysis of algal distribution in the caves in relation to light and humidity showed no relevant differences in algal distribution between the two caves. Three different algal groups were identified. The first one includes strains strictly dependent on low humidity, a second cluster was mainly associated with sites where humidity is not a severe constraint, and a third group, mainly represented by filamentous cyanobacteria, is probably dependent on high humidity, since it was detected only at Piscina Mirabilis.

Introduction

The algal flora of caves is drawing increasing attention due to the peculiarities of their environment. Reduced light intensity, low nutrient input, and absence of seasonality (Dayner and Johansen, 1991; Pedersen, 2000) are the predominant features that influence distribution and composition of algal assemblages in natural and artificial caves, but temperature, humidity, and occurrence of flowing water also play a role in the establishment of algal settlements (Mulec et al., 2007). Many cave habitats currently suffer the impact of increasing tourist fluxes; artificial lights and human traffic are strong factors that can deeply modify equilibria within algal populations (Chelius et al., 2009). An example is given by the anthropogenic caves occurring in the archaeological district of Campi Flegrei in Italy, an area that is the single largest feature of the Phlegraean Volcanic District, which includes the islands of Procida and Ischia, as well as submarine vents in the northwestern bay of Naples (Orsi et al., 1996). Campi Flegrei has been inhabited since prehistoric times and became an important center of civilization during antiquity. Different underground habitats have been dug in the district, and two of them have remarkable dimensions. The most ancient is the so-called Sybil's Cave (fourth century BCE), near Cuma, which is in fact a long gallery cut into the soft tuff, lighted by multiple openings to the surface. The other large cave (dating back to the first century CE) is the Piscina Mirabilis, located in Baia, a cistern also excavated in tuff, used to store drinking water. The two caves present some common features. They share the same external climatic conditions, being located less than 6 kilometers from each other, and similar viable algal propagules can be dispersed into both caves by air currents and transport by animals (Dobat, 1970). In addition, they have been dug in the same geological material that originated from the eruption of the Neapolitan Yellow Tuff (dated at 15 ka BP; Insinga et al., 2004), which produced the caldera collapse of the bay of Pozzuoli (Scarpati et al., 1993).

On the other hand, the two caves differ in some characteristics. The Sybil's Cave is, in part, directly lightened by daylight and is visited by numerous tourists throughout the year, whereas the Piscina Mirabilis does not receive direct light and is rarely open to the public. Moreover, it has been partially filled for centuries with freshwater with a high carbonate concentration, causing the formation of calcareous incrustations along the walls of the cave, and groundwater infiltrations are still frequent. The Sybil's Cave is a dry habitat, with very little water infiltration. The similarities and differences present an opportunity for observing how they influence the composition of the algal assemblages in the two caves and could help to clarify the contribution of microalgae to deterioration processes.

Biodeterioration in caves occurs as a consequence of the presence of microbial communities, formed of algae, bacteria, and fungi, that develop thick biofilms on any rock surface, leading to decay (Albertano et al., 2003). Subterranean algal communities are generally divided into

* Corresponding author: pcennamo@unina.it
[1] Facoltà di Lettere, Università degli Studi 'Suor Orsola Benincasa', Via S. Caterina da Siena 37, I-80135 Napoli, Italy
[2] Dipartimento delle Scienze Biologiche, Università degli Studi di Napoli 'Federico II', Orto Botanico, Via Foria 223, Napoli I-80139, Italy
[3] Dipartimento di Scienze della Vita, Seconda Università di Napoli, Via Vivaldi 43, Caserta I- 81100, Italy
[4] Dipartimento di Scienze della Terra, Università degli Studi di Napoli 'Federico II', Via Mezzocannone 8, Napoli I-80134, Italy

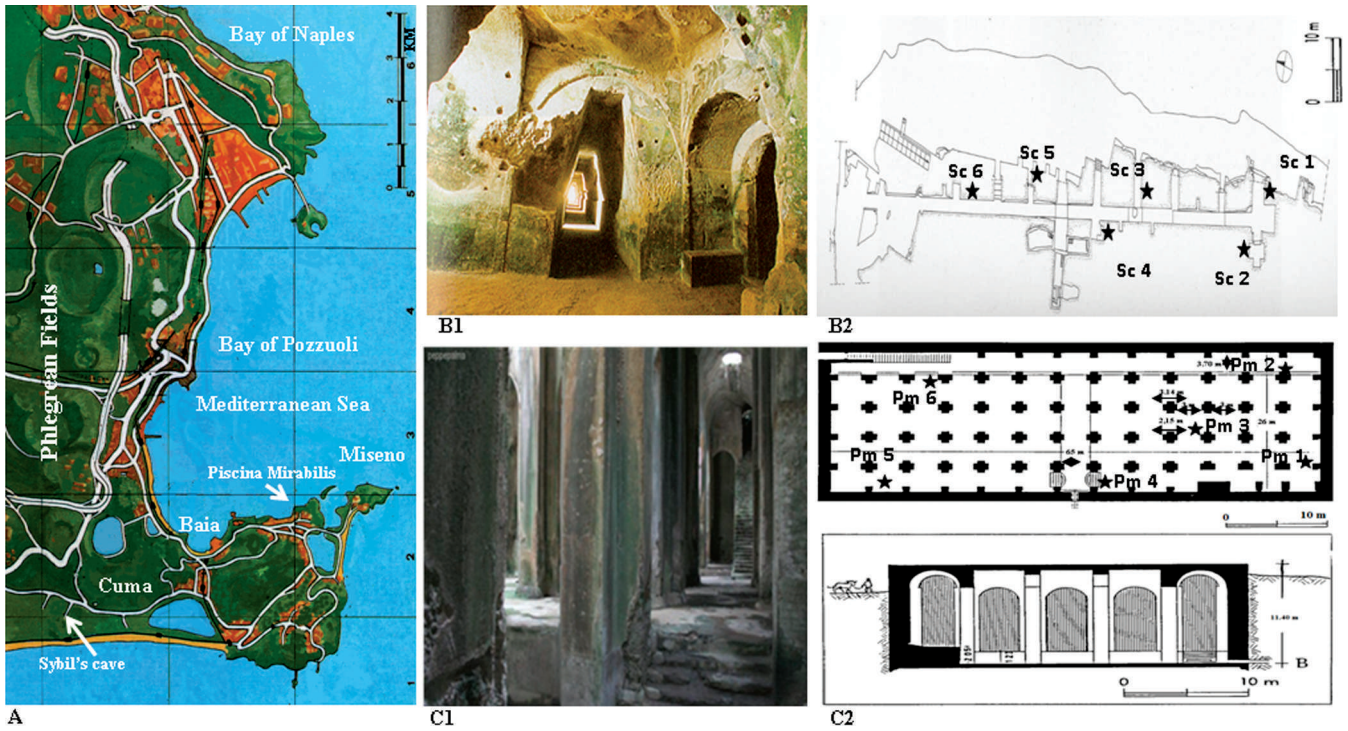

Figure 1. A, map of Phlegrean Fields. B1, picture of the Sybil's Cave. B2, map of and locations of the sampling sites in the Sybil's Cave (Pagano et al., 1982). C1, picture of the Piscina Mirabilis. C2, map of and locations of the sampling sites in the Piscina Mirabilis (Rajola et al., 1978).

the so-called lampenflora, formed by specialized organisms that thrive only in underground habitats in the presence of artificial light, and areophilic flora, composed by terrestrial microalgae, mainly belonging to Chlorophyta and diatoms that tolerate cave environmental conditions, especially at the openings of caves (Mulec et al., 2008). Cyanobacteria are the key organisms in the genesis of biofilms, being able to produce exopolymeric substances that allow the formation of the microbial community and its adhesion to rocks (Stal, 2000). Cyanobacteria exposed to high light intensities may have an endolithic phase of growth, changing the mineral structure of the rock and determining its decay (Asencio and Aboal, 2001).

In an attempt to ascertain the potential damage caused by the algal flora on the underground monuments of Campi Flegrei, a systematic survey of the algal flora from the two anthropogenic caves has been attempted. At the same time, considering that the algae living in these habitats cannot be considered solely as a threat, but also as an important source of biodiversity, an effort was undertaken to isolate and maintain the strains in the algal collection of University Federico II of Naples to study their ecophysiological features.

Experimental Methods

The Sybil's Cave, built in the fourth century BCE, is a trapezoidal passage over 131 m long running parallel to the side of the hill on which was built the Acropolis of Cuma at Campi Flegrei (Fig. 1 B1, B2). It was cut out in the volcaniclastic Neapolitan Yellow Tuff. The gallery leads to a more enclosed polygonal hall; the main entrance and the openings along the hallway ensure the entrance of light and a continuous flux of air.

The Piscina Mirabilis, built in the first century CE, is a cistern dug in the tuff , 70 m long, 25.50 m wide, and 15 m deep (Fig. 1 C1, C2). The cavity has a rectangular layout with forty-eight tuff pillars covered in *opus reticulatum*, a form of brickwork used in ancient Roman architecture consisting of diamond-shaped bricks of tuff placed around a core of concrete, and is divided into four corridors that compose the inner part of the cistern. The outer walls, in *opus reticulatum*, are covered with a thick layer of *cocciopesto*, mortar with potsherds. The Piscina Mirabilis supplied drinking water for the Roman fleet that was based in Misenum, near Baiae (Fig. 1 A).

Due to their orientation and position, the entrances of both caves are directly illuminated throughout the year. Moreover, the openings present in the Sybil's Cave allow penetration of light during the whole day, whereas the Piscina Mirabilis is always shady. Six sampling points were selected in each cave, on the basis of light, temperature, and relative humidity data (Fig. 1 B2, C2). They showed evidence of biodeterioration in the form of a green and brown patina. Ten samplings were carried out within a 20 × 20 cm square at each point.

Biofilm samples were collected in the autumn of 2009 by scraping the walls of the caves with a sterile scalpel and

Table 1. Temperature, light intensity and relative humidity of the Sybil's Cave (SC) and the Piscina Mirabilis (PM) sample sites.

Sample Sites	Temperature, °C	μE, m^{-2} s^{-1}	Relative Humidity, %
SC1	17 ± 2	0.05 ± 0.002	69 ± 1
SC2	18 ± 2	0.02 ± 0.001	69 ± 1
SC3	18 ± 2	0.16 ± 0.007	69 ± 2
SC4	19 ± 2	0.4 ± 0.02	68 ± 2
SC5	19 ± 2	0.407 ± 0.02	69 ± 2
SC6	19 ± 2	3.31 ± 0.15	72 ± 3
PM1	16 ± 1	0.15 ± 0.006	85 ± 1
PM2	16 ± 1	0.15 ± 0.006	86 ± 1
PM3	16 ± 1	0.22 ± 0.01	84 ± 1
PM4	16 ± 1	0.46 ± 0.02	81 ± 1
PM5	16 ± 1	0.05 ± 0.002	80 ± 2
PM6	16 ± 1	2.61 ± 0.13	75 ± 2

depositing materials into sterile vials containing either a specific medium for Cyanobacteria (BG11; Castenholz, 1988) or BBM (Bold Basal Medium; Bischoff and Bold, 1963) for all other microalgae. Samples were collected in September, October, and November (Table 1). Temperature, light intensity, and relative humidity were measured at each sampling site by using appropriate instruments (TESTO 174, TESTO 545, AG Germany). Light irradiance at each sampling point was measured by using a LI-COR radiation sensor (BIOSCIENCES).

The algal samples were inspected using an optical microscope (Nikon Eclipse E800 equipped with Nomarski interference, magnification ×100). Small fragments of biofilms, after critical-point drying, were gold-coated in an Emitech k550 Sputter Coater and observed by scanning electron microscopy (Philips EM 208S).

Quantitative mineralogical analysis and the chemical composition of rocks collected in the sampling areas were determined by means of x-ray powder diffraction and environmental scanning electron microscope. The x-ray diffraction was performed with a Panalytical X'Pert Pro modular diffractometer, and quantitative analyses were obtained by the Rietveld method (Bish and Post, 1993). Chemical elements were measured using a microanalysis system (ZAFPB).

Quantitative estimations of the identified taxa were also made. For algal counts, 0.5 g of fresh biofilm sample was suspended and fixed in 100 mL of aqueous solution of formaldehyde (3%) and counted with a hemocytometer within 24 hours. To establish species compositions, part of each suspension was put on a slide, and twenty randomly chosen microscope fields were counted using a grid (LUCIA version 4.60 System for Image Processing and Analysis); at least one hundred cells were counted per slide. Three such slides were counted for each sample, and the means were analyzed for significant variance (Student's t-test). The relative standard error was never higher than 5%. The count of filamentous Cyanobacteria was carried out by counting filaments in transects of a chamber filled with a few milliliters for sedimentation over night. Backcalculating to a ml of sample was carried out by considering the volume of the counting chamber and measuring the area of the transects and of the chamber bottom (Lawton et al., 1999).

Additionally, the identification of the microbial components of biofilms was accomplished by molecular techniques. DNA was extracted using a procedure described by Doyle and Doyle 1990. PCR amplification was carried out on an estimated 10 ng of extracted DNA. For Cyanobacteria, the primer set for 16S rDNA (Díez et al., 2001) was used; for algae, the primer set for 18S rDNA indicated by Huss et al. (1999) was used. PCR reactions were carried out in a final volume of 50 μL containing 5 μL of 10× PCR buffer, 100 mM of deoxynucleotide triphosphate, 2.5 mM of magnesium chloride, 0.5 mM of primers, and 1U of *Taq* polymerase (Quiagen, Hilden, Germany). The PCR program consisted of an initial denaturation at 95 °C for 4 min and 30 cycles including 1 min of denaturation at 94 °C, 45 s of annealing at 56 °C, and 2 min extension at 72 °C. A final extension of 7 min at 72 °C followed by cooling at 4 °C terminated the PCR program.

The identification of the entire community was obtained employing cloning libraries. An aliquot of purified PCR product was ligated into the pGEM-T easy Vector system (Promega, Vienna, Austria), and clones were screened and sequenced with a 3130 genetic analyzer (Applied Biosystems). The sequences obtained were compared with available sequences in the GeneBank database. Cluster analysis to detect possible grouping of algal taxa in terms of environmental preferences was carried out by using the SYNTAX vers. 5.1 computer program for data analysis in ecology and systematics (Podani, 2001).

Results and Discussion

At all the sampling points, mean midday temperature was 18 ± 2 °C in the Sybil's Cave (SC) and 16 ± 1 °C in the Piscina Mirabilis (PM). The mean amount of photosynthetically active radiation in SC ranged from 0.0165 to 3.31 μE $s^{-1}m^{-2}$, whereas in PM values at sampling points 1 to 6 ranged from 0.049 to 2.61 μE $s^{-1}m^{-2}$ (Table 1). Relative humidity in SC ranged from 69 to 72%; on the other hand, the relative humidity of PM was in the range 75 to 86% (Table 1).

Light microscopy revealed the presence of taxa belonging to Cyanobacteria, Chlorophyta, Bacillariophyta, and Rhodophyta. The variations in relative abundance of these taxa among the various sampling point in the two caves are shown in Figure 2. Cyanophyta were the dominant taxa at several sampling points, both in SC (sites 1 to 4) and in PM (sites 1 to 4), where Cyanobacteria cell percentages ranged from 50 to 80% in SC and from 70 to 85% in PM. At the same sites, Chlorophyta represented a minor percentage

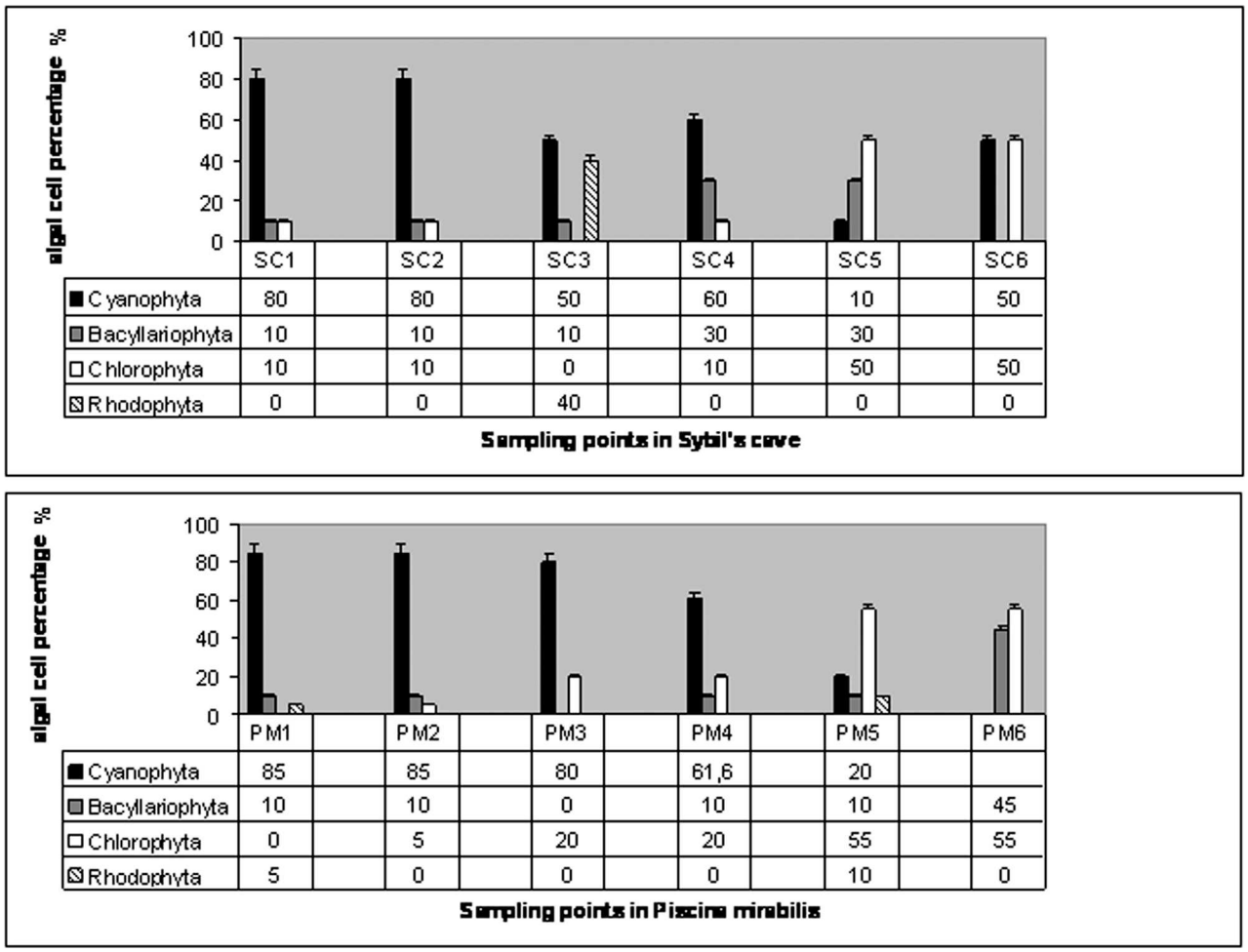

Figure 2. Microbial composition of biofilms in the Sybil's Cave and the Piscina Mirabilis.

(less than 25%) of the algal population, but at SC5, PM5, and PM6, where cyanophytes were scarcely represented, chlorophytes prevailed, with their relative abundance being directly proportional to the increase in light intensity. Bacillariophyta (diatoms) normally did not exceed 10% in SC and in PM; at SC4, SC5, and PM6, however, they were 30 and 45% respectively. Rhodophyta were abundant only at SC3, at relatively low light intensity, while in PM their percentages never exceeded 10%.

Microanalyses of the substrate, always composed of Neapolitan Yellow Tuff (NYT), revealed the presence of the same elemental composition in both sites (Al, Ba, Cd, Co, Cu, Fe, K, Mg, Mn, Na, Si, Sr, Ti, U, and Zn), albeit elements were present at different concentrations. Mineralogical composition of investigated samples confirmed the composition of NYT, mainly phillipsite, chabazite, and analcime, and hydrous aluminosilicates pertaining to the zeolite group, along with feldspars and minor amounts of clay minerals (de'Gennaro et al., 2000). Data from the literature (Morra et al., 2010) state high porosity values for NYT, which is characterized, moreover, by the presence of micropores causing a high capillary absorption of water that allows microbial growth. SEM observations showed that the microbial community is embedded in an exopolysaccharidic matrix that facilitates the establishment of strong bonds between biofilm and substrate (Fig. 3). In both sites, Cyanobacteria adhered strictly to NYT, offering an ideal environment for the growth of other organisms, giving endurance and thickness to the biofilm.

Identification of many algal strains is difficult because of the scarcity of useful features and the homoplasious morphology of some lineages. To minimize the risk of erroneous identifications, molecular techniques were also used. Only the most similar sequence matches (90% identity) with GenBank have been considered. Sequencing revealed a total of seventeen phylotypes for SC and thirteen for PM that were assigned to Cyanophyta (eleven taxa), Rhodophyta (two taxa), Chlorophyta (six taxa) and Bacillariophyta (two taxa) (Table 2).

A hierarchical clustering was carried out on a dissimilarity matrix based on the presence/absence of algal taxa in different sampling sites at different light intensities and relative humidities (Jaccard coefficient $1 - a / (a + b + c)$). Two classes of humidity were defined for the analysis, low humidity (less than

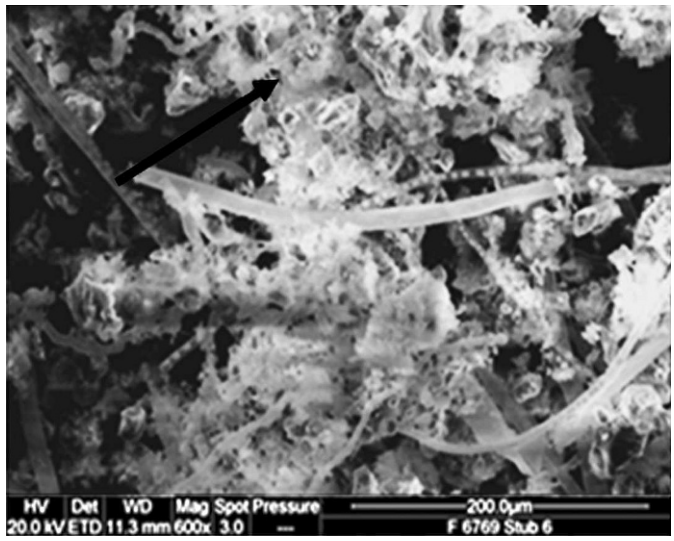

Figure 3. Scanning electron micrograph (SEM) showing microbial community embedded in an esopolysaccharidic matrix (arrow).

75%) and high humidity (77 to 82%), as well as three classes of light intensities, low intensity (from 0.017 to 0.198 $\mu E\ s^{-1}m^{-2}$), intermediate intensity (from 0.33 to 0.4125 $\mu E\ s^{-1}m^{-2}$), and high intensity (above 2.607 $\mu E\ s^{-1}m^{-2}$). As shown in Figure 4, algal strains are grouped in two distinct clusters: group A (eight strains), which includes strains found only at low humidity; *Aphanotecae* sp., *Chroococcus lithophilus, Gloeocapsa* sp., *Gloeocystis* sp., *and Scenedesmus arcuatus* sp. are grouped in the same subgroup, since they have been found in sampling sites with both medium and high light intensities. *Pseudococcomya simplex* and *Cyanobium bacillare* appear distantly related to this subgroup, as these taxa colonize low intensity sites and high intensity sites, respectively. A second cluster (group B) includes two subgroups. In subgroup B1, all species are not affected by humidity; *Chroococcus varius*, *Navicula* sp., *Chlorella* sp., *Stichococcus* sp. and *Scotiellopsis terrestis* are ubiquitous strains, while *Oscillatoria* sp., *Synechococcus* sp., *Cyanidium* sp., and *Phragnonema sordidum* have been detected only in sampling sites with low to medium light intensities. A third group representing Subgroup B2 includes *Leptolyngbya fragilis*, *L. foveolarum*, *Lyngbya* sp., and *Nostoc commune*; these strains were detected only in PM, thus suggesting that they are probably dependent on high humidity.

The Sybil's Cave and the Piscina Mirabilis share some important physico-chemical characters: location, anthropogenic origin, Mediterranean climate, and nature of the substrate. Microbial colonization of rock substrates is highly dependent on their features (Macedo et al., 2009), and in the case of SC and PM, surface roughness, porosity, and mineral composition of the rock promote in the same way the establishment of microbial assemblages. Temperature, irradiation, and relative humidity are relevant differences between SC and PM. In the inner part of the former, light intensity is very reduced ($< 0.01\ \mu E\ s^{-1}m^{-2}$), but temperature and relative humidity are comparable to open-air values. Similar values of relative humidity were reported by Hoffman (1989) for another anthropogenic cave, the Roman necropolis in Seville, Spain. SC cannot be considered a typical cave environment, but rather a poorly illuminated aerial habitat, where temperature and relative humidity are heavily influenced by the external climatic conditions due to the presence of large opening in the rock walls of the cave. On the other hand, PM is a dim environment with a mild temperature and a relative humidity comparable to that recorded from numerous natural caves, whose values range from 76 to 96% (Couté and Yéprémian, 2002).

In the dark area of SC, Cyanophytes are the dominant organisms, being represented by *Synechococcus* sp. and *Cyanobium bacillare* and *Oscillatoria* sp. *Oscillatoria* has been frequently encountered in European caves (Couté and Yéprémian, 2002). It is a pioneer organism because of its capacity to grow diazotrophically (Gallon et al., 1991). Moreover, as other members of Oscillatoriales, it is well adapted to extremely low irradiance compared to other filamentous Cyanophyta (Albertano et al., 2000). The presence of *Synechococcus* and of the closely related *Cyanobium bacillare* in sampling points 1 and 2 of SC confirms that the average temperature of SC during the year is not particularly low, since this species does not thrive in cold environments (Sakamoto and Bryant, 1999). *Synechococcus* is not a typical cave organism: its occurrence has been reported on both marble and granite monuments in different Mediterranean countries (Crispim and Gaylarde, 2005), and it also can grow endolithically (Saiz-Jimenez et al., 1990). *Chroococcus lithophilus* and *C. various*, together with *Gloeocapsa* sp., are the dominant Cyanobacteria in the whole Sybil Cave, where light intensity is greater than 0.01 $\mu E\ s^{-1}m^{-2}$. The increase in Chroococcacean species at low levels of irradiation seems to be a standard feature of cave algal assemblages (Asencio and Aboal, 2001), even though the occurrence of *Chroococcus* and *Gloeocapsa* has been reported not only in dim habitats, but also on monuments exposed to daylight (Scheerer et al., 2009), confirming the tolerance of these organisms to a wide range of environmental conditions.

The algal communities of PM can be split in two types: the first, found in points 1 through 3, is mainly composed by filamentous Cyanobacteria. *Nostoc commune* is the dominant species, responsible for the formation of thick mats containing also *Leptolynbya fragilis*, *L. foveolarum*, and *Lyngbya* sp. filaments, along with Chroococcacean species as *Synechococcus* sp. and *Cyanobium bacillare*. The dominant presence of filamentous cyanobacteria in stable conditions of low light intensity and high relative humidity has been reported for different caves (Martinez and Asencio, 2010; Roldàn and Hernández-Mariné, 2009). *Nostoc* is a cosmopolitan terrestrial genus that can endure desiccation, as well as very low temperatures (Dodds et al., 1995). However, the persistence of *Nostoc commune* seems to be determined

Table 2. List of algal taxa at sampling sites in the Sybil's Cave (SC) and in the Piscina Mirabilis (PM).

	Sampling Sites											
Species	S	SC2	SC3	SC4	SC5	SC6	PM1	PM2	PM3	PM4	PM5	PM6
PROKARYOTA												
CYANOPHYTA												
Aphanotecae sp.	…	…	…	X	X	X	…	…	…	…	…	…
Chroococcus lithophilus Ercegović	…	…	X	X	X	X	…	…	…	…	…	…
Chroococcus varius A. Braun in Rabehorst	…	…	X	X	X	X	…	…	…	X	X	X
Gloeocapsa sp.	…	…	X	X	X	X	…	…	…	…	…	…
Leptolyngbya foveolarum (Rabenhorst ex Gomont) Anagnostidis et komárek	…	…	…	…	…	…	X	X	…	…	…	…
Leptolyngbya fragilis (Gomont) Anagnostidis et komárek	…	…	…	…	…	…	X	X	…	…	…	…
Lyngbya sp.	…	…	…	…	…	…	X	X	…	X	…	…
Nostoc commune Vaucher ex Bornet & Flahault	…	…	…	…	…	…	…	…	X	…	…	…
Oscillatoria sp.	X	X	…	…	…	…	X	…	X	…	…	…
Synechococcus sp.	X	X	…	…	…	…	X	X	X	…	…	…
Synechococcus bacillaris Cyanobium bacillare (Butcher) J. Komárek, J. Kopeck & V. CepàK	X	X	…	…	…	…	…	…	…	…	…	…
EUKARYOTA												
BACILLARIOPHYTA												
Navicula sp.	…	…	…	X	X	X	…	…	…	X	X	X
Pinnularia obscura Krasske	…	…	…	X	X	…	…	…	…	…	….	…
CHLOROPHYTA												
Chlorella sp. Beijerinck	…	…	…	…	X	X	…	…	X	…	X	X
Gloeocystis sp.	…	…	…	X	X	X	…	…	…	…	…	…
Stichococcus sp.	…	…	…	X	X	X	…	…	…	…	X	X
Scenedesmus arcuatus Lemmrmanm	…	…	…	…	X	X	…	…	…	…	…	…
Scotiellopsis terrestris (H. Reislig) Pucocharova & Kalina	…	…	…	…	…	X	X	…	…	…	X	…
Pseudococcomya simplex (Mainx) Fott	…	…	…	…	…	X	…	…	…	…	…	…
RHODOPHYTA												
Cyanidium sp.	X	…	X	…	…	…	X	X	…	…	X	…
Phragnonema sordidum Zopf	X	…	X	…	…	…	X	…	…	X	…	…

by the occurrence of liquid water (Stal, 2000). This feature could account for the sharp difference observed in community composition between the Sybil's Cave and the Piscina Mirabilis; in the first, a dry habitat, *Nostoc commune* was not recovered at any light intensity, whereas in PM, an intense growth of this Cyanophyta was observed where light intensity was low.

Chlorophyta and diatoms found in points 4 to 6 of both SC and PM are typical members of algal aerial communities. Chlorophyta genera such as *Chlorella*, *Stichococcus*, and *Scotiellopsis* and diatom genera such as *Navicula*, and *Pinnularia* are ubiquitous and well-adapted to colonize a wide range of substrata, regardless of microclimatic and environmental conditions (Macedo et al., 2009). *Pinnularia obscura* has been detected in thermoacidic environments of Campi Flegrei (Ciniglia et al., 2007), and it is probably widely distributed in the whole district.

The cluster analysis of algal distribution in the Sybil's Cave and the Piscina Mirabilis as related to light and humidity showed that the most relevant differences in the algal distributions was the detection of filamentous Cyanobacteria exclusively in the Piscina Mirabilis. This group of organisms seems to prefer high and constant values of relative humidity together with low light intensities, which were not recorded in the Sybil's Cave.

Also noteworthy is the presence in both caves of two rare unicellular red algae, *Cyanidium* sp. and *Phragnonema sordidum*. The occurrence of *P. sordidum* in SC was reported for the first time by Sieminska (1962), who recovered the alga on a shady and damp wall of this

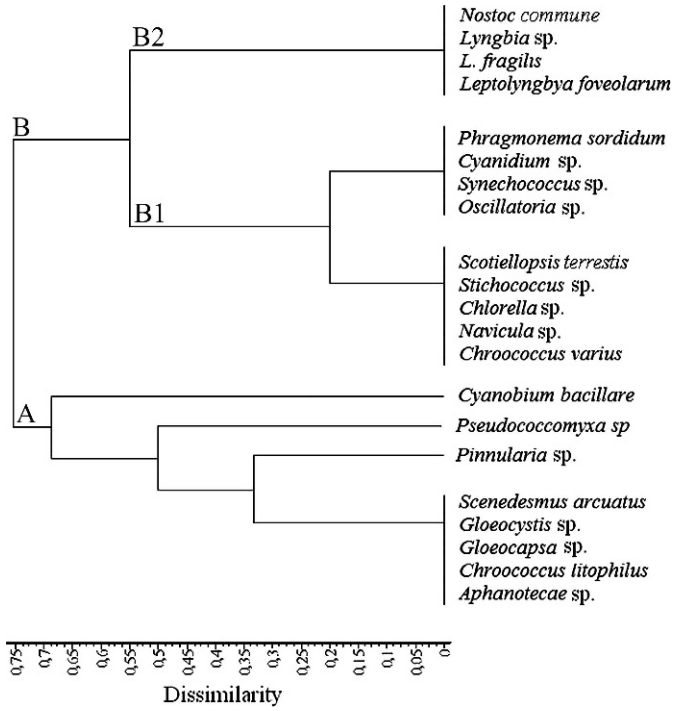

Figure 4. Hierarchical clustering of the algal strains based on light and humidity. The major clusters described in the text are, from the bottom up, A, B1, and B2.

cave. In SC, *P. sordidum* is frequently associated with *Synechococcus*, and it occurs in all the stages of its life cycle. The presence of *P. sordidum* has been recorded in other caves in the Mediterranean region (Friedmann, 1956), as well as on monuments in the Deux Sèvres district, France, under low light intensity (Le Clerc et al., 1983) and in hypogaean Roman archeological sites (Albertano, 1993).

The genus *Cyanidium* encompasses unicellular algae recently placed in the phylum Cyanidiophyta (Saunders and Hommerstand, 2004) among the Rhodophyta. This genus includes both thermoacidophilic organisms, such as the well known *C. caldarium*, ubiquitously present in thermoacidic environments (Pinto et al., 2007), as well as mesophilic ones, as reported by Schwabe (1936, 1944) on the walls of Chilean coastal caves with no water seepage. According to Ott and Seckbach (1994), the mesophilic strain is clearly different from *C. caldarium*, on the basis of its mesophilic character and its habitat, but its geographic distribution is presently not known. Since the studies of Schwabe (1936, 1944), cave *Cyanidium* taxa have been found in many other sites, from the Negev Desert, Israel (Friedmann, 1956) to France and Italy (Hoffmann 1986, Skuja, 1970).

Conclusions

The Campi Flegrei district presents many other hypogean monuments that have not yet been explored for their algal communities. Studies are in progress to extend our knowledge of the algal biodiversity occurring in these peculiar habitats.

References

Albertano, P., 1993, Epilithic algal communities in hypogean environments: Giornale Botanico Italiano, v. 127, no. 3, p. 386–392.

Albertano, P., Bruno, L., D'Ottavi, D., Moscone, D., and Palleschi, G., 2000, Effect of photosynthesis on pH variation in cyanobacterial biofilms from Roman catacombs: Journal of Applied Phycology, v. 12, p. 279–384. doi:10.1023/A:1008149529914.

Albertano, P., 2003, CATS—Cyanobacteria attack rocks: control and preventive strategies for avoiding damage caused by cyanobacteria and associated micro-organisms in Roman hypogean monuments, *in* Kozlowski, R., et al., eds., Proceedings of the 5th EC Conference on Cultural Heritage Research: a Pan-European Challenge, Cracow, EU-ICSC, 394 p.

Albertano, P., Moscone, D., Palleschi, G., Hermosin, B., Saiz-Jimenez, C., Sanchez-Moral, S., Hernandez-Marine, M., Urzi, C., Groth, I., Schroeckh, V., Saarela, M., Mattila-Sandholm, T., Gallon, J.R., Graziottin, F., Bisconti, F., and Giuliani, R., 2003, Cyanobacteria attack rocks (CATS): Control and preventive strategies to avoid damage caused by cyanobacteria and associated microorganisms in Roman hypogean monuments, *in* Saiz-Jimenez, C., ed., Molecular Biology and Cultural Heritage: Lisse, Netherlands, Zwets & Zeitlinger, p. 151–162.

Asencio, A.D., and Aboal, M., 2001, Biodeterioration of wall paintings in caves of Murcia (SE Spain) by epilithic and chasmoendolithic microalgae: Algological Studies/Archiv für Hydrobiologie, Supplement Volumes No. 103, p. 131–142.

Bish, D.L., and Post, J.E., 1993, Quantitative mineralogical analysis using the Rietveld full-pattern fitting method: American Mineralogist, v. 78, p. 932–940.

Bischoff, H.W., and Bold, H.C., 1963, Some soil algae from Enchanted Rock and related algal species: Austin, University of Texas Publication no. 6318, Phycological Studies no. 4, 95 p.

Castenholz, W., 1988, Culturing methods for Cyanobacteria, *in* Parker, L., and Glazer, A.N., eds., Cyanobacteria: Elsevier, Methods in Enzymology, no. 167, p. 68–93. doi:10.1016/0076-6879(88)67006-6.

Chelius, M.K., Beresford, G., Horton, H., Quirk, M., Selby, G., Simpson, R.T., Horrocks, R., and Moore, J.C., 2009, Impacts of alterations of organic inputs on the bacterial community within the sediments of Wind Cave, South Dakota, USA: International Journal of Speleology, v. 38, no. 1, p. 1–10.

Ciniglia, C., Cennamo, P., De Stefano, M., Pinto, G., Caputo, P., and Pollio, A., 2007, *Pinnularia obscura* Krasske (Bacillariophyceae, Bacillariophyta) from acidic environments: characterization and comparison with other acid-tolerant *Pinnularia* species: Fundamental and Applied Limnology: Archiv für Hydrobiologie, v. 170, p. 29–47. doi:10.1127/1863-9135/2007/0170-0029.

Couté, A., and Yéprémian, C., 2002, L'homme et les algues des cavernes, *in* M. F. Roquebert, M.F., ed., Les contaminants biologiques des biens culturels, Paris, Elsevier, Collection Patrimoine, p. 33–55.

Crispim, C.A., and Gaylarde, C.C., 2005, Cyanobacteria and biodeterioration of cultural heritage: a review. Microbial Ecology, v. 49, p. 1–9. doi:10.1007/s00248-003-1052-5.

Dayner, D.M., and Johansen, J.R., 1991, Observations on the algal flora of Seneca Caverns, Seneca County, Ohio: Ohio Journal of Science, v. 91, p. 118–121.

de'Gennaro, M., Cappelletti, P., Langella, A., Perrotta, A., and Scarpati, C., 2000, Genesis of zeolites in the Neapolitan Yellow Tuff: geological, volcanological and mineralogical evidence: Contributions to Mineralogy and Petrolology, v. 139, p. 17–35. doi:10.1007/s004100050571.

Díez, B., Pedrós-Alió, C., and Massana, R., 2001, Study of genetic diversity of eukaryotic picoplankton in different oceanic regions by small-subunit rRNA gene cloning and sequencing: Applied and Environmental Microbiology, v. 67, p. 2932–2941. doi:10.1128/AEM.67.7.2932-2941.2001.

Dobat, K., 1970, Considérations sur la végétation cryptogamique des grottes du Jura Souabe (sud-ouest de l'Allemagne): Annales de Spéléologie, v. 25, no. 4, p. 872–907.

Dodds, W.K., Gudder, D.A., and Mollenhauer, D., 1995, The ecology of *Nostoc*: Journal of Phycology, v. 31, p. 2–18. doi:10.1111/j.0022-3646.1995.00002.x.

Doyle, J.J., and Doyle, J.L., 1990, Isolation of plant DNA from fresh tissue: Focus, v. 12, p. 13–15.

Friedmann, I., 1956, Beiträge zu Morphologie und Formwechsel der atmophytischen Bangioidee *Phragmonema sordidum*: Zopf. Österreichische botanische Zeitschrift, v. 103, p. 613–633.

Gallon, J.R., Hashemm, M.A., and Chaplina, A.E., 1991, Nitrogen fixation by *Oscillatoria* spp. under autotrophic and photoheterotrophic conditions: Journal of General Microbiology, v. 137, p. 31–39. doi:10.1099/00221287-137-1-31.

Hoffmann, L., 1986, Cyanophycées aériennes et subaériennes du Grand-Duché de Luxembourg: Bulletin du Jardin Botanique National de Belgique, v. 56, p. 77–127.

Hoffmann, L., 1989, Algae of terrestrial habitats: Botanical Review, v. 55, p. 77–105. doi:10.1007/BF02858529.

Huss, V.A.R., Frank, C., Hartmann, E.C., Hirmer, M., Kloboucek, A., Seidel, B.M., Wenzeler, P., and Kessler, E., 1999, Biochemical taxonomy and molecular phylogeny of the genus *Chlorella* sensu lato (Chlorophyta): Journal of Phycology, v. 35, p. 587–598. doi:10.1046/j.1529-8817.1999.3530587.x.

Insinga, D., Calvert, A., D'Argenio, B., Fedele, L., Lanphere, M., Morra, V., Perrotta, A., Sacchi, M., and Scarpati, C., 2004, $^{40}Ar/^{39}Ar$ dating of the Neapolitan Yellow Tuff eruption (Campi Flegrei, southern Italy): volcanological and chronostratigraphic implications. European Geophysical Union 1st General Assembly, Nice, 2004 (abstract).

Lawton, L., Marsalek, B., Padisák, J., and Chorus, I., 1999, Determination of Cyanobacteria in the laboratory, *in* Chorus, I., and Bartram, J., eds., Toxic Cyanobacteria in Water: A Guide to Their Public Health Consequences, Monitoring and Management, London, E & FN Spon Press, p. 347–368.

Le Clerc, J.C., Couté, A., and Dupuy, P., 1983, Le climat annuel de deux grottes et d'une église du Poitou, ou vivent des colonies pures d'algues sciaphiles: Cryptogamie Algologie, v. 4, p. 1–19.

Macedo, M.F., Miller, A.Z., Dionísio, A., and Saiz-Jimenez, C., 2009, Biodiversity of cyanobacteria and green algae on monuments in the Mediterranean Basin: an overview: Microbiology, v. 155, p. 3476–3490. doi:10.1099/mic.0.032508-0.

Martínez, A., and Asencio, A.D., 2010, Distribution of cyanobacteria at the Gelada Cave (Spain) by physical parameters: Journal of Cave and Karst Studies, v. 72, no. 1, p. 11–20. doi:10.4311/jcks2009lsc0082.

Morra, V., Calcaterra, D., Cappelletti, P., Colella, A., Fedele, L., de' Gennaro, R., Langella, A., Mercurio, M., and de' Gennaro, M., 2010, Urban geology: relationships between geological setting and architectural heritage of the Neapolitan area, *in* Beltrando, M., Peccerillo, A., Mattei, M., Conticelli, S., and Doglioni, C., eds., The Geology of Italy: tectonics and life along plate margins, Journal of the Virtual Explorer, v. 36, paper 27. doi:10.3809/jvirtex.2010.00261.

Mulec, J., Kosi, G., and Vrhovšek, D., 2007, Algae promote growth of stalagmites and stalactites in karst caves (Škocjanske jame, Slovenia): Carbonates and Evaporites, v. 22, no. 1, p. 6–10. doi:10.1007/BF03175841.

Mulec, J., Kosi, G., and Vrhovšek, D., 2008, Characterization of cave aerophytic algal communities and effects of irradiance levels on production of pigments: Journal of Cave and Karst Studies, v. 70, no. 1, p. 3–12.

Orsi, G., De Vita, S., and di Vito, M., 1996, The restless, resurgent Campi Flegrei nested caldera (Italy): constraints on its evolution and configuration: Journal of Volcanology and Geothermal Research, v. 74, p. 179–214. doi:10.1016/S0377-0273(96)00063-7.

Ott, F.D., and Seckbach, J., 1994, New classification for the genus *Cyanidium* Geitler 1933, *in* Seckbach, J., ed., Evolutionary Pathways and Enigmatic Algae: *Cyanidium caldarium* (Rhodophyta) and Related Cells, New York, Springer, Developments in Hydrobiology, v. 91, p. 145–152.

Pagano, M., Redd, M., and Roddaz, J.-M., 1982. Campi Flegrei Marsilio Editore.

Pedersen, K., 2000, Exploration of deep intraterrestrial microbial life: current perspective: FEMS Microbiology Letters, v. 185, p. 9–16. doi:10.1111/j.1574-6968.2000.tb09033.x.

Pinto, G., Ciniglia, C., Cascone, C., and Pollio, A., 2007, Species composition of Cyanidiales assemblages in Pisciarelli (Campi Flegrei, Italy) and description of *Galdieria phlegrea* sp. nov., *in* Seckbach, J., ed., Algae and Cyanobacteria in Extreme Environments, Dortrecht, Netherlands, Springer, Cellular Origin, Life in Extreme Habitats, and Astrobiology, v. 11, p. 487–502. doi:10.1007/978-1-4020-6112-7_26.

Podani, J., 2001, SYN-TAX 2000 Computer Program for data analysis in Ecology and Systematics: User's Manual, Budapest, Scientia, 53 p.

Rajola, T., and N. Fiorillo *in* Paoli, P.A., 1978, Table 60 Naples, Biblioteca Nazionale Vittorio Emanuele III, Roma.

Roldán, M., and Hernández-Mariné, M., 2009, Exploring the secrets of the three-dimensional architecture of phototrophic biofilms in caves. International Journal of Speleology, v. 38, no. 1, p. 41–53.

Saiz-Jimenez, C., Garcia-Rowe, J., Garcia Del Cura, M.A., Ortega-Calvo, J.J., Roekens, E., and Van Grieken, R., 1990, Endolithic cyanobacteria in Maastricht limestone: Science of the Total Environment, v. 94, no. 3, p. 209–220. doi:10.1016/0048-9697(90)90171-P.

Sakamoto, T., and Bryant, D.A., 1999, Nitrate transport and not photoinhibition limits growth of the freshwater Cyanobacterium *Synechococcus* species PCC 6301 at low temperature: Plant Physiology, v. 119, p. 785–794. doi:10.1104/pp.119.2.785.

Saunders, G.W., and Hommersand, M.H., 2004, Assessing red algal supraordinal diversity and taxonomy in the context of contemporary systematic data: American Journal of Botany, v. 91, no. 10, p. 1494–1507. doi:10.3732/ajb.91.10.1494.

Scarpati, C., Cole, P., and Perrotta, A., 1993, The Neapolitan Yellow Tuff—A large volume multiphase eruption from Campi Flegrei, Southern Italy: Bulletin of Volcanology, v. 5 5, p. 343–356. doi:10.1007/BF00301145.

Scheerer, S., Ortega-Morales, O., and Gaylarde, C., 2009, Microbial deterioration in stone monuments—an updated overview, *in* Laskin, A., Gadd, G., and Sariaslani, S., eds., Advances in Applied Microbiology, Volume 66: San Diego, Academic Press, p. 97–130.

Schwabe, G.H., 1936, Über einige Blaualgen aus dem mittleren und südlichen Chile: Verhandlungen des Deutschen Wissenschaftlichen Vereins zu Santiago de Chile, v. 3, p. 113–174.

Schwabe, G.H., 1944, Umraumfremde Quellen, Shanghai, M. Nössler, Mitteilungen der Deutschen Gesellschaft für Natur- und Völkerkunde Ostasiens supplement 21, 300 p.

Sieminska, J., 1962, The red alga *Phragmonema sordidum* in the Sibyl cave nearby Naples: Acta Hydrobiologie, v. 4, no. 2, p. 225–227.

Skuja, H., 1970, Alghe cavernicole nelle zone illuminate delle grotte di Castellana (Murge di Bari): Le Grotte d'Italia, Ser. 4, v. 2, p. 193–202.

Stal, L.J., 2000, Cyanobacterial mats and stromatolites, *in* Whitton, B., and Potts, M., eds., Ecology of the Cyanobacteria: Their Diversity in Space and Time, Dortrecht, Netherlands, Kluwer, p. 61–120.

M. Komac and J. Urbanc – Assessment of spatial properties of karst areas on a regional scale using GIS and statistics – the case of Slovenia. *Journal of Cave and Karst Studies,* v. 74, no. 3, p. 251–261. DOI: 10.4311/2010ES0188R

ASSESSMENT OF SPATIAL PROPERTIES OF KARST AREAS ON A REGIONAL SCALE USING GIS AND STATISTICS – THE CASE OF SLOVENIA

Marko Komac and Janko Urbanc
Geological Survey of Slovenia, Dimičeva ul. 14, SI – 1000 Ljubljana, Slovenia, marko.komac@geo-zs.si

Abstract: In Slovenia, 43% of the territory is karst, including 42% of all protected water sources and 53% of all water-protection areas in the country. Over 95% of drinking water is obtained from groundwater, so assessment of karst areas and their spatial distribution is essential to better understand the water in the lithosphere and for the assessment of the hydrogeochemical properties of the groundwater in a large part of Slovenia. These groundwater resources are susceptible to degradation or pollution, and a regional karstification-intensity map was developed to assist in the management of these water resources and to interpret the chemical composition of the groundwater. For the purpose of classifying stratigraphic units into karstification-level classes, three parameters were analyzed in the outcrops of units with carbonate content using GIS and simple spatial statistics: the presences of sinks and cave entrances and the absence of a surficial drainage network. Where at least two of the three parameters showed a positive relation with karstification, the unit was regarded as intensely karstified, while the rest were regarded as less karstified. The former areas cover 24% and the latter 21% of Slovenian territory.

Introduction

Due to its natural features, Slovenia is a cradle of karst research. According to Gams (2003), 43% of Slovenian territory is karst. Figure 1 (generalized after Gams, 2003) shows the general distribution of karst types in Slovenia. Karst is a terrain, generally underlain by limestone or dolomite, in which the topography is chiefly formed by the dissolution of rock and that may be characterized by sinkholes, sinking streams, closed depressions, subterranean drainage, and caves (Monroe, 1970).

Karst areas have very specific hydrogeological properties, and hence, a karst map of high quality is essential for the purpose of better understanding the flow and chemical composition of water in the almost half of Slovenia's territory that consists of carbonate rocks. For the purpose of studying the characteristics of Slovenian aquifers in a later stage, a better and newer map of karst areas on a general scale is needed. Such a map will also be very useful for assessing groundwater vulnerability and siting of ecologically problematic projects, but the intention of this paper is not to address the vulnerability issue. An assessment of these is the next step, which will be done in the future when additional parameters will have to be considered, such as soil cover and the thickness of the vadose zone. The intention of this paper is merely to assign different intensities of karstification to areas in Slovenia on the basis of available data by using GIS methods.

In the past, there were several attempts to map karst areas in Slovenia (among others, Blaeu and Blaeu, 1645; Valvasor, 1977; Gams, 2003), but none were based upon a statistical approach or directly on stratigraphic levels. The recently published Geological map of Slovenia at a scale of 1:250,000 (Buser, 2010) enabled a novel approach to assessing karst-prone areas for the whole Slovenian territory at an acceptable resolution.

Various studies have dealt with the analysis of karst terrains and karst features using GIS, remote-sensing techniques, and field work to derive large-area karst maps. Florea et al. (2002) used systematic mapping of karst features and GIS to produce a karst map of an area of Kentucky. Veni (2002) based his karst (and pseudokarst) map of the United States on lithology, rather than on karst features. Armstrong et al. (2003) analyzed the relation between hydraulic conductivity and karst surface features and found a good correlation between the two in western Florida. Also in Florida, Denizman (2003) investigated morphometric parameters of karst surface features and concluded that GIS provides good tools for karst studies. Florea (2005) used sinkhole information to identify known and unknown structural features in Kentucky. For the smaller area in Kentucky, Taylor et al. (2005) derived sinkhole data from digital elevation models. Stafford et al. (2008) used karst features data to develop a karst-potential map in evaporates. They discovered that using a GIS approach exclusively underestimates the actual extent and development of karst features. Gao and Zhou (2008) gave a thorough overview of past GIS and database application in karst research.

Study Area

Slovenia lies in central Europe, at the contact of the Alpine arch with the Dinaric chain and Pannonian basin. Its surface measures slightly over 20,200 km^2 (Fig. 2). Elevations extend from sea level up to 2864 m, and the landscape varies from Pannonian plains to hilly slopes and Alpine mountains,

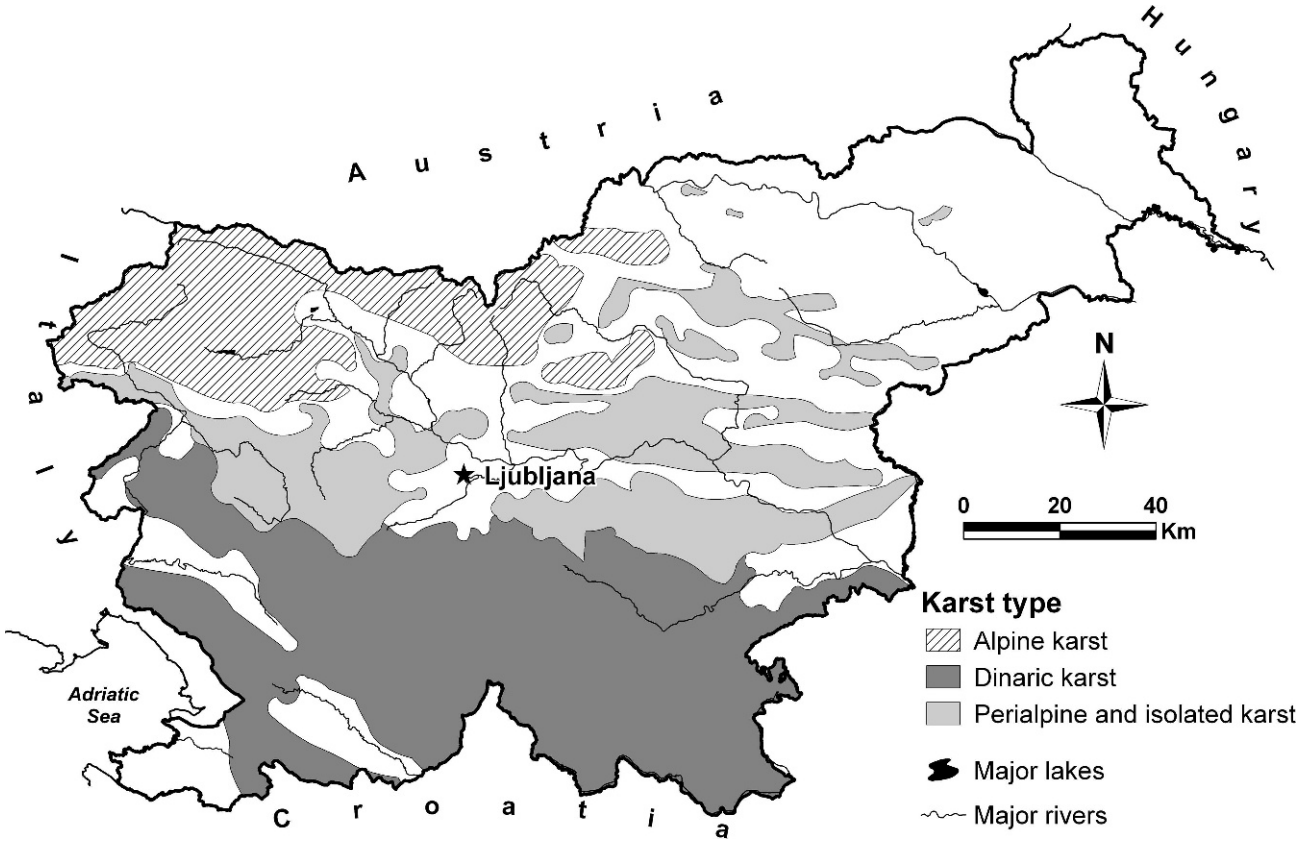

Figure 1. Karst regions in Slovenia, generalized after Gams (2003).

all with areas of karst morphology. Due to its richness in carbonate formations, more than 40% of Slovenia is karst or semi-karst. According to Komac (2005) almost 92% of the carbonates are of Mesozoic age in Slovenia, where karst is only developed on carbonate rocks. Of the territory of Slovenia, 49.25% is composed of clastic rocks, carbonate rocks cover 39.31%, and a mixture of the two covers 4.27% of the area. The least area is occupied by igneous rocks (1.49%), followed by pyroclastic rocks (1.78%) and metamorphic rocks (3.9%). In Slovenia, almost all karst phenomena are the product of hypergenic karst processes, and there is virtually no hypogenic karst.

DATA AND METHODS USED

The analysis potentially covered the area of the whole country, and a reasonable scale for the data was selected. The digital Geological Map of Slovenia at a scale of 1:250,000 (Buser, 2010) in ESRI shape format was used as a basis for stratigraphic information. Lithologies of the strata and thicknesses mentioned in the text were obtained from the booklets accompanying the geological maps at a scale of 1:100,000. A digital elevation model with a cell size of 25 meters (GURS, 2005) was used for morphologic analyses, particularly for sink occurrence. The chosen DEM is the best available raw and unbiased information on Slovenia's surface, and, due to the scale and coarse positional precision of the lithologic data, a 25 m DEM was detailed enough. We are aware that more precise results could be achieved with more detailed data, but for the purpose of the project, the chosen scale and resolution were satisfactory. Drainage network data at a scale at 1:50,000 were obtained from the Environmental Agency (ARSO, 2005) and used to assess the abundance of surface water flows. A highly detailed catalog of cave entrance was collected by the Speleological Association of Slovenia (JZS, 2010). All analyses were conducted with ESRI ArcGIS software.

The approach we chose was based on surface karst features. Because of the resolution and other limitations in the input datasets, a combination of three factors, cave, sink, and drainage-network densities, was chosen as a measure of karstification intensity. The method presented in this paper is obviously applicable only for the assessment of hypergenic karst, while for the purpose of assessment of hypogenic karst its use is very limited.

Before the analyses, all areas selected for the study were classified by an experienced hydrogeologist with long-term experience in karst hydrology as at least potentially karstified areas. The analysis covered the area of the whole country, and a reasonable scale for the data was selected.

Prior to analyses performed in GIS on a 25 m cell basis, data used in the analyses had to be selected. Given the fact that karst can only develop on soluble rocks (Monroe, 1970), stratigraphic formations were used as the basis for the analysis. For this purpose we extracted from the Geological

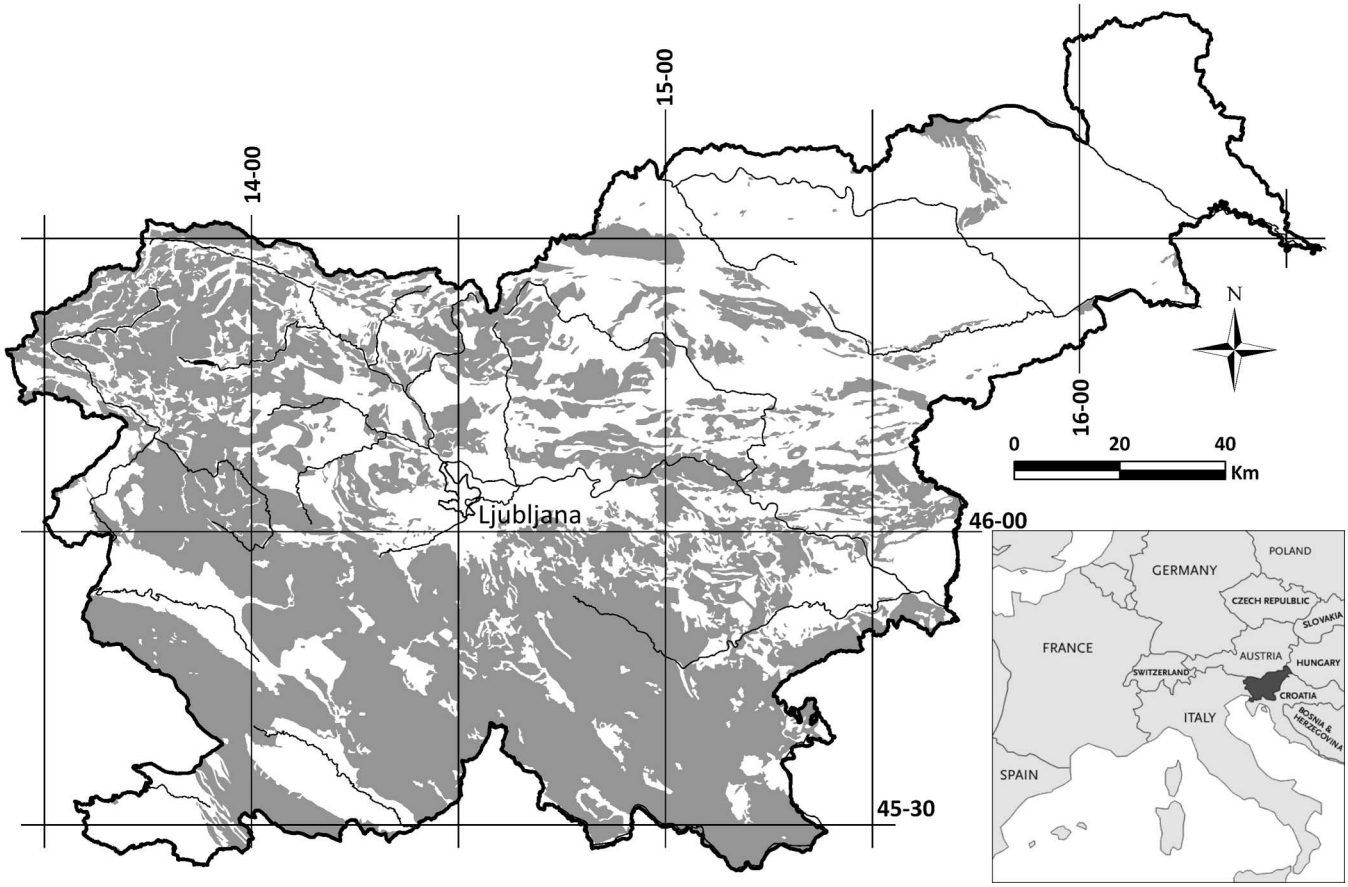

Figure 2. Map of Slovenia with outcrops of selected units shown in gray. Location of Slovenia in Europe is shown in the lower right.

map of Slovenia all stratigraphic formations containing the words limestone, calcite, or dolomite in their lithologic descriptions to get a subgroup of units (and hence outcrop areas) that could be potential carbonate-karst areas. Out of 114 units, 47 were selected, represented by 2048 polygons covering 44.7% of Slovenia. Purely non-carbonate units were ignored in our study, though several of the selected units contain both carbonate and non-carbonate rocks, mainly clastic rocks. We expected that this simple selection would include some formations that are less susceptible to karstification, as not all were pure carbonates. In fact, in some formations, carbonates are a minor lithology or only occur in small areas and limited thickness, and those may not host frequent or well-developed karst features. In Slovenia, dolomites, which are by definition pure carbonates, are generally not karstified, but rather form fractured aquifers with completely different hydrogeological characteristics than limestone areas. We acknowledge these potential sources of error and also point out that, given the coarse spatial resolution of the DEM and generalization of the stratigraphic map, some small areas of carbonates that do have karst development may not be represented in our analysis. Karst fields (poljes) were not included in this selection since they are stratigraphically classified as Quaternary sediments. Stratigraphic units were classified as one of four lithologic classes, clastic rocks, dolomites, limestones, and mixed limestones and dolomites.

The chosen DEM is the best available raw and unbiased information on Slovenia's surface, and, due to the scale and coarse positional precision of the lithologic data, a 25 m DEM was detailed enough. We are aware that more precise results could be achieved with more detailed data, but for the purpose of the project, the chosen scale and resolution were satisfactory.

The occurrence of sinks indicates the presence of karst processes. Numbers of sinkholes were derived for the whole study area from the 25 m DEM using the Sink function in ArcMap software. Obviously not all features derived were karst sinks, because a proportion of them (and the most obvious ones) occurred in flat alluvial basins or in the vicinity of rivers. After a field-check at representative locations, we decided to exclude, in addition to non-carbonate outcrops, areas on alluvial plains within a 75 m (3 cells) buffer zone near rivers. Our fieldwork experience has shown that in the vicinity of rivers no sinks occur, and those derived there from a DEM are artifacts, most probably related to small relic channels or ditches. The buffer zone width was defined by trial, because in many areas—mainly valleys—the alluvial sediments are shown disproportionally narrow

due to the scale of the geological map and their being of less importance on the geological map than bedrock, especially because there is no surface water flow in valleys in karst areas. Altogether there were 129,485 accepted sink occurrences in the analyzed areas. Density varied from 0 to 43.7 sinks/km^2, with a mean of 10.6 sinks/km^2 and a standard deviation of 11.2. We acknowledge that due to the automatic derivation of the sink data some bias in the form of spurious sinks still exists, especially in flat terrain where alluvial sediments partially composed of carbonate rocks were included in the analysis. Hence the sink-index values of these lithologic units need to be interpreted with caution.

The occurrence of caves is obviously the most definitive proof that an area can be classified as karst. At the same time, the cave data may be biased, since the data were collected by incidental discoveries and generally not by a systematic search of the terrain. Despite its limitations, the cave catalog is the only available resource of this type covering all of Slovenia that could be used in GIS analysis, so it was used as one of the bases for the evaluation of karstification intensity. The cave catalog includes records of entrances to various types and stages of karst caves, fully developed horizontal or sub-horizontal caves, vertical caves, inactive caves, freezing or ice caves, and rock-shelters. The information regarding cave occurrence was the only data set that was used in a raw form for the analyses. There were 7554 cave entrances mapped in the study area. Cave density values varied from 0 to 2.1 caves/km^2, with a mean of 0.6 cave/km^2 and a standard deviation of 0.5.

The absence of a surface drainage network on a given formation can also indicate the presence of karst areas where subsurface drainage is predominant. To avoid losing the information on the surface drainage network density when performing raster-based analyses, we calculated the density of the drainage network by simply dividing the total length of this network by the area of a given stratigraphic unit's outcrop. The total length of surface drainage network with flowing water in the analysis area was 6082.3 km. The surficial drainage network density was expressed in km/km^2, and values varied from 0 to 2.5 km/km^2, with a mean of 0.95 km/km^2 and a standard deviation of 0.75. Our approach was based on the assumption that lower drainage network densities imply higher karstification intensities.

Table 1 shows the extent of the studied features within each stratigraphic outcrop that was included, as well as its area. The average densities of features in the overall area was 0.83 caves per km^2, 14.3 sinks per km^2, and 0.67 km of surface drainage network per km^2.

For a quantitative assessment of the importance of the presence of caves or sinks and the absence of surface drainage in each stratigraphic unit, a non-parametric chi-squared (X^2) was computed as $(O-E)^2/E$ for each of the observed quantities, where O was the observed quantity and E was the expected value of that quantity in the area of the particular unit based on the average over all units. From this, an index was computed by negating the X^2 value if ($O - E$) was negative in the cases of numbers of caves and sinks and if it was positive in the case of drainage networks. (A more extensive drainage network implies less karstification.) Hence in all cases, a negative index indicates that the unit appears less karstified than average based on that particular quantity, and a positive index indicates that the unit appears more karstified. The resulting cave indexes (CI), sink indexes (SI), and surface drainage network indexes (SDNI) are listed in Table 2 and displayed in Figure 3.

For each feature index in each stratigraphic unit, a normalized value was computed. For example, $CI_{norm} = (CI - CI_{min})/(CI_{max} - CI_{min})$, where CI_{max} and CI_{min} are the maximum and minimum values of CI observed for any unit. Normalized values for SI and SDNI were computed similarly, and the three normalized values for each unit were averaged to give a single average of normalized indexes (ANI). The ANIs are also listed in Table 2.

All correlation tests were performed using Pearson product-moment correlation coefficient (r) formula, and values represent linear correlation coefficients.

RESULTS AND DISCUSSION

GENERAL RESULTS

Chi-square analyses showed that the three phenomena we expected to be related to karst areas were the correct choice. For all tests the degrees of freedom (df) was 46. In the case of cave occurrence, X^2 had the score of 3975.7 and the p-value < 0.001; in the case of sink occurrence, X^2 had the score of 74070.2 and the p-value < 0.001; and in the case of density of surficial drainage network, X^2 had the score of 4795.9 and the p-value < 0.001.

For each stratigraphic unit, the number of indexes that were greater than 0 (IIC) is shown in Table 2. An indication of karstification intensity, we presumed that units with IIC ≥ 2 are intensely karstified, and that other units are less karstified. In most cases, the intensely karstified areas have ANIs that exceed those of the areas less karstified. A threshold of ANI ≥ 0.4344 coincides rather well with the simplified threshold of at least two positive indexes, except for the units 13 and 48, which have ANI values above that threshold but have only one positive index. The high value of ANI (0.602) for unit 13 is the consequence of very high SI value, while the other two indexes are negative. Despite the fact that in the area of unit 13 the number of sinks is high, the other two indexes indicate that the unit should be classified among the less karstified areas. The reason for a high SI value is probably a combination of errors of the automatically derived sink data and of the fact that parts of the exposure of unit 13 with widely differing intensities of karstification were not separated on the geological map. Unit 48 is a very heterogeneous formation, composed of limestones, marls, and coal and bauxite beds that has, like unit 13, some intensely karstified areas, while in general, the karstification is very limited due to its composition. So

Table 1. Amounts of inventoried features in each stratigraphic unit and their areas. SDN is length of surface drainage network.

No.[a]	Caves	Sinks	SDN, km	Area, km^2
13	24	6627	162.3	151.6
27	6	450	290.5	206.9
29	19	912	155.3	171.0
34	0	37	22.3	9.9
42	10	166	60.2	30.4
45	4	45	1.7	1.9
46	181	2544	72.8	188.0
48	92	1585	28.3	112.0
50	2	22	2.6	8.9
52	26	405	66.7	70.4
53	24	225	81.8	81.6
54	186	1793	18.2	104.6
55	8	208	0.0	9.4
56	9	100	84.6	58.7
57	1116	11886	66.9	584.3
58	4	294	0.0	17.6
59	1463	28334	107.5	1097.5
61	543	10614	26.2	334.5
63	13	67	62.8	34.2
64	277	7182	22.1	277.4
65	74	4060	20.1	123.5
66	195	8099	16.7	281.4
67	111	4349	31.0	177.6
68	15	34	16.6	23.6
70	3	41	18.3	9.6
71	333	8200	38.0	333.0
72	324	7750	85.0	390.3
73	3	34	96.4	41.4
74	4	292	2.8	15.1
75	4	69	5.7	15.2
76	1504	6617	386.1	914.3
77	283	11177	1133.2	1096.8
78	20	131	239.0	150.1
80	32	447	291.5	180.6
81	1	36	38.5	25.7
82	0	1	7.7	6.6
83	2	27	102.9	41.9
84	387	2247	643.3	641.1
85	30	28	54.3	45.5
86	11	479	110.4	112.7
87	32	290	30.7	48.8
91	67	505	458.3	325.1
92	85	996	806.7	445.9
93	13	50	87.7	44.7
96	0	7	2.7	1.1
97	11	23	20.5	19.2
102	3	0	5.7	5.1
Σ	7554	129485	6082.3	9066.7

[a] Lithological description of units/formations is given in the second column in Table 2.

despite the relatively large values of ANI, the IIC test places both units in the less karstified class.

Analyses of the correlation values (r) between the three sets of indexes show that the connection between cave occurrence and sink occurrence is not very strong (0.26), while the correlation between the absence of surficial drainage network and cave (0.58) or sink (0.66) occurrence is stronger. The weaker correlation value of the cave occurrence could be explained with the fact that caves were not systematically mapped, but were registered by pure chance, and that most probably, there are still some caves to be discovered. Also, the cave data only record entrances and do not reflect the size of the caves. Correlations between the types of indexes might imply that they are not independent; this is in fact expected for hypergenic karst. Although the relations between the studied features may not apply outside the study area, for Slovenia the correlation between the absence of surface drainage network and sink or cave occurrence is a fact that was also checked and proved in the field.

Caves are absent (density = 0.0 km^{-2}) in three units (34, 82, 96), sinks in one (102), and surficial drainage network in two (55, 58). The highest density of caves (2.1 km^{-2}) was found in unit 45, the highest density of sinks (43.7 km^{-2}) in unit 13, and the highest density of surface drainage network (2.45 km/km^2) in unit 83. Results for the different types of index values can be discussed in more detail with reference to Table 2 and Figure 3 and additional information, not shown, about the lithology of the stratigraphic units.

The composition of units with highly positive value of the cave index (54, 57, 59, 61, 71, and 76) indicate that these units are either composed of 200 to 1500 m of relatively pure $CaCO_3$ (units 54, 57, 76), or are composed of $CaCO_3$ and limited impurities, mainly bituminous dolomite (units 59, 61, 71). For units where the other two indexes, SI and SDNI, were negative, low CI values correspond well to the low karstification intensity. When the other two indexes are positive, negative CI values, which from the cave-occurrence perspective indicate less karstified areas, are probably result of random and sporadic cave discovery. In the case of homogeneous carbonate lithologic units, it would be expected that even one cave occurrence would indicate well-developed karst, so that the unit should be classified as intensely karstified. Since almost all lithologic units used in this study were not pure carbonates but rather heterogeneous formations of clastic rocks and carbonates, the assumption that one cave in the stratigraphc unit proves that the whole area of that outcrop is intensely karstified is oversimplified and could be wrong. Even in hypergenic karst, basing the distinction between intensely and less karstified areas strictly on the basis of CI values alone could be misleading because of overlooked caves. This is why supplementary indexes of sinks and surface drainage have been used.

Sink index values for stratigraphic units are in general agreement with their classification according to karstification intensity, except in the case of the Triassic Dachstein limestone (76). Extremely low SI value in the Dachstein limestone

Table 2. Short statement of the lithology of each stratigraphic unit, and results of the statistical analysis of the data in Table 1. CI, cave index; SI, sink index; SDNI, surface drainage network index; ANI, average normalized index; IIC, number of indexes that are greater than 0, indicating proneness to karstification; LC, lithological class of the unit (C = clastic rocks; D = dolomite; L = limestone; LD = mixed limestone and dolomite). Table is sorted first by increasing IIC and then by increasing ANI.

No.	Lithological unit (formation) description	CI	SI	SDNI	ANI	IIC	LC
92	Dolomite, micaceous siltstone, sandstone, claystone, oolitic limestone and dolomite, marlstone, marly limestone (Lower Triassic)	−220.9	−4531.4	−861.6	0.0720	0	C
77	Thick-bedded Main Dolomite (Upper Triassic - Norian-Rhaetian)	−435.4	−1284.9	−214.7	0.2390	0	D
91	Thick-bedded and massive dolomite, subordinately limestone (Middle Triassic - Anisian)	−153.4	−3687.6	−264.6	0.2505	0	D
84	Massive coarse-crystalline dolomite and limestone (Upper Triassic - Rhaetian)	−40.5	−5213.9	−105.7	0.2856	0	D
27	Lithothamnium limestone, marly limestone and marl (Middle Miocene - Badenian)	−160.6	−2123.0	−165.8	0.3059	0	C
80	Marly limestone, marlstone, dolomite, shale (Upper Triassic - Carnian)	−93.3	−1762.9	−239.4	0.3141	0	C
78	Platy Bača Dolomite with chert (Upper Triassic - Norian-Rhaetian)	−88.2	−1889.2	−190.1	0.3245	0	D
83	Alternation of claystone and sandstone, platy limestone in the upper part - Amphiclina beds (Upper Triassic - Carnian)	−31.1	−546.2	−198.7	0.3667	0	C
73	Platy micritic limestone and calcarenite with chert (Lias)	−28.7	−525.0	−169.6	0.3747	0	L
29	Lithothamnium limestone (Middle Miocene - Badenian)	−107.0	−959.3	−14.3	0.3815	0	L
93	Thick-bedded dolomite, subordinately limestone (Upper Permian)	−15.8	−542.8	−110.9	0.3918	0	D
86	Massive dolomite, subordinately limestone (Middle and Upper Triassic - Anisian-Norian)	−73.2	−794.4	−16.0	0.3937	0	D
56	Platy limestone with chert in alternation with red marlstone - Krško beds (Upper Cretaceous - Upper Cenomanian-Turonian)	−32.6	−650.7	−51.8	0.3991	0	C
53	Platy Volče limestone with chert, red marly limestone and marlstone (Upper Cretaceous - Coniacian-Campanian)	−28.5	−759.4	−13.3	0.4070	0	C
63	Platy Biancone limestone with chert (Upper Jurassic-Lower Cretaceous - Tithonian-Berriasian)	−8.4	−362.9	−69.5	0.4075	0	L
42	Limestone-dolomite conglomerate - Škofja Loka and Okonina Conglomerate (Middle Oligocene - Rupelian)	−9.3	−165.6	−77.7	0.4096	0	C
81	Platy limestone and dolomite with chert. marlstone. marly limestone - Tamar Formation (Upper Triassic - Carnian)	−19.4	−298.0	−26.3	0.4163	0	C
85	Massive Wetterstein Limestone and dolomite. thick-bedded limestone (Middle and Upper Triassic - Ladinian-Cordevol)	−1.7	−595.6	−18.5	0.4164	0	LD
52	Coarse-grained limestone breccia with intercalations of flysch (Upper Cretaceous - Maastrichtian)	−18.2	−358.3	−8.0	0.4197	0	C
34	Lithothamnium-Lepidocyclina limestone, sand, silt and clay (Lower Miocene - Ottnangian-Eggenburgian)	−8.2	−76.4	−37.0	0.4215	0	C
70	Massive crinoidal and oolitic limestone (Lias. Dogger)	−3.2	−67.9	−21.6	0.4267	0	L
97	Light-gray to red limestone - Dovžanova soteska and Trogkofel Formations (Lower Permian)	−1.5	−229.6	−4.5	0.4277	0	L
68	Reddish and greyish nodular limestone of Ammonitico Rosso type limestone breccias, marlstone and claystone (Upper and Lower Jurassic)	−1.1	−273.1	0.0	0.4280	0	C
82	Chert, platy limestone, claystone and siltstone - Kobla Formation (Upper Triassic - Carnian)	−5.5	−92.9	−2.4	0.4301	0	C

Table 2. Continued.

No.	Lithological unit (formation) description	CI	SI	SDNI	ANI	IIC	LC
102	Thick-bedded limestone in the lower part, reef limestone in the middle part, thick-bedded micritic limestone in the upper part (Devonian)	−0.4	−72.7	−1.5	0.4321	0	L
96	Neoschwagerina reef limestone, limestone breccia (Middle Permian)	−0.9	−4.8	−5.2	0.4326	0	L
87	Platy micritic limestone with chert nodules - Pokljuka Formation (Middle and Upper Triassic)	−1.8	−237.3	0.1	0.4286	1	L
75	Reef limestone with corals (Upper Triassic - Rhaetian)	−5.9	−100.9	2.0	0.4309	1	L
50	Reddish and gray marly limestone and marlstone (Turonian-Campanian)	−4.0	−87.3	1.9	0.4317	1	C
48	Thick-bedded micritic limestone - Vreme and Kozina beds (Lower Paleocene - Upper Cretaceous - Danian-Maastrichtian)	0.0	−0.1	29.2	0.4411	1	L
13	Coherent fluvial deposits; terraces (limestone conglomerate with gravel intercalations) (Quaternar)	−82.9	9195.7	−36.1	0.6020	1	C
74	Limestone, dolomite and limestone-dolomite breccia (Upper Triassic and Lower Jurassic (Rhaetian and Lias))	−5.9	26.9	5.3	0.4344	2	LD
58	Platy limestone with chert - Komen beds (Upper Cretaceous - Upper Cenomanian-Turonian)	−7.7	7.4	11.8	0.4351	2	L
45	Alveolina-nummulites limestone (Middle Eocene)	3.8	12.4	−0.2	0.4354	2	L
46	Alveolina-nummulites and miliolida limestone (Lower Eocene)	3.8	−7.4	22.5	0.4404	2	L
67	Reef limestone with corals, hydrozoans and sponges (Lower part of Upper Jurassic - Lower Kimeridgian-Oxfordian)	−9.3	1294.2	65.2	0.4752	2	L
72	Micritic and oolitic limestone, limestone breccia and bituminous dolomite (Lower and Middle Lias)	0.0	849.8	119.4	0.4810	2	LD
65	Oolitic and micritic limestone (Upper part of Upper Jurassic - Upper Kimeridgian-Tithonian)	−8.1	2986.7	47.5	0.5078	2	L
66	Thick-bedded micritic and oolitic limestone (Lower part of Upper Jurassic - Lower Kimeridgian-Oxfordian)	−6.6	4142.5	156.9	0.5592	2	L
76	Thick-bedded Dachstein Limestone with transitions to dolomite (Upper Triassic - Norian-Rhaetian)	723.1	−3177.2	84.2	0.5787	2	L
55	Platy limestone with chert - Dutovlje Formation (Upper Cretaceous - Campanian)	0.0	40.8	6.3	0.4365	3	L
54	Rudist limestone and calcarenite - Lipica Formation (Upper Cretaceous - Coniacian-Campanian)	112.2	60.1	38.5	0.4746	3	L
64	Alternation of dolomite and limestone (Upper part of Upper Jurassic - Upper Kimeridgian-Tithonian)	9.1	2617.2	144.5	0.5275	3	LD
71	Micritic and oolitic limestone, bituminous dolomite (Upper Lias-Dogger)	11.1	2495.1	153.9	0.5277	3	LD
61	Alternation of limestone and dolomite (lower part). micritic limestone (upper part) (Lower Cretaceous - Berriasian-Barremian)	250.7	7132.8	175.0	0.6968	3	LD
57	Rudist and micritic limestone - Sežana Formation (Upper Cretaceous - Turonian)	813.3	1503.3	269.5	0.7480	3	L
59	Thick-bedded micritic limestone and bituminous dolomite (Lower Cretaceous and lower part of Upper Cretaceous)	329.2	10226.7	536.8	0.8708	3	LD

could be explained by the fact that the average slope angle of this unit is 26.4°, while average slope angles of other intensive karst areas are below 13°. For the intensely karstified outcrops analyzed in this paper, the correlation between the number of sinks in a given slope angle class and the area of the same slope angle classes was 0.79. The distribution of the slope angle classes' areas correlates well with the distribution of sinks; hence this dependence can be used to test the correlation between slope angle and sink distribution. Correlation test of the later showed that at higher slopes the

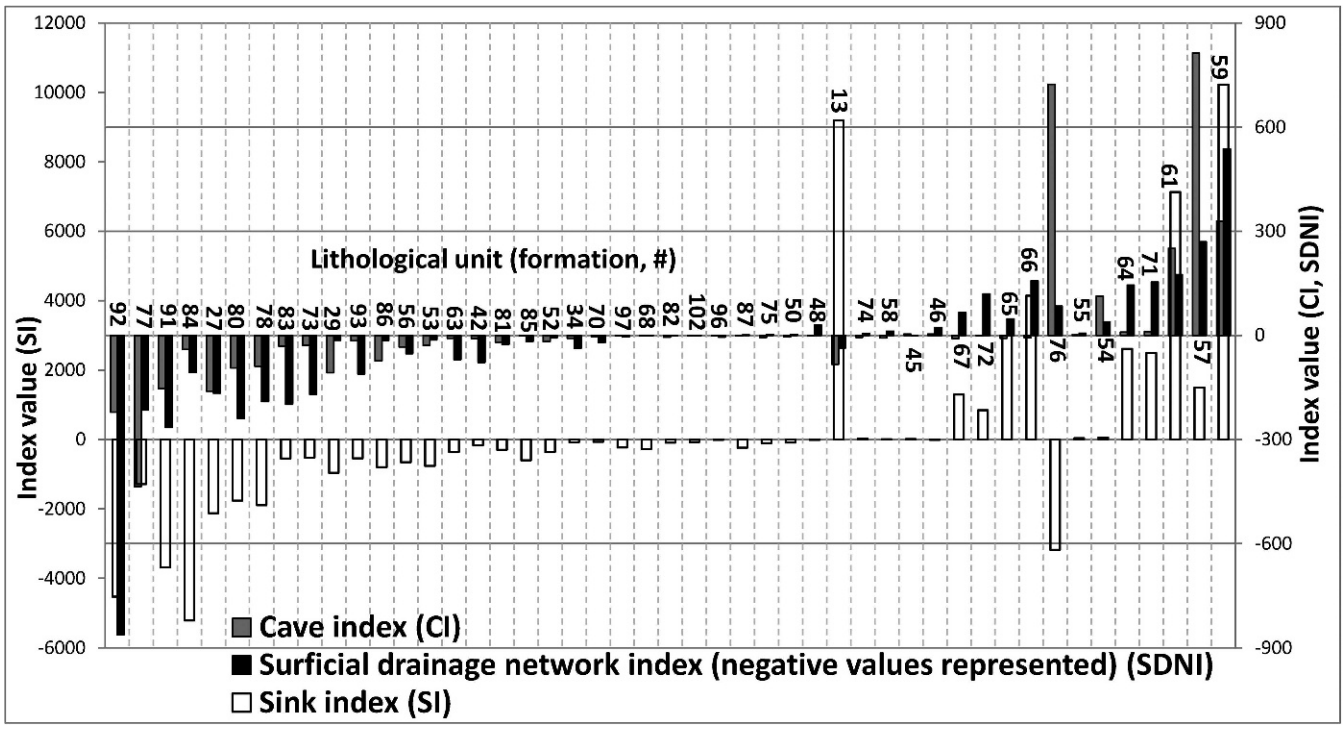

Figure 3. Cave, sink, and surface drainage network density index values, computed as described in the text, for each stratigraphic unit included in the analyses. Units are arranged from left according to increasing average normalized index (ANI; see text). Units determined to be intensely karstified are to the right of conspicuous unit 13.

occurrence of sinks is lower and the correlation between sink occurrence distribution and slope angle distribution was −0.797. This agrees with Gams (2003, p. 170), who claims that the occurrence of sinks has a negative correlation with slope angle. In addition to its greater slopes, unit 76 is located at relatively high elevation, an average of 1200 m, while the average elevation of all the other intensely karstified units is 708 m. The steeper slopes that result in higher surface runoff, extreme conditions of precipitation, winds, and temperature variations, and the absence of vegetation cover at high elevations could hinder the development of sinks.

High surface drainage network values, corresponding to small amounts of surface drainage, agree well with the selection of highly karstified units. As expected from field observations, high SDNI values are related to two lithological classes, limestones and mixed limestone and dolomite. The reason is rather trivial; units classified as limestones or limestones and dolomites have little or no soil cover that would, to some extent, prevent vertical percolation of water through small cracks and fractures to the subsurface. Where considerable surface drainage flow is present, there are usually fluvial sediments, and on the geological map such areas are labeled as Quaternary alluvial sediments.

Table 3 shows some of the data in Tables 1 and 2 averaged over the stratigraphic units, both as divided into less karstified units and intensely karstified units and as divided into the lithological classes clastic, dolomite, limestone, and mixed limestone and dolomite. Index and density values clearly show the distinction between classes that have higher (limestone and mixed limestone and dolomites) and lower (clastics and dolomites) karstification intensities. Nevertheless, the comparison of lithologic class with karstification intensity shows that not all limestones, and to a lesser extent, not all mixed limestones and dolomites, can be simply classified as intensely karstified areas. The differentiation is clearly visible in a three-dimensional plot where axes are CI, SI, and SDNI values (Fig. 4). The low average normalized indexes of nine units classified as limestone and one unit classified as limestones and dolomites that are exceptions (see Table 2) could be due to thin (5 to 10 cm) bedding with total thicknesses of several meters up to only 30 meters (unit 63), to high content of intercalations in limestone such as quartzite pebbles, marls, cherts, and sandstones (units 29, 73, 96), siltstones and sandstones (unit 97), or siltstones and marls (unit 102), or to very steep average slopes above 20° (units 70, 75, 85, 87). The last possibility is supported by the fact that the correlation of sink density with slope angle for limestone and mixed limestone and dolomite, among units with at least one positive index, is −0.797. The effect of the slopes of those limestone and mixed carbonate units in which the actual sink occurrence is much lower than expected (63, 70, 75, 85, and 87), is probably exaggerated by the fact that these units cover small areas where a low number of caves have been discovered, and result in low ANI values. Based on results of sink distribution analyses within slope ranges, critical

Table 3. Average values of indexes (CI, cave index; SI, sink index; SDNI, surface drainage network index), the average normalized index (ANI), and other parameters over the stratigraphic units by lithological class (C = clastic rocks; D = dolomite; L = limestone; LD = mixed limestone and dolomite) and by degree of karstification (LKA, less karstified area; IKA, intensely karstified area).

Rock Type	CI	SI	SDNI	ANI	Elevation (m a.s.l.)	Slope angle (degrees)	Cave density (km^{-2})	Sink density (km^{-2})	SDN density (km/km^2)
C	−51.11	−180.67	−122.59	0.387	688.6	16.9	0.18	7.13	1.52
D	−134.44	−2235.46	−150.32	0.314	743.6	19.95	0.33	6.15	1.13
L	73.33	215.11	22.38	0.464	774	16.12	1.25	15.01	0.36
LD	84.66	3250.41	159.49	0.565	628.6	11.38	1.19	25.03	0.13
LKA	−54.25	−616.08	−93.28	0.533	708.8	18.8	0.06	6.25	1.26
IKA	138.67	1888.21	114.84	0.382	678.6	13.5	1.47	20.93	0.19

slope angles above which sinks are unlikely to develop at a 95% (99%) probability level, are 17° (21°) for unit 63, 15° (20°) for unit 70, 20° (22°) for unit 75, 23° (26°) for unit 85, and 19° (25°) for unit 87. In each case, the 95% slope-angle values are either somewhat lower than the average slope angles for a given unit (23.5° for unit 63, 20.1° for unit 70, 28.8° for unit 85, 20.3° for 87) or much lower than the average slope angle (32.3° for unit 75). This remains true even for the 99% threshold, except in unit 87. The distribution of sink occurrence on shallower slopes in units 63, 70, 75, 85, and 87 that have relatively high average slope angles, indicates that the sparse occurrence of sinks within these units could be related to those high average slopes.

In the intensely karstified areas, the average density of caves is about 25 times greater than in less karstified areas (Table 3).

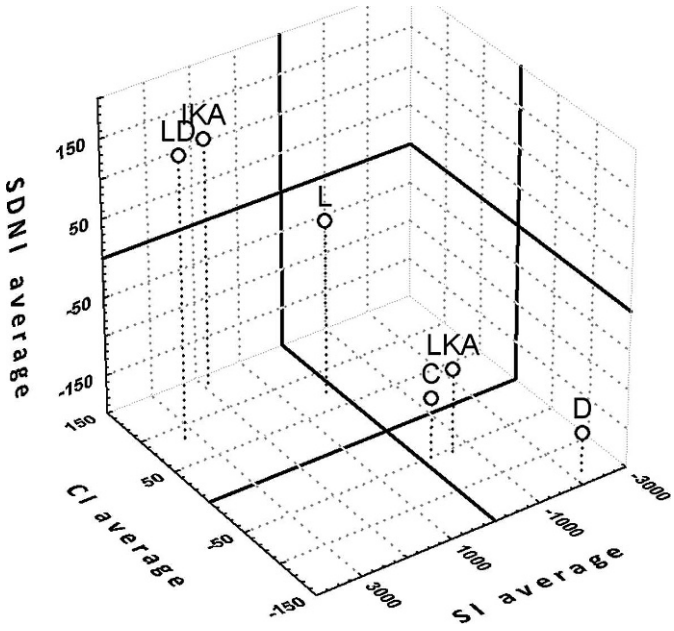

Figure 4. 3D plot of average values of the three indexes over the analyzed units sorted by lithology (C, clastic rocks; D, dolomites; L, limestones; LD, mixed limestone and dolomite) and by degree of karstification (LKA, less karstified areas; IKA, intensely karstified areas), as given in Table 3.

For sink density, the ratio between intensely and less karstified areas is greater than 3. Surface drainage network density in intensely karstified areas is almost 7 times lower than in less karstified areas.

Results of the analyses are best comprehended if displayed graphically. Figure 5 shows maps of the three feature indexes, for caves, sinks, and surface drainage network, in parts A–C, and the result of combining the data into average normalized indexes in part D. The difference between the sink index SI and the other two indexes is most obvious in the Alpine region in the northwest and the north-central Quaternary terraces. The summary Figure 5D, showing the ANI values divided into the two karstification-intensity classes, shows that 23.9% of Slovenia's area (outcrops of sixteen stratigraphic units represented by 550 polygons that cover 4850.35 km^2) can be classified as intensely karstified and 20.8% (thirty-one units represented by 1498 polygons covering 4216.36 km^2) can be classified as less karstified.

Conclusions

The results derived by GIS for Slovenia show that it is possible, using a combination of appropriate indicative features, to identify hypergenic karst areas, and to a certain extent, also assess the degree of their karstification. We've shown that useful parameters are lithology, sink and cave density, and the absence of a surficial drainage network. Among some of these parameters, we noticed some correlation. We've also shown a general negative correlation between slope angles and sink density with high reliability. Average densities of caves, sinks, and surface drainage networks in intensely karstified areas are several times higher for the first two and several times lower for the latter than in less karstified areas. The results presented show regional karstification levels can vary on a local scale in comparison to the general scale.

The map in Figure 5D provides a basis for the general assessment of groundwater vulnerability, which is especially high in the karstified areas, and for water-resource protection planning. In addition, the map could be used in preliminary studies of land-planning issues such as the siting of

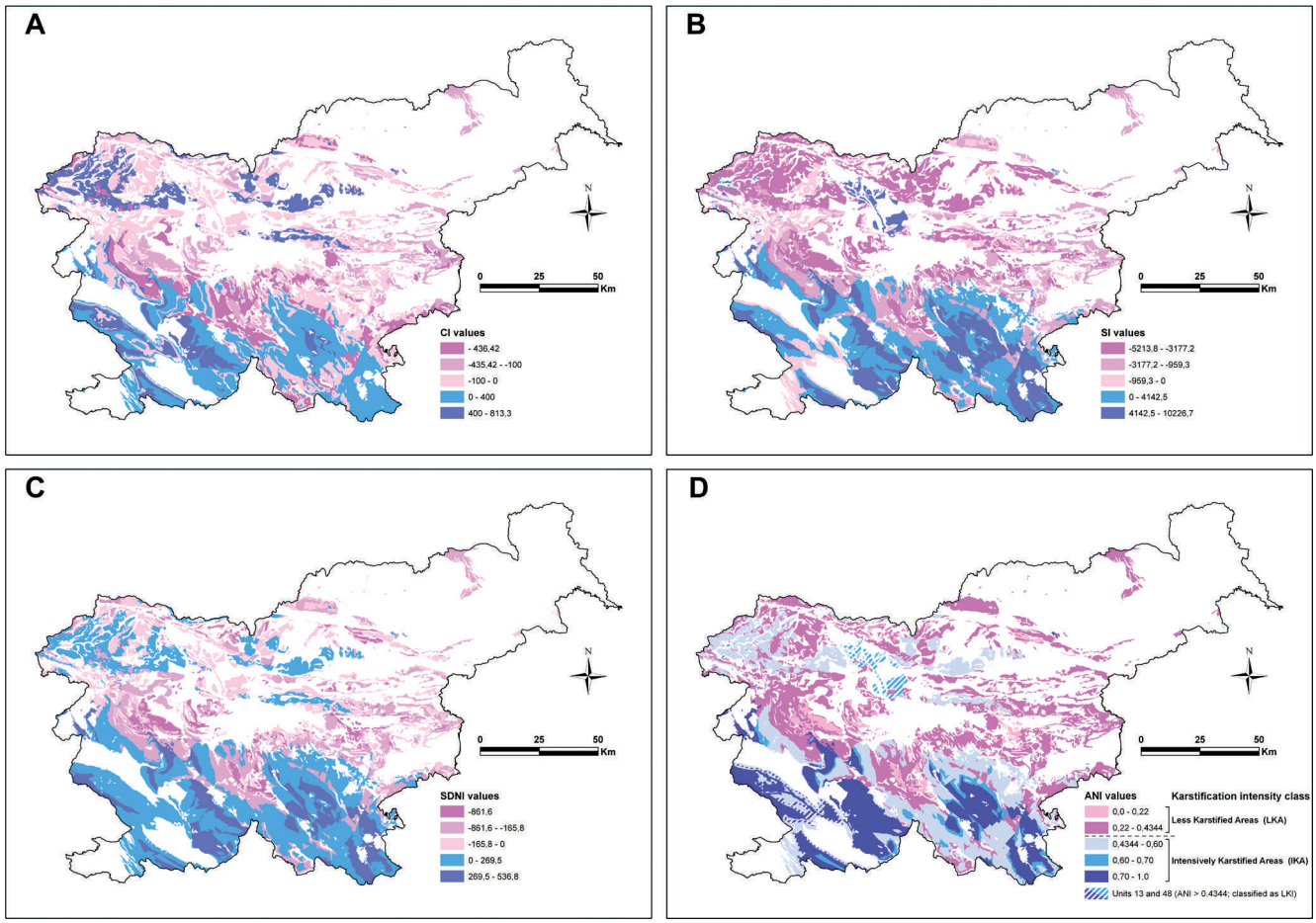

Figure 5. Maps of the analyzed areas, with colors based on A, cave index (CI); B, sink index (SI); C, surface drainage network density index (SDNI); and D, average normalized index (ANI). In D, the division between less and intensely karstified areas is shown in the key; units13 and 48 are shown hatched because they are classified as less karstified, despite their ANI values.

problematic infrastructure (landfills, industrial plants, gas stations, etc.) or for assessment of karst hazards in engineering geology. But the limitations of the presented approach need to be taken into account, including the coarse scale of the geological data, the low digital-elevation-model resolution, and problems with the automated derivation of surface karst from the DEM. The results can be used as guidance at a regional scale to prioritize areas of future more detailed assessment of local karst areas.

ACKNOWLEDGEMENTS

The authors wish to thank the Slovenian Research Agency for funding the project "A spatial model of groundwater hydrochemical composition in Slovenia in GIS environment" within which this research was performed.

REFERENCES

Armstrong, B., Chan, D., Collazos, A., and Mallams, J.L., 2003, Doline and aquifer characteristics within Hernando, Pasco, and northern Hillsborough counties: GSA Annual Meeting, Seattle, November 2–5, 2003, p. 39–51.

ARSO, 2005, European Environmental Information and Observation Network (Evropsko okoljsko informacijsko in opazovalno omrežje), Ljubljana, Environmental Agency of Republic of Slovenia: http://nfp-si.eionet.europa.eu/Dokumenti/GIS/ (accessed April 10, 2010).

Blaeu, W., and Blaeu, J., 1645, Karstia, Carniola, Histria et Windorum Marchia, *in* Theatrum Orbis Terrarum, sive Atlas Novus in quo Tabulæ et Descriptiones Omnium Regionum, Editæ a Guiljel et Ioanne Blaeu: http://www.library.ucla.edu/yrl/reference/maps/blaeu/index.htm#description (accessed August 21, 2010)

Buser, S., 2010, Geological Map of Slovenia at scale 1:250,000 (Geološka karta Slovenije 1 : 250.000): Geological Survey of Slovenia, 1 sheet.

Denizman, C., 2003, Morphometric and spatial distribution parameters of karstic depressions, lower Suwannee River basin, Florida: Journal of Cave and Karst Studies, v. 65, no. 1, p. 29–35.

Florea, L.J., 2005, Using state-wide GIS data to identify the coincidence between sinkholes and geologic structure: Journal of Cave and Karst Studies, v. 67, no. 2, p. 120–124.

Florea, L.J., Paylor, R.L., Simpson, L., and Gulley, J., 2002, Karst GIS advances in Kentucky: Journal of Cave and Karst Studies, v. 64, no. 1, p. 58–62.

Gams, I., 2003, Kras v Sloveniji v prostoru in času: Ljubljana, ZRC SAZU, 487 p.

Gao, Y., and Zhou, W., 2008, Advances and challenges of GIS and DBMS applications in karst: Environmental Geology, v. 54, p. 901–904. doi:10.1007/s00254-007-0894-4.

GURS, 2005, Digital elevation model – DMV25, 1998–2005 (DEM with resolution 25×25 m), Surveying and Mapping Authority of the Republic of Slovenia.

JZS, 2010, Catalog of caves in Slovenia: Speleological Association of Slovenia.
Komac, M., 2005, Statistics of the Geological Map of Slovenia at scale 1:250 000: Geologija, v. 48, no. 1, p. 117–126.
Monroe, W.H., 1970, A Glossary of Karst Terminology: U.S. Geological Survey, Water-Supply Paper 1899, 26 p.
Stafford, K.W., Rosales-Lagarde, L., and Boston, P.J., 2008, Castile evaporite karst potential map of the Gypsum Plain, Eddy County, New Mexico and Culberson County, Texas: A GIS methodological comparison: Journal of Cave and Karst Studies, v. 70, no. 1, p. 35–46.
Taylor, C.J., Nelson, H.L. Jr., Hileman, G., and Kaiser, W.P., 2005, Hydrogeologic-framework mapping of shallow, conduit-dominated karst—Components of a regional GIS-based approach, *in* Kuniansky, E.L., ed., U.S. Geological Survey Karst Interest Group Proceedings. Rapid City, South Dakota, September 12–15, 2005, U.S. Geological Survey, Scientific Investigations Report 2005-5160, p. 103–113.
Valvasor, J.V., 1977, Slava vojvodine Kranjske: Ljubljana, Mladinska knjiga, 365 p.
Veni, G., 2002, Revising the karst map of the United States: Journal of Cave and Karst Studies, v. 64, no. 1, p. 45–50.

A.S. Hsiou, P.V. de Oliveira, C.L. Ximenes, and M.S.S. Viana – Lizards and snakes (Lepidosauria, Squamata) from the late Quaternary of the state of Ceará in northeastern Brazil. *Journal of Cave and Karst Studies,* v. 74, no. 3, p. 262–270. DOI: 10.4311/2011PA0239

LIZARDS AND SNAKES (LEPIDOSAURIA, SQUAMATA) FROM THE LATE QUATERNARY OF THE STATE OF CEARÁ IN NORTHEASTERN BRAZIL

Annie Schmaltz Hsiou[1], Paulo Victor de Oliveira[2], Celso Lira Ximenes[3], and Maria Somália Sales Viana[4]

Abstract: We present the first formal report on the squamate assemblage from Parque Nacional de Ubajara. This park contains the most important cave complex in the state of Ceará in northeastern Brazil, called Província Espeleológica de Ubajara. The material comes from the Urso Fóssil cave at Pendurado Hill. All previously reported fossil remains found in this cave are tentatively attributed to the Quaternary (late Pleistocene-early Holocene). Probably only *Arctotherium brasiliense* represents a relictual fossil bear from the late Pleistocene megafauna. The taxa recognized in this paper belong to *Tropidurus* sp., *Ameiva* sp., cf. *Epicrates*, and cf. *Crotalus durissus*, adding to the knowledge of the Brazilian Quaternary squamate fauna as a whole, and contribute to a major taxonomic refinement of the squamate assemblages from the early Holocene of northeastern Brazil.

Introduction

The Brazilian Quaternary record of Squamata (i.e, lizards, amphisbaenians, and snakes) has been documented mainly in the southeast and northeast regions, with several taxa correlated to the current Brazilian herpetofauna (Camolez and Zaher, 2010; Hsiou, 2010). Many records, however, have not been formally studied and described (Lund, 1840; Paula-Couto, 1978; Lino et al., 1979; Barros-Barreto et al., 1982; Guérin, 1991; Guérin et al., 1993; Faure et al., 1999) and their taxonomic and systematic status remains unclear.

Some of the most diverse squamate faunas from the late Pleistocene–Holocene of Brazil were recently studied. The fossils were collected in caves and rock shelters in the states of Bahia (northeastern Brazil), Goiás, Mato Grosso (midwestern Brazil), Minas Gerais, and São Paulo (southeastern Brazil; Camolez and Zaher, 2010). A large number of lizards (Tropiduridae, Leiosauridae, Polychrotidae, Teiidae, and Anguidae), snakes (Boidae, Colubridae, Viperidae, and Elapidae) and amphisbaenians (Amphisbaenidae) were described, and the majority of fossils were attributed to extant neotropical species (Camolez and Zaher, 2010). All fossils were identified based on osteological comparison with extant species. However, there is only a single record of snakes (Viperidae) from the late Pleistocene of southwestern Brazilian Amazonia (Hsiou and Albino, 2011). Beyond these records, some extinct species including two amphisbaenians, *Amphisbaena braestrupi* and *A. laurenti,* were reported from the late Pleistocene–Holocene of Lagoa Santa region, Minas Gerais State (Gans and Montero, 1998), as was the extinct teiid lizard *Tupinambis uruguaianensis*, from the late Pleistocene of the Touro Passo Formation, Rio Grande do Sul State, southern Brazil (Hsiou, 2007).

Recent fieldwork was undertaken at Parque Nacional de Ubajara, where the most important cave complex in the state of Ceará in northeastern Brazil is located, part of a notable karstic system (Oliveira, 2010). Small mammals, such as bats, rodents, and marsupials (Ximenes and Machado, 2004), were among the taxa recorded. Other records include artiodactyls (deer and peccaries), perissodactyls (tapirs), xenarthrans (armadillos), and felids (Ximenes and Machado, 2004; Oliveira, 2010), as well as a single member of the late Pleistocene megafauna, the fossil bear *Arctotherium brasiliense* (Trajano and Ferrarezzi, 1995). Other records are from deposits in *tanques* (natural depressions formed in granitic rocks that accumulate sediments and fossils), such as undetermined remains of lizards and snakes reported by Paula-Couto (1980) as being recorded from Pleistocene deposits of the Itapipoca region.

Recently, Hsiou et al. (2009) briefly reported on some snake vertebrae of the families 'Colubridae' and Viperidae from the late Quaternary in Província Espeleológica de Ubajara. Their report did not contain stratigraphic data (see also Trajano and Ferrarezzi, 1995; Ximenes and Machado, 2004) or radiometric (geochronologic) control. Here we describe new material from the early Holocene in the state of Ceará in Brazil based on the most recent

[1] Departamento de Biologia, FFCLRP, Universidade de São Paulo; Av. Bandeirantes 3900, Ribeirão Preto-SP, Brazil. *anniehsiou@ffclrp.usp.br*

[2] Programa de Pós-Graduação em Geociências/CNPq, Departamento de Geologia, Centro de Tecnologia e Geociências da Universidade Federal de Pernambuco (UFPE); Av. Acadêmico Hélio Ramos, s/n°- Cidade Universitária, CEP 50740-530, Recife-PE, Brasil. *victoroliveira.paleonto@gmail.com*

[3] Museu de Pré-História de Itapipoca (MUPHI); Avenida Anastácio Braga, 349, 62500-000, Itapipoca- CE, Brasil. *clx.ximenes@gmail.com*

[4] Laboratório de Paleontologia, Museu Dom José, Universidade Estadual Vale do Acaraú (UVA); Av. Dom José, 878, CEP 62010-190, Sobral-CE, Brasil. *somalia_viana@hotmail.com*

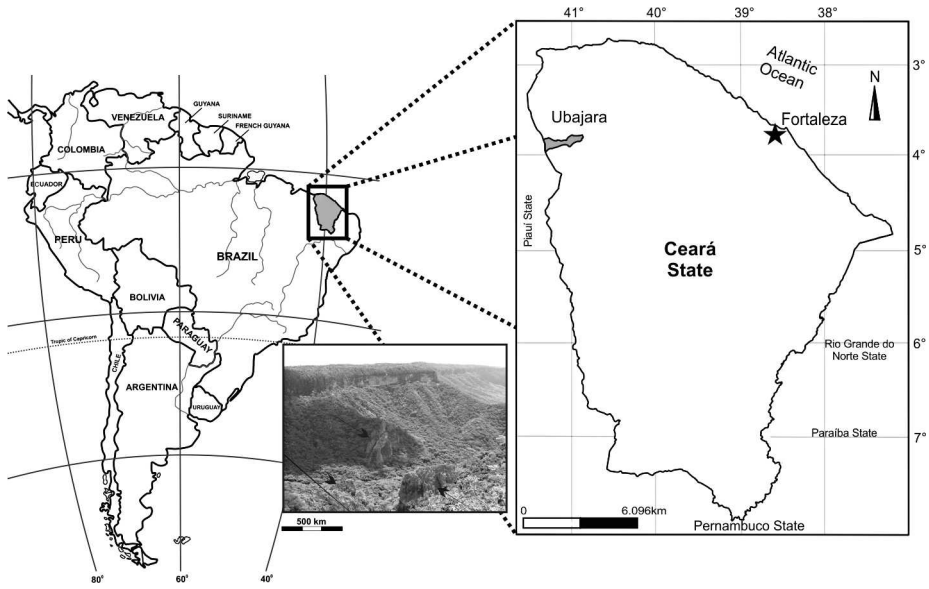

Figure 1. Location map of late Quaternary of Província Espeleológica de Ubajara, Ceará State, Brazil.

fieldwork done in the Ubajara region, during July 2009, with precise stratigraphic and radiometric control.

Location And Geological Setting

The Parque Nacional de Ubajara is located in Ubajara Municipality (Fig. 1), in Ibiapaba Cuesta in the northwestern portion of the state of Ceará (northeastern Brazil), which possesses a notable karst system. The speleological province of the Ubajara region consists of nine limestone hills with fourteen known caves (IBAMA, 2002). The limestone rock cropping out in the region corresponds to the Frecheirinha Formation of the Ubajara Group, Neoproterozoic of the Ubajara Graben (Quadros, 1996; CPRM, 2003). The Ubajara Group has an unconformable contact with the rocks of the Serra Grande Group, Silurian-Devonian of the Parnaíba Basin (Nascimento et al., 1981). Among the limestone hills in the studied area, the Pendurado Hill includes two important fossiliferous caves: Urso Fóssil and Pendurado.

All fossil remains are attributed to the Quaternary (late Pleistocene-early Holocene), however, the fossil bear *Arctotherium brasiliense* is probably the only relict in this fauna of the Pleistocene megafauna (Trajano and Ferrarezzi, 1995), found at Urso Fóssil cave (03°49′58″S, 40°53′34.4″W). The material studied was found in one room of this cave, called Sala de Entrada. A controlled stratigraphic excavation in this room exposed three layers of sedimentary deposits, and all fossil remains belong to the early Holocene. A geological section provided information about unconsolidated accumulations of allochthonous (biogenic and siliciclastic from outside the cave) and autochthonous (generated inside the cave) material. The stratigraphic layers include sediments from the bottom to top (Fig. 2):

Layer 1 has a thickness of 0.20 m and is comprised of carbonaceous silt-clay sediments, containing smaller autochthonous fragments of limestone and large, angular fragments of speleothems. In this layer, there are shells of freshwater clams and several carbonized bone fragments. As in layer 2, a sample was collected for thermoluminescence dating; more details can be found in Oliveira et al. (in press). Remains of squamate reptiles and mammals such as Didelphimorphia, Xenarthra, Rodentia, and Artiodactyla were found.

Layer 2 has a thickness of about 0.35 m and is composed of light gray clay containing autochthonous fragments of limestone (> 2 cm), some small geodes, and fragments of stalactites (approximately 10 cm diameter) and other speleothems, in some cases, showing concentrations of iron oxide. The top of the layer contains a high concentration of two types of undetermined seeds. At the bottom of the layer, some complete shells of freshwater clams and several fragments of shells had accumulated. There are small feces covered by powdered carbonate, but still unconsolidated. Some 20 cm from the top of this level, sediment samples were collected in PVC pipe for thermoluminescence dating, and below that, samples were obtained for recovery of palynomorphs. Gastropods and several fragments of Didelphimorphia, Xenarthra, and Rodentia, were collected.

Layer 3, with a 0.15 m thickness, is composed of light yellowish, silty-clay sediments of carbonate-rich composition, containing small autochthonous fragments (0.5–1 cm) of amorphous and angular limestone, and a great amount of recent seeds and fecal matter.

Material and Methods

The material studied includes isolated dentaries and vertebrae deposited in the collection of Museu Dom José

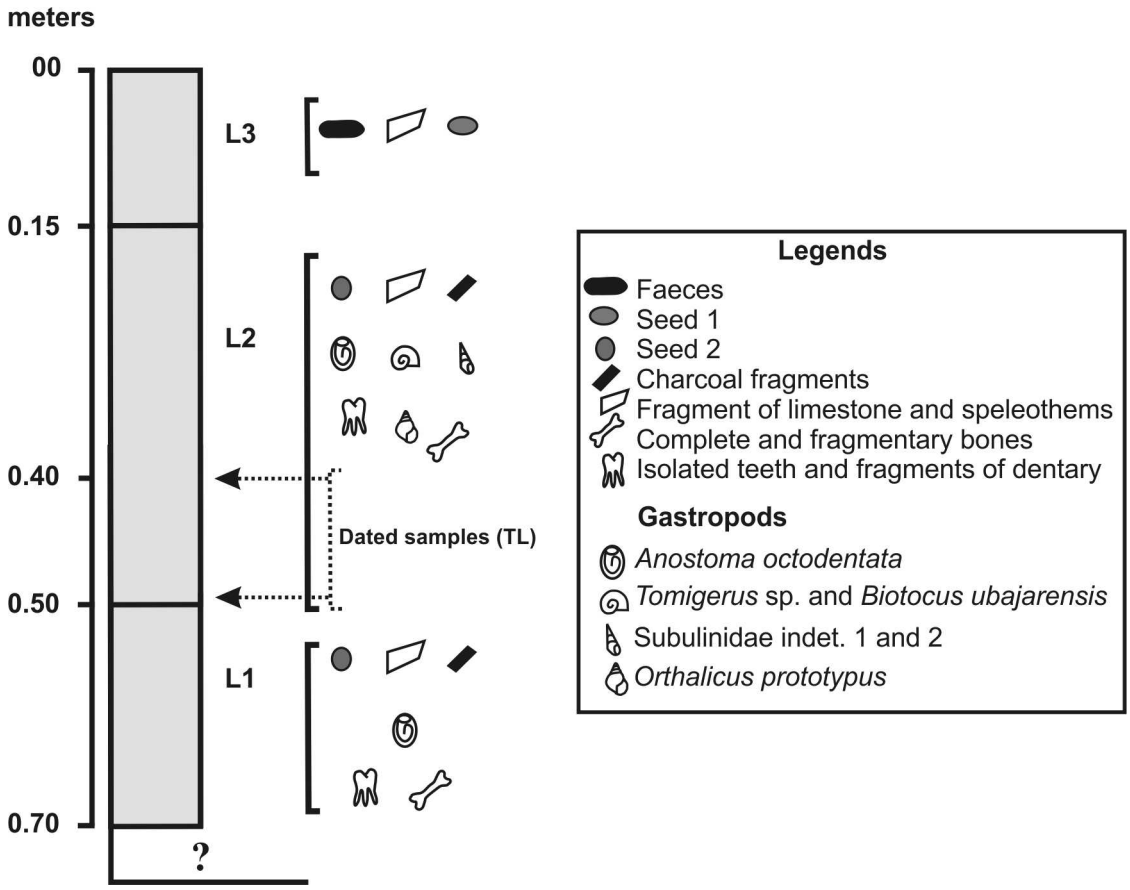

Figure 2. Stratigraphic section showing the layers L1, L2 and L3; and their associated fossils.

(MDJ), in the State Ceará, Brazil. The material consists of two lizard dentaries (MDJ R-004 and 005) and five vertebrae of snakes (MDJ R-006, 020, 024, 026, and 027). The osteological nomenclature and systematics follow Estes (1983), Presch (1974), Estes et al. (1988), Frost et al. (2001a,b), Nydam and Cifelli (2002), and Nydam et al. (2007) for lizards; and Auffenberg (1963), Hoffstetter and Gasc (1969), Rage (1984), Zaher (1999), and Holman (2000) for snakes.

SYSTEMATIC PALEONTOLOGY

SQUAMATA Oppel, 1811
IGUANIA Cope, 1864
TROPIDURIDAE Frost and Etheridge 1989 *sensu* Frost, Janies, and Titus, 2001a
Tropidurus Wied, 1824
Tropidurus sp.
(Fig. 3)

Material: MDJ R-005, complete right dentary.

Stratigraphic provenance: Parque Nacional de Ubajara, Pendurado Hill, Urso Fóssil Cave, Sala da Entrada, layer 1 (TL 8,200 ± 980 years BP), early Holocene.

Description: MDJ R-005 is a complete and delicate right dentary with four mental foramina in labial view. The dentary bears thirteen pleurodont teeth preserved in eighteen tooth positions. The mesial teeth are anteriorly inclined and unicuspid. The distal ones are tricuspid, with two accessory cusps, a mesial and a distal one, smaller than the main central cusp. Under the last two posterior teeth, the subdental shelf of the dentary possesses a notch that extends obliquely until the last teeth (Camolez and Zaher, 2010). The symphysis is small and slightly dorsally oriented. Meckel's groove is extensively closed, with an anterior opening restricted to an elongate foramen and a posterior notch under the last two distal tooth positions. The posterior process of the dentary is long when compared to the total size of the dentary. In labial view, the dorsal margin of the posterior process of the dentary shows a flattened surface, for the contact with the anterior process of the coronoid.

Discussion: Species of *Tropidurus* are widely distributed in open areas in the tropical and subtropical regions, from southern Venezuela east through the Guianas to north-eastern Brazil, and from there southwest of the Amazonian region to eastern Bolivia, northernmost Uruguay, and central Argentina (Etheridge, 1964; Ávila-Pires, 1995; Frost et al., 2001b). There are four species groups formally diagnosed within the genus: *T. spinolusus* group, the *T. borgeti* group, the *T. semitaeniatus* group, and the *T.*

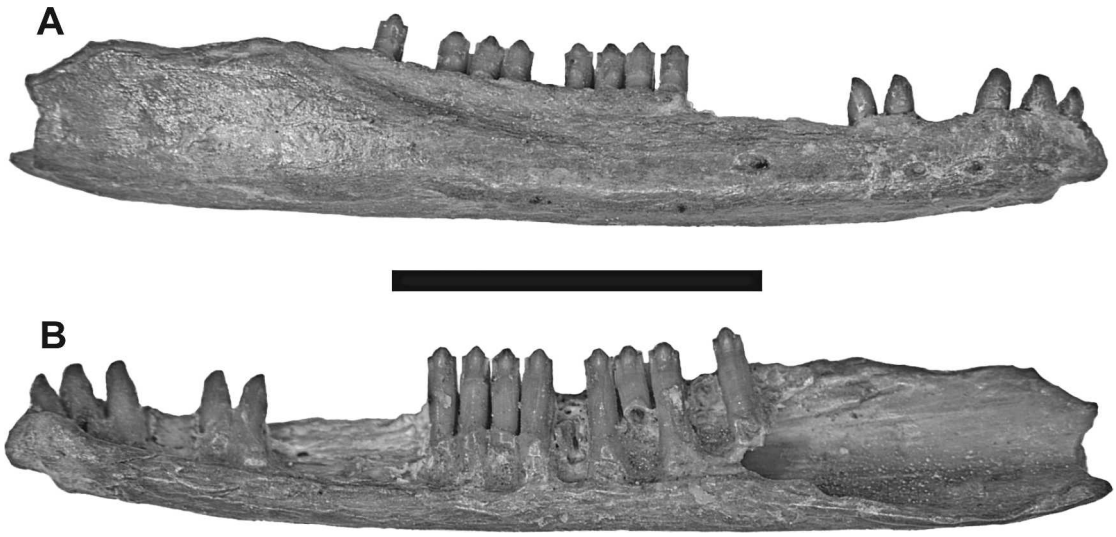

Figure 3. ***Tropidurus*** **sp. complete right dentary, MDJ R-005: A, labial view; B, lingual view. Scale bar = 10 mm.**

torquatus group (Frost et al., 2001b). Attribution to the species level of MDJ R-005 was not possible; but the presence of a longitudinal impression of the labial surface of the posterior part of the dentary, which rises posteriorly (slight ''erosion'' of the alveolar shelf) should be an apomorphy supporting assignment of MDJ R-005 to the ''*Tropidurus* group'' (Frost, 1992; Frost et al. 2001b).

SCLEROGLOSSA Estes, de Queiroz and Gauthier, 1988
SCINCOMORPHA Camp, 1923
TEIIOIDEA Estes, de Queiroz and Gauthier, 1988
TEIIDAE Gray, 1827
TEIINAE Presch, 1974
Ameiva Meyer, 1795
Ameiva sp.
(Fig. 4)

Material: MDJ R-004, incomplete right dentary.

Stratigraphic provenance: Parque Nacional de Ubajara, Pendurado Hill, Urso Fóssil Cave, Sala da Entrada, layer 1 (TL 8,200 ± 980 years BP), early Holocene.

Description: MDJ R-004 is a robust but incomplete right dentary. Its anterior portion is fragmented at the symphysis, and the ventral, lingual and labial portions also are broken. There are three mental foramina in labial view. The dentary rises posteriorly toward its labial and lingual articulations with the coronoid. Lingually, only the anterior portion of the splenial is preserved. Meckel's groove is restricted to the anterior region of dentary by the development of the subdental shelf showing a straight groove (Brizuela, 2010). There are eleven subpleurodont teeth preserved in sixteen tooth positions, within a *sulcus dentalis* and with heavy deposits of cementum at tooth bases (Estes et al., 1988; Nydam and Cifelli, 2002). The third mesial tooth preserved is conical and apparently unicuspid, relatively smaller than the distal ones. The fourth tooth is damaged, but two accessories cusps can be seen, a mesial and distal one, both slightly posteriorly oriented. The fifth, sixth, and seventh are replacement teeth within the replacement pit and show two accessory cusps, both cusps being almost vertical and aligned with one another. The eighth tooth is broken at the base. From the ninth to the eleventh tooth, tooth size and interdental spacing increases (''enlarged posterior teeth: a greater degree of molariformy'', Estes and Williams, 1984). Two accessory cusps are present, as on the fourth preserved tooth.

Discussion: The genus *Ameiva* displays a wide geographical distribution, occurring in southern Mexico, Central and South America, and in many Caribbean islands, with different species (Ávila-Pires, 1995; Pianka and Vitt, 2003). The genus has been considered a paraphyletic group (Presch, 1974; Reeder et al., 2002; Giugliano et al., 2006, 2007), although some authors defended monophyly (Hower and Hedges, 2003). Among the *Ameiva* species, the most studied is *A. ameiva,* commonly found in open habitats, coastal and forests environments, and frequently seen in perianthropic situations (Ávila-Pires, 1995).

Following Camolez and Zaher (2010), the largest size among small Teiidae (such as *Cnemidophorus*, *Kentropix* and *Crocodilurus*) and the dental morphology would allow referral of MDJ R-004 to the species *Ameiva ameiva*. Nevertheless, no additional osteological materials have been found to support this attribution. Currently, we cannot identify MDJ R-004 to species.

SERPENTES Linnaeus, 1758
ALETHINOPHIDIA Nopcsa, 1923
MACROSTOMATA Müller, 1831
BOOIDEA Gray, 1825
BOIDAE Gray, 1825

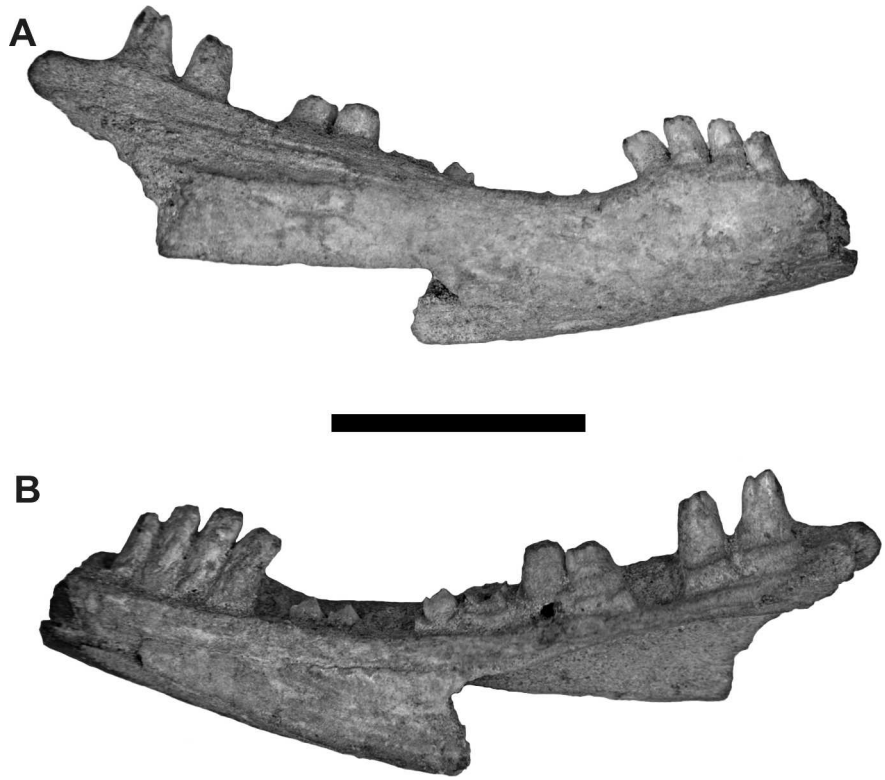

Figure 4. *Ameiva* sp., incomplete right dentary, MDJ R-004: A, labial view; B, lingual view. Scale bar = 10 mm.

Epicrates Wagler, 1830
cf. *Epicrates* sp.
(Fig. 5)

Material: MDJ R-020, incomplete midtrunk vertebrae.

Stratigraphic provenance: Parque Nacional de Ubajara, Pendurado Hill, Urso Fóssil Cave, Sala da Entrada, layer 1 (TL 8,200 ± 980 years BP), early Holocene.

Description: MDJ R-020 lacks most of the dorsal part of the neural arch. The specimen is small, relatively robust and high, with a short centrum. The vertebra probably is a midtrunk vertebra, given the presence of a well marked and anteroposteriorly developed haemal keel. In general view, the prezygapophyses are slightly inclined dorsally, anterolaterally oriented, and display a short prezygapophyseal process. The articular facets of the prezygapophyses are triangular. There are small lateral foramina. The centrum is triangular, widened anteriorly, and rather narrow. A deep paracotylar depression is present to either side of the cotyle, but foramina are absent there. The paradiapophyses are broken, but were apparently robust and oriented dorsoventrally, surpassing the ventral edge of the cotyle. The haemal keel is well-marked and begins on the ventral edge of the cotyle. The subcentral ridges are weakly marked; the subcentral grooves are shallow, but this is more evident in the middle portion of the centrum, lateral to the haemal keel. There is one pair of subcentral foramina.

Discussion: The endemic Neotropical genus *Epicrates* is currently recognized as a paraphyletic group in relation to *Eunectes*, owing to recent studies that found mainland *Epicrates* in a sister-group relationship with *Eunectes* (Burbrink, 2005; Noonan and Chippindale, 2006). The genus contains ten species (Kluge, 1989; McDiarmid et al., 1999) and comprises two monophyletic groups (Kluge, 1989; Passos, 2003; Burbrink, 2005; Noonan and Chippindale, 2006; Passos and Fernandes, 2008). An insular group distributed in the West Indian islands contains twenty-one taxa (Henderson and Powell, 2007), whereas *Epicrates cenchria* (Linnaeus) is a continental endemic (McDiarmid et al., 1999; Passos and Fernandes, 2008). Of the previous nine subspecies of *E. cenchria*, five are now recognized as distinct species *E. alvarezi, E. assisi, E. cenchria, E. crassus*, and *E. maurus* based on statistically robust delimitation of species boundaries (Passos and Fernandes, 2008). The taxonomic assignment of the specimen described above is based on the following combination of vertebral characters shared with the genera of extant neotropical boines: robust, short and wide vertebra, low inclination of the articular facet of the prezygapophysis (less than 15°); short prezygapophyseal process, vertebral centrum short, marked precondylar constriction, haemal keel well developed in the midtrunk vertebrae, and presence of subcentral and lateral foramina (Rage, 2001; Lee and Scanlon, 2002; Szyndlar and Rage, 2003; Albino and Carlini, 2008; Hsiou and Albino, 2009, 2010). Within the neotropical boines, the trunk vertebra is similar to samples from individuals of the genera *Epicrates* and *Corallus*, differing from *Eunectes* and

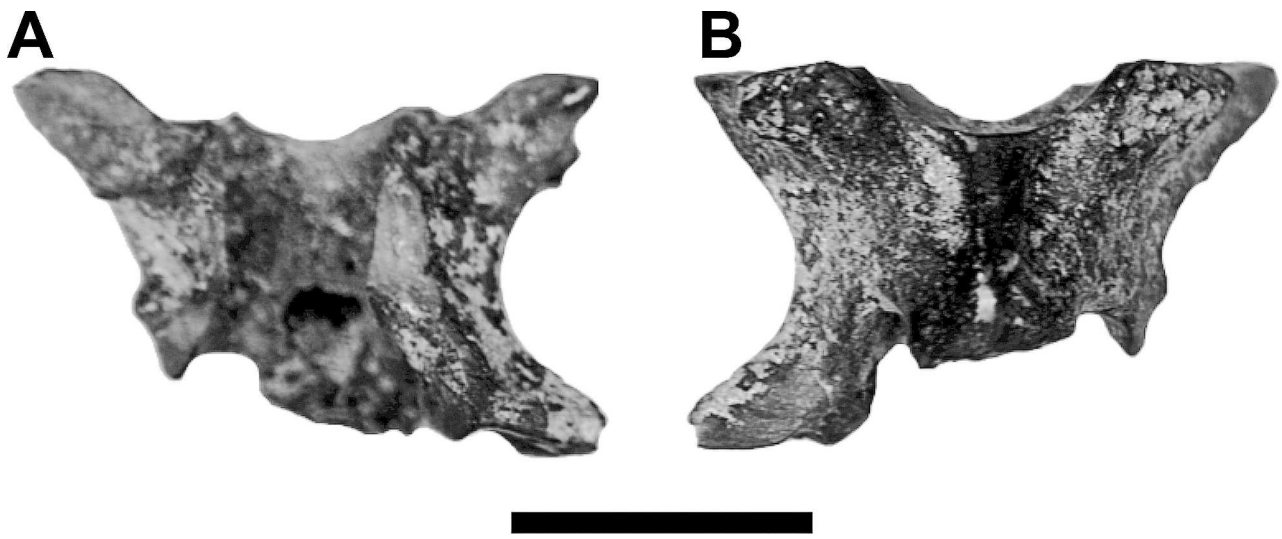

Figure 5. cf. *Epicrates* sp., incomplete midtrunk vertebra, MDJ R-020:A, dorsal view; B, ventral view. Scale bar = 5 mm.

Boa in its smaller size (Hsiou and Albino, 2009, 2010). According to Hsiou and Albino (2010), *Epicrates* and *Corallus* could be distinguished by the morphology of the anterior lobe on the anterior edge of the zygosphene, but MDJ R-020 lacks most of the neural arch. In *Corallus* the prezygapophyses are mostly horizontal in anterior view, whereas they are relatively more inclined above the horizontal plane in *Epicrates* (Hsiou and Albino, 2010). For this reason, we tentatively assigned the trunk vertebrae MDJ R-020 to cf. *Epicrates.*

CAENOPHIDIA Hoffstetter, 1939
COLUBROIDEA Oppel, 1811
VIPERIDAE Oppel, 1811
Crotalus Linnaeus, 1758
Crotalus durissus Linnaeus, 1758
cf. *Crotalus durissus*
(Fig. 6)

Material: MDJ R-006, 024, 026 and 027, incomplete trunk vertebrae.

Stratigraphic provenance: Parque Nacional de Ubajara, Pendurado Hill, Urso Fóssil Cave, Sala da Entrada, layer 2 (MDJ R-006, TL 8,000 ± 990 years BP) and layer 1 (MDJ R-024, 026, 027, TL 8,200 ± 980 years BP), early Holocene.

Description: The preservation of the vertebrae varies among specimens. MDJ R-006 and 024 lack most part of the neural spine, hypapophysis, right prezygapophysis and parapophyseal process, and both paradiapophyses; MDJ R-026 lacks the hypapophysis and right prezygapophysis and parapophyseal process; MDJ R-027 lacks most of the neural arch, zygosphene, hypapophysis, and left prezygapohysis and paradiapophysis. The zygosphene is thin and shows a concave anterior margin, with small and dorsally angled articular facets. The neural arch is wider than long, is moderately depressed, and bears a deep posterodorsal notch. The neural canal is subtriangular, low and wide. The articular facets of the prezygapophyses are slender, longer than broad, with the main axis rather laterally oriented. A small prezygapophyseal process projects slightly beyond the articular facets of the prezygapophysis. The paradiapophyses are clearly oriented dorsoventrally as a whole. The diapophysial and parapophysial surfaces are distinct from each other. The paradiapophyses are well developed, with a prominent and spherical diapophysis, distinct from a large and concave parapophysis (seen in MDJ R- 024). A well-developed and strongly inclined parapophyseal process is spatulated projecting anteriorly, and extends clearly beyond the ventral rim of the cotyle. The postzygapophyses are elongated and inclined dorsolaterally. The zygantra are large and deep, with a small foramen within each side of zygantrum. The neural spine is very well developed, high, and considerably elongated anteroposteriorly, seen in MDJ R-026. The interzygapophyseal constriction is deep and curved. Small lateral foramina are evident on the side walls of the neural arch, more or less positioned at the diapophysial level. The cotyle and condyle are nearly circular, and one pair of small paracotylar foramina is evident; one foramen is located on each side of the cotyle, placed in a shallow depression. The centrum is triangular and bears a very prominent hypapophysis (broken in MDJ R-006, 0026, and 027). The centrum is delimited by subcentral ridges that are well defined anteriorly but vanish in the posterior half of the centrum.

Discussion: The *Crotalus durissus* complex (Neotropical rattlesnakes) occurs in dry areas from Mexico to northern Argentina, but is absent from Central American and Amazonian rainforests, resulting in a highly disjunctive distribution (Wüster et al., 2005). The Brazilian *Crotalus durissus* complex is represented by a single species, *Crotalus durissus*, which has a large geographical distribution among the central region of Cerrado, semi-arid and arid environments of northern region, savannas and open areas

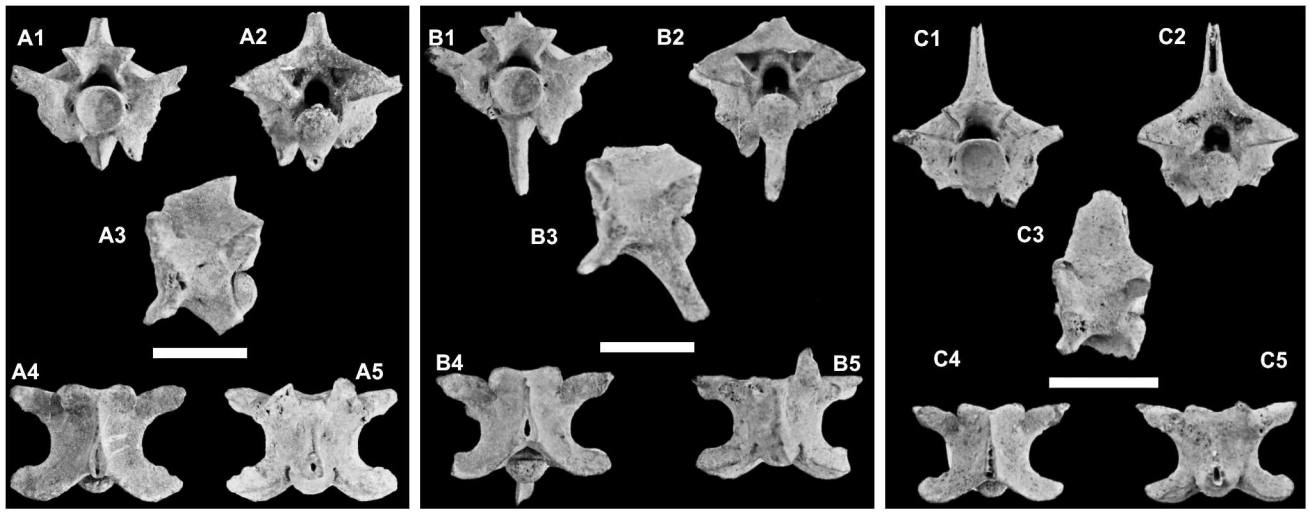

Figure 6. cf. *Crotalus durissus*, midtrunk vertebrae, MDJ R-006 (A), MDJ R-024 (B), and MDJ R – 026 (C), in anterior (A1–C1), posterior (A2–C2), lateral (A3–C3), dorsal (A4–C4), and ventral (A5–C5) views. Scale bar: 10 mm.

of southern, southeastern and northern regions of Brazil (Melgarejo, 2003). The great distribution of *C. durissus* in Brazil is represented by the presence of five geographical forms, *C. d. terrificus, C. d. cascavella, C. d. collineatus, C. d. ruruima,* and *C. d. marajoensis*. All vertebrae described here share the only vertebral synapomorphy recognized for the Viperidae family: a well-developed and strongly anteroventrally oriented parapophyseal process (Zaher, 1999). However, the distinction among the Brazilian species on osteological features still requires further studies. At present, the vertebrae described here are similar to those of *Crotalus durissus* in the anterior edge of zygosphene concave, great anteroposterior extent of the neural spine, spatulate parapophyseal process, and presence of small paracotylar foramina. All of these subtle characters can distinguish *Crotalus durissus* from species of *Bothrops*, another genus with broad geographical distribution that occurs in most open areas in both northern and southern regions of Brazil.

CONCLUDING REMARKS

The new squamate assemblage from the late Quaternary Província Espeleológica de Ubajara described here comprises the lizard families Tropiduridae (*Tropidurus* sp.) and Teiidae (*Ameiva* sp.), and the snake families Boidae (cf. *Epicrates* sp.) and Viperidae (cf. *Crotalus durissus*), in addition to undetermined ''colubrid'' snakes reported by Hsiou et al. (2009). Unfortunately, all specimens are very fragmentary, and specific assignment is not possible. Camolez and Zaher (2010) reported some squamate assemblages from several regions of Brazil, but this work constitutes the first formally described record from the state of Ceará. Hence, the taxa reported in this paper contribute to a better understanding of the Brazilian Quaternary squamate fauna as a whole. Most of the previous records from northeastern Brazil were made based on uninformative reports, lacking a formal description, and their taxonomic validity is still unclear (Paula-Couto, 1980; Guérin, 1991; Guérin et al., 1993; Faure et al., 1999). For this reason, the present paper contributes to a major taxonomic refinement of the squamate faunas during the late Quaternary of northeastern Brazil. All material described here comes from levels with dating around 8,000 years BP, corresponding to the early Holocene. According to Oliveira et al. (in press) the age is consistent with the vertebrate fauna, because representatives of the Pleistocene South American megafauna have not been found in these levels. Like the tayassuids, marsupials, xenarthrans, and caviomorphs from these levels, the squamates do not indicate faunistic alteration during the early Holocene in comparison with the current fauna (Oliveira, 2010; Oliveira et al., in press). The paleoecological data indicated by the taxa reported are in accordance with the mosaic composition of the current environments of the Ubajara region, having humid forest in higher altitudes and open and dryer areas in the plains (Oliveira et al., in press).

ACKNOWLEDGEMENTS

We thank Conselho Nacional de Desenvolvimento Científico e Tecnológico (CNPq) for financial support of the project ''Estudo Paleontológico dos Mamíferos das Cavernas do Parque Nacional de Ubajara, Ceará'' (Universal/n° 473952/2008-4) headed by A.M. Ribeiro (MNC/FZBRS). Thanks also to A.M. Ribeiro (MCN/FZBRS), G. Lessa (UFV), and S. Teixeira (MUPHI) for help and camaraderie during fieldwork in July 2009; to Fundação Cearense de Apoio à Pesquisa e ao Desenvolvimento Científico e Tecnológico (FUNCAP, BPI 0341-1.07/08), and especially to Museu Dom José (MDJ) for the loan

of the specimens. A.S. Hsiou also thanks to CNPq in the form of Postdoctoral Fellowship (n°. 150803/2010-9); and P.V. Oliveira thanks Coordenação de Aperfeiçoamento de Pessoal de Nível Superior (CAPES) and CNPq for Master and Doctoral Fellowships developed at Programa de Pós-Graduação em Geociências at UFRGS and UFPE, respectively. We also thank to the three anonymous referees for their careful reviews and helpful suggestions.

References

Albino, A.M., and Carlini, A.A., 2008, First record of *Boa constrictor* (Serpentes, Boidae) in the Quaternary of South America: Journal of Herpetology, v. 42, p. 82–88.

Auffenberg, W., 1963, The fossil snakes of Florida: Tulane Studies in Zoology and Botany, v. 10, no. 3, p. 131–216.

Ávila-Pires, T.C.S., 1995, Lizards of Brazilian Amazonia (Reptilia: Squamata): Zoologische Verhandelingen, no. 299, 706 p.

Barros-Barreto, C.N.G., De Blasis, P.D., Dias Neto, C.M., Karmann, I., Lino, C.F., and Robrahn, E.M., 1982, Abismo Ponta de Flecha: um projeto arqueológico, paleontológico e geológico no médio curso de Ribeira de Iguape, São Paulo. Revista de Pré-História, v. 3, p. 195–215.

Brizuela, S., 2010, Los lagartos continentales fósiles de la Argentina (excepto Iguania) [Ph.D. thesis]: La Plata, Faculdad de Ciencias Naturales y Museo, Universidad Nacional de La Plata, 442 p.

Burbrink, F.T., 2005, Inferring the phylogenetic position of *Boa constrictor* among the Boinae: Molecular Phylogenetics and Evolution, v. 34, p. 167–180. doi:10.1016/j.ympev.2004.08.017.

Camolez, T., and Zaher, H., 2010, Levantamento, identificação e descrição da fauna de Squamata do Quaternário Brasileiro (Lepidosauria): Arquivos de Zoologia, Museu de Zoologia da Universidade de São Paulo, v. 41, p. 1–96.

CPRM (Serviço Geológico do Brasil), 2003, Atlas Digital de Geologia e Recursos Minerais do Ceará, Brasília, Ministério das Minas e Energia, CD-ROM.

Estes, R., 1983, Sauria terrestria, Amphisbaenia, Handbuch der Paläoherpetologie (Teil 10A): Stuttgart, Gustav Fisher Verlag, 249 p.

Estes, R., De Queiroz, K., and Gauthier, A., 1988, Phylogenetic relationships within Squamata, *in* Estes, R., and Pregill, G., eds., Phylogenetic Relationships of the Lizard Families: Essays Commemorating Charles L. Camp: California, Stanford University Press, p. 119–281.

Estes, R., and Williams, E.E., 1984, Ontogenetic variation in the molariform teeth of lizards: Journal of Vertebrate Paleontology, v. 4, p. 96–107. doi:10.1080/02724634.1984.10011989.

Etheridge, R., 1964, The skeletal morphology and systematic relationships of sceloporine lizards: Copeia, v. 1964, p. 610–631.

Faure, M., Guérin, C., and Parenti, F., 1999, Découverte d'une mégafaune Holocène à la Toca do Serrote do Artur (aire archéologique de São Raimundo Nonato, Piauí, Brésil): Comptes Rendus de l'Académie des Sciences, Ser. II, Sciences de la Terre et des Planètes, v. 329, p. 443–448.

Frost, D.R., 1992, Phylogenetic analysis and taxonomy of the *Tropidurus* group of lizards (Iguania: Tropiduridae): American Museum Novitates, no. 3033, 68 p.

Frost, D.R., and Etheridge, R., 1989, A Phylogenetic analysis and taxonomy of Iguanian Lizards (Reptilia: Squamata): The University of Kansas, Museum of Natural History, Miscellaneous Publications, no. 81, 65 p.

Frost, D.R., Etheridge, R., Janies, D., and Titus, T.A., 2001a, Total evidence, sequence alignment, evolution of polychrotid lizards, and a reclassification of the Iguania (Squamata: Iguania): American Museum Novitates, no. 3343, 38 p.

Frost, D.R., Rodrigues, M.T., Grant, T., and Titus, T.A., 2001b, Phylogenetics of the lizard genus *Tropidurus* (Squamata: Tropiduridae: Tropidurinae): direct optimization, descriptive efficiency, and sensitivity analysis of congruence between molecular data and morphology: Molecular Phylogenetics and Evolution, v. 21, p. 352–371. doi:10.1006/mpev.2001.1015.

Gans, C., and Montero, R., 1998, Two new fossil amphisbaenids (Reptilia: Squamata) from the Pleistocene of Lagoa Santa (Minas Gerais, Brasil): Steenstrupia, v. 24, p. 9–22.

Giugliano, L.G., Contel, E.P.B., and Colli, G.R., 2006, Genetic variability and phylogenetic relationships of *Cnemidophorus parecis* (Squamata, Teiidae) from Cerrado isolates in southwestern Amazonia: Biochemical Systematics and Ecology, v. 34, p. 383–391. doi:10.1016/j.bse.2005.12.007.

Giugliano, L.G., Collevatti, R.G., and Colli, G.R., 2007, Molecular dating and phylogenetic relationships among Teiidae (Squamata) inferred by molecular and morphological data: Molecular Phylogenetics and Evolution, v. 45, p. 168–179. doi:10.1016/j.ympev.2007.05.017.

Guérin, C., 1991, La faune de vertébrés du Pléistocène supérieur de l'aire archéologique de São Raimundo Nonato (Piauí, Brésil): Comptes Rendus de l'Académie des Sciences, Ser. II, Sciences de la Terre et des Planètes, v. 312, p. 567–572.

Guérin, C., Curvello, M.A., Faure, M., Hugueney, M., and Mourer-Chauviré, C., 1993, La faune pléistocène du Piauí (Nordeste du Brésil): implications paléoécologiques et biochronologiques: Quaternaria Nova, v. 3, p. 303–341.

Henderson, R.W., and Powell, R., 2007, The biology of boas and pythons: a retrospective look to the future, *in* Henderson, R.W., and Powell, R., eds., Biology of the Boas and Pythons: Eagle Mountain, Utah, Eagle Mountain Publishing, p. 2–22.

Hoffstetter, R., and Gasc, J.P., 1969, Vertebrae and ribs of modern reptiles, *in* Gans, C., Bellairs, A.d'A., and Parsons, T.S., eds., Biology of the Reptilia, Volume 1, Morphology A: London, Academic Press, p. 201–310.

Holman, J.A., 2000, Fossil Snakes of North America: Origin, Evolution, Distribution, Paleoecology: Bloomington, Indiana University Press, 357 p.

Hower, L.M., and Hedges, S.B., 2003, Molecular phylogeny and biogeography of West Indian teiid lizards of the genus *Ameiva*: Caribbean Journal of Science, v. 39, p. 298–306.

Hsiou, A.S., 2007, A new Teiidae species (Squamata, Scincomorpha) from the late Pleistocene of Rio Grande do Sul State, Brazil: Revista Brasileira de Paleontologia, v. 10, p. 181–194.

Hsiou, A.S., 2010, Lagartos e serpentes (Lepidosauria, Squamata) do Mioceno médio-superior do norte da Região Norte América do Sul [Ph.D. thesis]: Porto Alegre, Universidade Federal do Rio Grande do Sul, 239 p.

Hsiou, A.S., and Albino, A.M., 2009, Presence of the genus *Eunectes* (Serpentes, Boidae) in the Neogene of Southwestern Amazonia, Brazil: Journal of Herpetology, v. 43, p. 612–619. doi:10.1670/08-295.1.

Hsiou, A.S., and Albino, A.M., 2010, New snake remains from the Miocene of northern South America: Herpetological Journal, v. 20, p. 249–259.

Hsiou, A.S., and Albino, A.M., 2011, First record of Viperidae snakes from the Pleistocene of southwestern Brazilian Amazonia: Alcheringa, v. 35, p. 389–395. doi:10.1080/03115518.2011.519646.

Hsiou, A.S., de Oliveira, P.V., and Ximenes, C.L., 2009, Presença de Colubroidea (Squamata, Serpentes) no Quaternário da Província Espeleológica de Ubajara, Estado do Ceará, *in* Livro de Resumos do Congresso Brasileiro de Paleontologia, 21th, Belém, Universidade Federal do Pará/Museu Emílio Goeldi, 189 p.

IBAMA (Instituto Brasileiro do Meio Ambiente e dos Recursos Renováveis), 2002, Parque Nacional de Ubajara: Plano de Manejo, Brasília, Ministério do Meio Ambiente, CD-ROM.

Kluge, A.G., 1989, A concern for evidence and a phylogenetic hypothesis of relationships among *Epicrates* (Boidae: Serpentes): Systematic Zoology, v. 35, p. 7–25. doi:10.1093/sysbio/38.1.7.

Lee, M.S.Y., and Scanlon, J.D., 2002, Snake phylogeny based on osteology, soft anatomy and ecology: Biological Reviews, v. 77, p. 333–401. doi:10.1017/S1464793102005924.

Lino, C.F., Dias-Neto, C.M., Trajano, E., Gusso, G.L.N., Karmann, I., and Rodrigues, R., 1979, Paleontologia das cavernas do Vale do Ribeira, Exploração I Abismo do Fóssil (SP-145): Resultados parciais, *in* Atas do Simpósio Regional de Geologia, 2th, Rio Claro, Sociedade Brasileira de Geologia, p. 257–268.

Lund, M., 1840, Nouvelles recherches sur la faune fossile du Brésil: Annales des Sciences Naturelles, Zoologie, ser. 2, v. 13, p. 310–319.

McDiarmid, R.W., Campbell, J.A., and Touré, T.A., 1999, Snakes Species of the World: A Taxonomic and Geographic Reference, Volume 1: Washington D.C., The Herpetologist's League, 511 p.

Melgarejo, A.R., 2003, Serpentes peçonhentas do Brasil, *in* Cardoso, J.L.C., França, F.O.S., Wen, F.H., Málaque, C.M.S., and Haddad, Jr., V., eds., Animais Peçonhentos do Brasil: Biologia, Clínica e Terapêutica dos Acidentes: São Paulo, Sarvier, p. 33–61.

Nascimento, D.A. do., Gava, A., Pires, J. de., and Teixeira, W., 1981, Geologia da folha SA. 24 – Fortaleza: Projeto Radambrasil, DNPM, v. 21, p. 23–212.

Noonan, B.P., and Chippindale, P.T., 2006, Dispersal and vicariance: the complex evolutionary history of boid snakes: Molecular Phylogenetics and Evolution, v. 40, p. 347–358. doi:10.1016/j.ympev.2006.03.010.

Nydam, R.L., and Cifelli, R.L., 2002, A new teiid from the Cedar Mountain Formation (Albian-Cenomanian boundary) of Utah: Journal of Vertebrate Paleontology, v. 22, p. 276–285. doi:10.1671/0272-4634(2002)022[0276:ANTLFT]2.0.CO;2.

Nydam, R.L., Eaton, J.G., and Sankey, J., 2007, New taxa of transversely-toothed lizards (Squamata: Scincomorpha) and new information on the evolutionary history of ''teiids'': Journal of Paleontology, v. 81, p. 538–549. doi:10.1666/03097.1.

Oliveira, P.V. de., 2010, Mamíferos de Neopleistoceno–Holoceno do Parque Nacional de Ubajara, Ceará [M.S. thesis]: Porto Alegre, Universidade Federal do Rio Grande do Sul, 167 p.

Oliveira, P.V. de., Ribeiro, A.M., Kerber, L., Lessa, G., and Viana, M.S.S., (in press) Late Quaternary caviomorph rodents (Rodentia: Hystricognathi) from Ceará State, northeast Brazil: Journal of Cave and Karst Studies.

Passos, P., 2003, Sistemática do complexo *Epicrates cenchria* (Linnaeus, 1758), com aproximações sobre a filogenia de *Epicrates* Wagler, 1830 (Serpentes, Boidae) [M.S. thesis]: Rio de Janeiro, Universidade Federal do Rio de Janeiro, 125 p.

Passos, P., and Fernandes, R., 2008, Revision of the *Epicrates cenchria* complex (Serpentes: Boidae): Herpetological Monographs, v. 22, p. 1–30. doi:10.1655/06-003.1.

Paula-Couto, C., 1978, Mamíferos fósseis do Pleistoceno do Espírito Santo: Anais da Academia Brasileira de Ciências, v. 50, p. 365–379.

Paula-Couto, C., 1980, Fossil Pleistocene to sub-recent mammals from northeastern Brasil: I – Edentata, Megalonychidae. Anais da Academia Brasileira de Ciências, v. 52, p. 144–151.

Pianka, E.R., and Vitt, L.J., 2003, Lizards—Windows to the Evolution of Diversity: Berkeley, University of California Press, series Organisms and Environments 5, 333 p.

Presch, W., 1974, A survey of the dentition of the macroteiid lizards (Teiidae: Lacertilia): Herpetologica, v. 30, p. 344–349.

Quadros, M.L.E.S., 1996, Estudo tectono-sedimentar da Bacia de Jaibaras, na região entre as cidades de Pacujá e Jaibaras, noroeste do Estado do Ceará [M.S. thesis]: Belém, Universidade Federal do Pará, 134 p.

Rage, J.-C., 1984, Serpentes, Handbuch der Paläoherpetologie, Part 11: Stuttgart, Gustav Fisher Verlag, 80 p.

Rage, J.-C., 2001, Fossil snakes from the Paleocene of São José de Itaboraí, Brazil. Part II. Boidae: Palaeovertebrata, v. 30, p. 111–150.

Reeder, T.W., Cole, C.J., and Dessauer, H.C., 2002, Phylogenetic relationships of whiptail lizards of the genus *Cnemidophorus* (Squamata: Teiidae): a test of monophyly, reevaluation of karyotypic evolution, and review of hybrid origins: American Museum Novitates, no. 3365, 61 p.

Szyndlar, Z., and Rage, J.-C., 2003, Non-erycine Booidea from the Oligocene and Miocene of Europe: Kraków, Institute of Systematics and Evolution of Animals, Polish Academy of Sciences, 109 p.

Trajano, E., and Ferrarezzi, H., 1995, A fossil bear from northeastern Brazil, with a phylogenetic analysis of the South American extinct Tremarctinae (Ursidae): Journal of Vertebrate Paleontology, v. 14, p. 552–561. doi:10.1080/02724634.1995.10011577.

Wüster, W., Ferguson, J.E., Quijada-Mascareñas, A., Pook, C.E., Salomão, M.C., and Thorpe, R.S., 2005, Tracing an invasion: landbridges, refugia, and the phylogeography of the Neotropical rattlesnake (Serpentes: Viperidae: *Crotalus durissus*): Molecular Ecology, v. 14, p. 1095–1108. doi:10.1111/j.1365-294X.2005.02471.x.

Ximenes, C.L., and Machado, D.A.N., 2004, Diagnóstico paleontológico da Província Espeleológica de Ubajara, Estado do Ceará, *in* Resumos do Encontro Brasileiro de Estudos do Carste, 1th, Belo Horizonte: Redespeleo Brasil e Associação Brasileira de Águas Subterrâneas (ABAS), 40 p.

Zaher, H., 1999, Hemipenial morphology of the South American xenodontine snakes, with a proposal for a monophyletic Xenodontinae and a reappraisal of colubroid hemipenes: Bulletin of the American Museum of Natural History, no. 240, 168 p.

A. Romano, S. Salvidio, R. Palozzi, and V. Sbordoni – Diet of the newt, *Triturus carnifex* (Laurenti, 1768), in the flooded karst sinkhole Pozzo del Merro, central Italy. *Journal of Cave and Karst Studies,* v. 74, no. 3, p. 271–277. DOI: 10.4311/2011JCKS0208

DIET OF THE NEWT, *TRITURUS CARNIFEX* (LAURENTI, 1768), IN THE FLOODED KARST SINKHOLE POZZO DEL MERRO, CENTRAL ITALY

Antonio Romano[1*], Sebastiano Salvidio[2], Roberto Palozzi[1,3], and Valerio Sbordoni[1]

Abstract: Karst habitats host a high number of specialized organisms that contribute to complex and peculiar food webs. In underground aquatic habitats, vertebrates are the top predators that strongly influence and regulate prey communities. In this study, the diet of the Italian crested newt, *Triturus carnifex*, in the world's deepest karst phreatic sinkhole, the Pozzo del Merro in Latium, central Italy, was analyzed. We obtained both stomach and fecal contents from twenty adult newts (ten females and ten males) sampled in summer 2010. Availability of prey in the sinkhole also was determined. Prey items were identified and classified into ten ecological groups. At Pozzo del Merro, during the summer, the aquatic stage of *T. carnifex* was specialized on the pre-imaginal stages of the small China-mark, *Cataclysta lemnata*. The recently described endemic stygobitic crustacean *Niphargus cornicolanus* was not found in stomach contents. Finally, our results showed that analyses of stomach and fecal contents may provide different information on the diet of newts in their aquatic phase.

Introduction

Flooded sinkholes are typical elements of karst and may host a relatively high level of biological diversity (e.g., Schmitter-Soto et al., 2002). Among vertebrates, few amphibian species are restricted to karst environments (Weber, 2004; Köhler et al., 2010; Sket, 1997), but more typically, they utilize karst as one of a variety of suitable habitats. In the Mediterranean, karst habitats are mainly associated with carbonate rocks (Lewin and Woodward, 2007). Although Mediterranean amphibians are widespread in surface habitats in the karst (Romanazzi and Bonato, 2011; Romano et al., 2010; Schmitter-Soto et al., 2002), few studies have examined their ecology in karst ecosystems (e.g., Schabetsberger and Jersabek, 1995; Schabetsberger et al., 1995). Scanty ecological information is available for amphibian populations living in flooded sinkholes.

In Europe, most amphibians are strictly protected by the European directive 92/43/EEC (the so-called habitats directive), which is aimed at the creation of an ecological network in Europe to preserve biodiversity. Among newts that occur in Italy, only the Italian crested newt, *Triturus carnifex* (Laurenti, 1768), is in annex II of the habitats directive that lists animals of community interest whose conservation requires the designation of special areas of conservation.

When a strictly protected amphibian species and an endemic or rare invertebrate species coexist, their ecological relationships as predator and prey are of importance for planning adequate conservation measures. In the study site, a deep, flooded sinkhole in central Italy (Fig. 1), ecological studies were particularly required because, beginning in 2003, the invasive aquatic Brazilian tropical fern *Salvinia molesta* D.S. Mitchell spread and soon covered the surface of the lake in the bottom of the study site, replacing the previously dominant *Lemna minor* L. with an approximately 5 cm thick vegetative layer upon which terrestrial vegetation had begun to grow (Giardini, 2003, 2004). The ecological consequences of this rampant invasion were unknown, and in March 2009 a *Salvinia molesta* eradication program started, as recommended in Giardini (2003). As a result, *L. minor* had largely been reestablished as the dominant water surface vegetation by spring 2009.

We studied the diet of the Italian crested newt to determine whether the endemic crustacean recently discovered in Pozzo del Merro was preyed upon by newts, to examine whether the newts show selectivity in feeding, and to compare the information obtained analyzing both stomach and fecal contents. We also checked to see whether the sex of the newts biased their choice of prey.

Study Site

The sinkhole Pozzo del Merro is located at 140 m a.s.l., on the southern slopes of Cornicolani Mountains (Lat. N 42°02′21″, Long. E 12°40′55″, Latium, central Italy) and is included in the natural reserve Macchia di Gattaceca e Macchia del Barco (Fig. 1a). The sinkhole is the deepest

* Corresponding author: antonioromano71@gmail.com
[1] Dipartimento di Biologia, Università di Roma "Tor Vergata", Via Della Ricerca Scientifica, I-00133 Roma, Italy
[2] DIP.TE.RIS., Università di Genova, Corso Europa, 26, I-16132 Genova, Italy
[3] DAF, Dipartimento di tecnologie, ingegneria e scienze dell'Ambiente e delle Foreste, Università di Viterbo "Tuscia", Via S. C. de Lellis, 01100, Viterbo, Italy

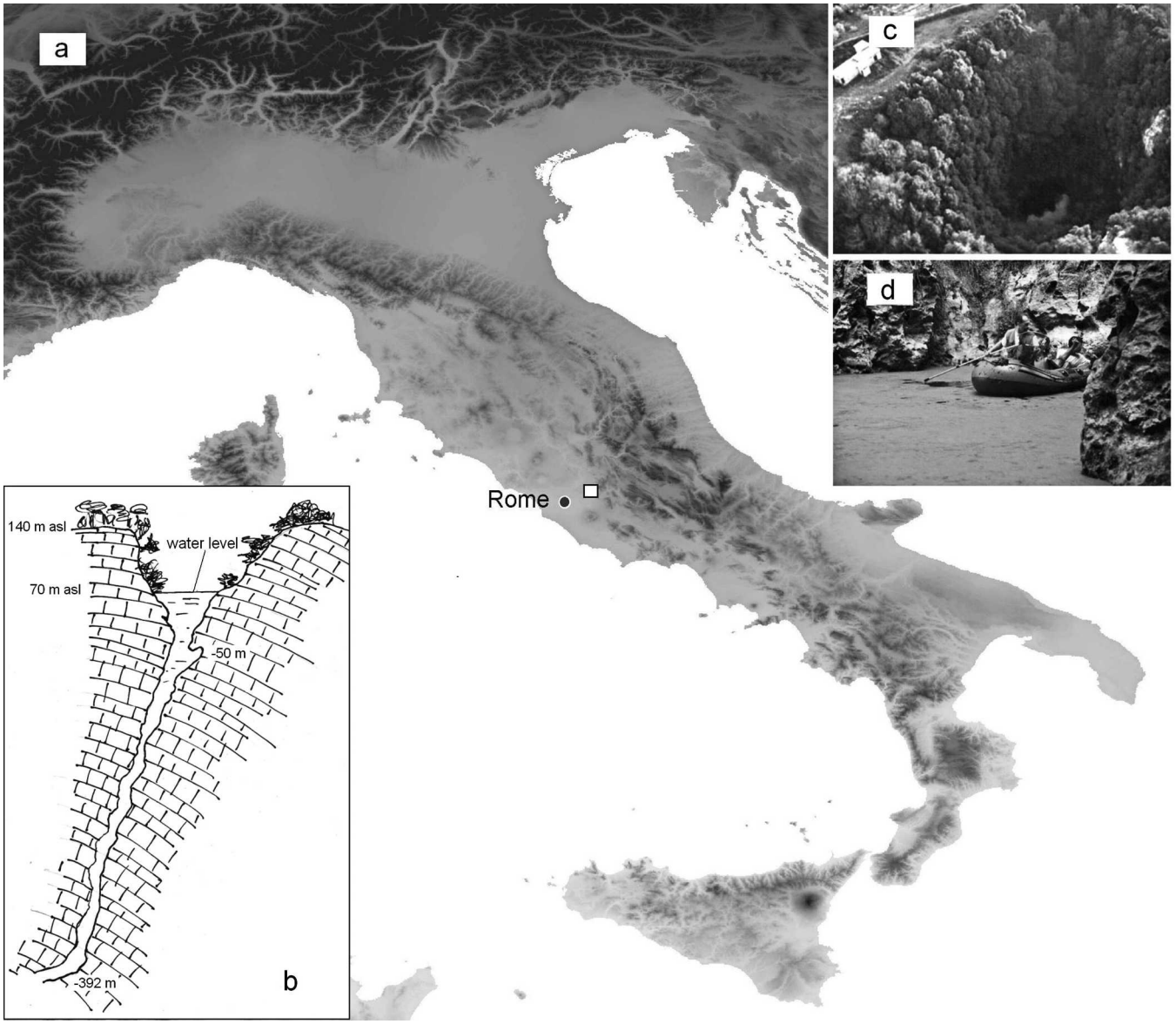

Figure 1. (a) Location of the study site, the flooded sinkhole Pozzo del Merro, in central Italy (white square). (b) Vertical geologic section. (c) The sinkhole as seen from above. (d) Sampling of the newt *Triturus carnifex* with a long-handled dip net maneuvered from a rubber boat.

flooded karst sinkhole in the world (about 460 m; Caramanna, 2002; Gary et al., 2003); its flooded part extends at least 392 m below the water table (Fig. 1b). Pozzo del Merro is funnel-shaped, with a diameter of about 160 m at ground level, narrowing to 25 m at the water surface at about 70 m depth (Fig. 1b,d). Below this depth the flooded sinkhole continues down as a nearly vertical conduit with several minor cavities along the walls (Fig. 1b). The water temperature of 15.9 °C is constant throughout the sinkhole (Palozzi, et al., 2010). The water chemistry is bicarbonate-calcic, and samples collected down the water column showed a progressive reduction of pH from neutrality up to a minimum value of 6.57 at about 100 m (Palozzi et al., 2010).

BIODIVERSITY ASSESSMENT

In 2005, an endemic species of amphipod crustacean was described from Pozzo del Merro, *Niphargus cornicolanus* Iannilli & Vigna Taglianti, 2005. Four amphibians are found there, the Italian crested newt *Triturus carnifex* (Laurenti, 1768), the smooth newt *Lissotriton vulgaris* (Linnaeus, 1758), the Apennine frog *Rana italica* Dubois 1987, and the common toad *Bufo bufo* (Linnaeus, 1758). However the two anurans are found only sporadically, while *T. carnifex* is the dominant newt (capture ratio *T.carnifex*/*L.vulgaris* = 30:1, A. Romano, unpublished data). The Italian crested newt is a large-bodied newt that occurs in Italy, southern Switzerland, Slovenia, Istria, and some regions of Austria, the Czech Republic, and Hungary

(see Vanni et al., 2007). *Triturus carnifex* prefers deep and permanent water bodies (Andreone and Marconi, 2006; Vanni et al., 2007).

Methods

Sampling Method

For this study, only adult newts were sampled. Twenty-two newts were captured on August 12, 2010, with a long-handled dip net 3.5 m in length, maneuvered from a boat (Fig. 1d). Newts were captured when surfacing to breathe. Newts were measured by snout-vent length, weighed, anesthetized in tricaine methanesulphonate (MS-222; Novartis). Their stomachs were flushed using a 20 ml syringe filled with water joined to a silicone catheter 1.0 mm in diameter. The flushing was repeated until no further content came out (Joly, 1987; Salvidio, 1992; Vignoli et al., 2007). Two newts had empty stomachs, leaving twenty subject to further analysis. Food items still present in the oral cavity after flushing were carefully removed by entomological forceps. Newts were housed in an aquarium for approximately sixteen hours after flushing to verify their return to normal activity and then released at the capture site. Fecal matter produced by the newts during their housing were also collected to obtain digested prey. Thus feeding material was obtained from two sources, stomach contents (STO) and feces (FEC). STO were individually assigned, but since newts were housed in the same aquarium all FEC were pooled.

Prey availability (AVA) was sampled in the aquatic environment of the sinkhole by a dip net measuring 60 cm by 30 cm with a 0.1 mm mesh. We attempted to obtain samples that were representative of the three groups into which aquatic invertebrates may be divided. We used the dip net to sample pleustonic invertebrates near the water surface, nektonic invertebrates within the top 3 m of the water column, and benthic invertebrates from the top 3 m on the walls of the sinkhole below the water surface. All those habitats were sampled ten times. STO, FEC, and AVA samples were preserved in 90% ethanol, and identification was made using a stereomicroscope.

The newt sex ratio was expressed as the proportion of mature males: males/(males + females) (Wilson and Hardy, 2002). The vacuity index was calculated as the percentage of empty stomachs out of the total examined. Because variances were not homogeneous, Welch's test for unequal variances was used to determine males-females snout-vent length and weight differences. The Mann-Whitney U test was used to disclose differences in the number of prey swallowed by males and females. The non-parametric Spearman's rank correlation was used to detect any differences in prey between the two sources, stomach and feces, and between prey (STO + FEC) and trophic availability. To compare the results obtained using two different sources (STO and FEC) and to detect sex-related feeding differences, three diversity indices were used, the number of taxa, the Simpson index, which measures evenness of the community from 0 to 1 and is the most-used statistic to compare small samples (Magurran, 2004), and the analysis of similarity (ANOSIM) on the Bray–Curtis dissimilarity measure, which is widely used to analyze animal communities, and in particular, those of freshwater invertebrates, with Bonferroni correction. ANOSIM is a non-parametric significance test between two or more groups, based on any distance measure (Clarke, 1993). Costello's (1990) graphical representation, modified by using prey-specific abundance (PI) instead of percentage abundance (Amundsen et al., 1996), was made to estimate the importance of particular food items in the diet of the newts and to assess their foraging strategy. This method classifies prey selection by plotting prey-specific abundance PI on the Y-axis against frequency of occurrence on the X-axis in the predator stomachs (Fig. 2). PI is defined as the proportion of a prey type among of all prey items in only those individuals in which that prey type occurs (Amundsen et al., 1996). This graphical approach allows for determination of prey importance, the feeding strategy of the predator, and the two components that contribute to the population's total niche width, within-phenotypic and between-phenotypic. The modified Costello's graph provides information on feeding patterns that might not be inferred from single-diet indexes.

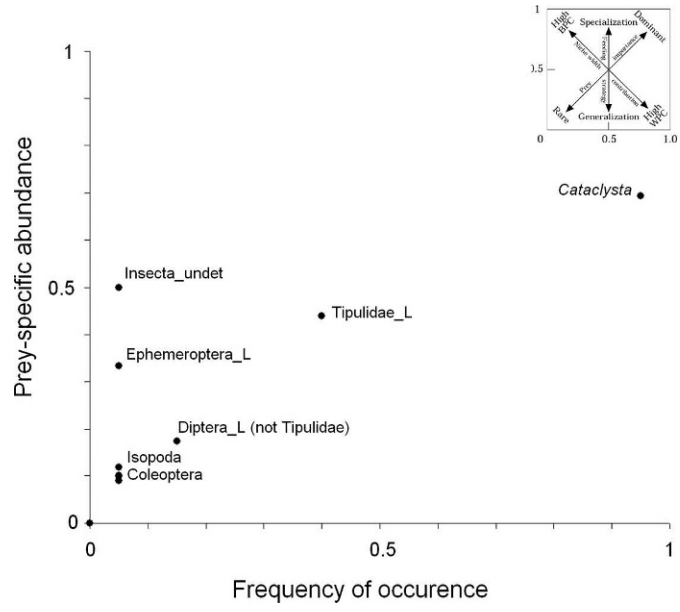

Figure 2. Feeding strategy, based on stomach contents, of the newt *Triturus carnifex* in the Pozzo del Merro visualized using the Costello graphic as modified by Amundsen et al. (1996). The small square shows the interpretation of the plot, where BPC is between-phenotype component of the population's total niche width and WPC is the within-phenotype component. Some taxa with low abundance and low frequency of occurrence in the predated samples are omitted for clarity.

RESULTS

No newt mortality was observed during or after stomach flushing. The sex ratio of *Triturus carnifex* was 0.5 ($n = 22$) and the stomach vacuity was 9%. Thus, we obtained data on the diet of ten male and ten female Italian crested newts. Sexes did not differ significantly in body size and weight ($n = 20$; snout-vent length = 6.37 ± 0.44 cm and 6.20 ± 0.25 cm for females and males, respectively; weight = 8.26 ± 1.80 g and 8.33 ± 1.20 g for females and males, respectively; $p > 0.1$ for all comparisons).

The results of sampling available prey are presented in Table 1. Based on their taxonomy and ecology, terrestrial or aquatic, the prey detected in stomach contents were divided into nine groups plus undetermined insects (Table 2). Overall, lepidopterans (*Cataclysta lemnata*) and dipterans were preyed upon by newts most frequently (95% and 55% respectively; Table 2). Invertebrates that would appear on the horizontal axis in Figure 2 are those that are available in the environment but were not eaten by the newts.

The average number of prey per stomach was 7.55 ± 11.66 and 5.22 ± 8.52 for males and females, respectively, and did not differ significantly (Mann-Whitney, U = 38, $p = 0.82$). There was no overall difference in the diet composition between the sexes (ANOSIM, $n = 20$; global $R = -0.06$, $p = 0.92$). Table 2 shows the numbers in each prey group found in the stomachs of males and females. Table 3 shows the diversity indexes for stomach and feces separately, with the sexes pooled, and for stomach contents for the sexes separately. The correlation between STO and FEC was not significant (flying diptera was pooled with the diptera that were not Tipulidae, giving $n = 9$; $r = 0.34$, $p = 0.37$), suggesting that some prey groups were degradated during digestion.

The overall richness of the types of invertebrates listed in Table 1 in the diet of *Triturus carnifex*, pooling the stomach and fecal contents, was less than trophic availability ($n = 15$; $r = -0.17$, $p = 0.95$). The numbers of groups preyed upon was eight and five, respectively, for females and males (Table 2). In the modified Costello's graphic representation (Fig. 2), almost all prey items are in the lower left corner, while *Cataclysta lemnata* is in the upper right quadrant.

DISCUSSION

The occurrence in the sinkhole Pozzo del Merro of the endemic amphipod *Niphargus cornicolanus* and the newt *Triturus carnifex* was the main motivation to study the trophic niche of the Italian crested newt. If a prey-predator relationship was demonstrated, conservation implications concerning these species, the former strictly endemic and the latter protected by the European Directive 92/43/EEC, would have to be considered. *Niphargus* specimens are often preyed upon by newts, and in general, by aquatic salamanders, in cases where they share the same microhabitat (Racca et al., 2002; Schabetsberger and Jersabek, 1995). However, in the Pozzo del Merro, *N. cornicolanus* is found mainly between 10 and 20 m of depth, and occasionally up to 74 m (Palozzi et al., 2010; R. Palozzi, unpublished data). In the study site, *T. carnifex* has been found (by RP) only up to 7 or 8 m deep, but definite data on this issue are lacking. Since many newts feed at more than 8 m of depth (Schabetsberger and Jersabek, 1995), and at least up to 12 m (George et al., 1977), a small overlap in the depth distributions of *T. carnifex* and *N. cornicolanus* seems possible. However, *Niphargus cornicolanus* was not found in the newt diet. The presence of *Niphargus* in the newt diet cannot be completely rejected, due to our limited sample size. However, even if it is preyed upon, the amphipod appears to be a relatively rare prey item, and its conservation, in relation to the potential predation of this large Italian newt, should not require specific measures or management plans.

Triturus carnifex feeds primarily on aquatic animals and on terrestrial arthropods falling on the water surface, showing a generalist dietary habit (Fasola and Canova, 1992; Ancona and Bolzern, 1993; Vignoli et al., 2009). However, the feeding strategy of the Italian crested newt in the Pozzo del Merro revealed that there is a dominant food item, the larvae of the lepidopteran *Cataclysta lemnata*, the point for which is in the upper right corner of Figure 2 and which has high specific abundance in the water and high occurrence in samples of prey remains. The population of *T. carnifex* inhabiting the sinkhole Pozzo del Merro is specializing in this one prey type. Almost all individuals had been feeding on the dominant prey, but a significant proportion of other available prey was included occasionally in the diet of some individuals (Table 1; Fig. 2). Since prey types range from the upper right to the lower left in Figure 2, the newt population possesses a relatively broad trophic niche. The diet of males and females was similar, but the number of taxa in the female stomachs was twice that of the males, and the confidence limit of the number of taxa diversity index (Table 3b) are just slightly overlapping, suggesting that analysis of a larger sample could allow a difference to be statistically confirmed. The comparison of the data obtained from fecal and stomach analyses is also interesting. Indeed, the study of fecal samples in salamanders may lead to a drastic underestimate in the number and diversity of prey taxa (Table 3a), because small and delicate prey tend to be completely digested by salamanders (Corvetto et al., 2012). This selective digestion may be a problem when searching for specific prey-predator relationships in a given context. Therefore, the use of stomach flushing should be preferred to fecal sampling, which does not assure a complete evaluation of a salamander's diet.

Table 1. Trophic availability (AVA) in the Pozzo del Merro and diet composition of twenty *Triturus carnifex* as determined from the analyses of their stomach contents (STO) and feces (FEC). All taxa or life stages are aquatic except where indicated by an asterisk (*).

Taxon		Life Stage									Total (prey)
		Larvae			Pupae			Adult			
Class/Order	Family	AVA	STO	FEC	AVA	STO	FEC	AVA	STO	FEC	
INSECTA											
Collembola								1872			
Lepidoptera	Piralidae (1 sp.)	1139	59	5	52	21	53				138
Diptera	Tipulidae	9	25	1							26
Diptera	not Tipulidae	4	4						1*		4
Ephemeroptera		1	1								1
Coleoptera	Elmintidae							17	1	1	2
Coleoptera*									1		1
undetermined									1	4	5
CRUSTACEA											
Isopoda	Asellidae							61	2	3	5
Concostraca								1			
ARACHNIDA											
Acarina								131			
GASTEROPODA											
Pulmonata	Planorbidae							5			
TURBELLARIA											
Seriata	Planariidae							15			
NEMATODA											
undetermined								1	1		1
OLIGOCHAETA											
undetermined								8			

Table 2. Summary of the number of specimens of prey found in stomachs only for groups of the taxa in Table 1, sorted by female (FF) and male (MM). The percentage of the ten newts of each species that had eaten each group is also given.

	FF		MM		Total	
Organism	N, prey	% of newt	N, prey	% of newt	N, prey	% of newt
Lepidoptera (*Cataclysta lemnata*)	37	90	43	100	80	95
Diptera Tipulidae (larvae)	11	30	20	50	21	40
Diptera non Tipulidae (larvae)	5	10	3	20	8	15
Flying Diptera (terrestrial and not Tipulidae)	1	10	0	0	1	5
Ephemeroptera (larvae)	1	10	0	0	1	5
Coleoptera (aquatic);	1	10	0	0	1	5
Coleoptera (terrestrial)	1	10	0	0	1	5
Insecta undetermined	1	10	0	0	1	5
Crustacea, Asellidae	0	0	2	10	2	5
Nematoda	0	0	1	10	1	5
Total	58		69		117	

CONCLUSIONS

This paper is the first study on the feeding behavior of a newt in a deep, flooded karst sinkhole. A previous study on the diet of newts during the 2003–2009 invasion of *Salvinia molesta* would have been useful to determine the effect of this invasive plant on the newt population. The importance of the native aquatic plant *Lemna minor* in sustaining the population of *Triturus carnifex* was strongly suggested by the present study. Alterations to the natural status of this karst ecosystem, such as the permanent replacement of autochthonous *Lemna* with *Salvinia*, could likely lead to ecological consequences, because the most importance food resource used by newts in the summer would be unavailable.

Other Italian crested newt populations living in different ecosystems such as shallow karst ponds and other lakes seem to be characterized by an opportunistic feeding behavior (Vanni et al., 2007). A study of a population from a flooded tuff quarry abandoned in central Italy suggested the *Triturus carnifex* may have a mixed feeding strategy (dominant-generalized) and some individuals may feed on prey with a relatively high frequency of occurrence (Vignoli et al., 2009). The population living in the Pozzo del Merro exhibited, at least in the summer, a different feeding behavior, because all newts were specialized predators of an invertebrate with high frequency of occurrence. Generalist feeding behavior of *T. carnifex* in habitats with variable environmental parameters may vary slightly over seasons and years, depending on resources (Ancona and Bolzern, 1993). Although in the sinkhole physical and chemical parameters are relatively stable (Palozzi et al., 2010), further research should aim at establishing the feeding strategy adopted by the Italian crested newts during the fall and winter, when the plant *Lemna minor* and the associated small China-mark *Cataclysta lemnata* are absent. Furthermore, in winter time, pleustonic prey would become less available, and the newts might move deeper in the water to forage on *Niphargus*.

Finally, the analysis of the diet of the smaller smooth newt *Lissotriton vulgaris* and of *Triturus carnifex* larvae, which may show a specialization towards aquatic crustaceans (Vignoli et al., 2009; Stoch and Dolce, 1984), should also be undertaken to completely reveal the trophic relationships between the endemic *Niphargus cornicolanus* and the sympatric amphibians which live in the Pozzo del Merro.

Table 3. Indexes of prey taxa diversity, with 95% confidence limits, of *Triturus carnifex* in the Pozzo del Merro (Central Italy).

	Stomach and Fecal Contents Compared for Pooled Male and Female Specimens						Stomach and Fecal Contents Compared for Females and Males					
	STO (sexes pooled)			FEC (sexes pooled)			Diversity STO Females			Diversity STO Males		
		Boostrap (95%)			Boostrap (95%)			Boostrap (95%)			Boostrap (95%)	
Index Type		Min.	Max.		Min.	Max.		Min.	Max.		Min.	Max.
Index of Taxa Diversity	9	5	9	5	3	5	8	3	8	4	3	4
Simpson Index	0.476	0.371	0.552	0.245	0.114	0.38	0.392	0.226	0.539	0.511	0.394	0.590

Acknowledgements

Capture and stomach flushing were performed with the permit from the Ministero dell'Ambiente e della Tutela del Territorio e del Mare (permit reference: DPN/2010/0002708). The Province of Rome provided the research grant for this study. We are indebted to Giovanni Forcina for help in field sampling. We thank two anonymous referees for many useful suggestions that surely improved our manuscript.

References

Amundsen, P.-A., Gabler, H.-M., and Staldvik, F.J., 1996, A new approach to graphical analysis of feeding strategy from stomach contents data—modification of the Costello (1990) method: Journal of Fish Biology, v. 48, no. 4, p. 607–614. doi:10.1111/j.1095-8649.1996.tb01455.x.

Ancona, N., and Bolzern, A.M., 1993, Alimentazione di *Triturus carnifex* e *T. vulgaris meridionalis* (Amphibia Caudata) in due stagni dell'Appenino Ligure: Rendiconti Scienze Chimiche e Fisiche, Geologiche, Biologiche e Mediche, Istituto Lombardo, v. B126, p. 123–137.

Andreone, F., and Marconi, M., 2006, *Triturus carnifex* (Laurenti, 1768), *in* Sindaco, R., Doria, G., Razzetti, E., and Bernini, F., eds., Atlante degli Anfibi e dei Rettili d'Italia / Atlas of Italian Amphibians and Reptiles: Firenze, Societas Herpetologica Italica, Edizioni Polistampa, p. 220–225.

Caramanna, G., 2002, Exploring one of the world's deepest sinkholes: the Pozzo del Merro (Italy), Underwater Speleology, February, p. 4–8.

Clarke, K.R., 1993, Non-parametric multivariate analysis of changes in community structure: Australian Journal of Ecology, v. 18, p. 117–143. doi:10.1111/j.1442-9993.1993.tb00438.x.

Costello, M.J., 1990, Predator feeding strategy and prey importance: a new graphical analysis. Journal of Fish Biology, v. 36, no. 2, p. 261–263. doi:10.1111/j.1095-8649.1990.tb05601.x.

Crovetto, F., Romano, A., and Salvidio, S., 2012, A comparison of two non-lethal methods for dictary studies in terrestrial salamanders. Wildlife Research, v. 39, p. 266–270.

Fasola, M., and Canova, L., 1992, Residence in water by the newts *Triturus vulgaris*, *T. cristatus* and *T. alpestris* in a pond in northern Italy: Amphibia-Reptilia, v. 13, no. 3, p. 227–233. doi:10.1163/156853892X00436.

Gary, M.O., Sharp, J.M. Jr., Caramanna, G., and Havens, R.H., 2003, Volcanically influenced speleogenesis: forming El Sistema Zacatón, Mexico, and Pozzo del Merro, Italy, the deepest phreatic sinkholes in the world: Geological Society of America Abstracts with Programs, vol. 34, no. 7, session 19-4, 52 p.

George, C.J., Boylen, C.W., and Sheldon, R.B., 1977, The presence of the red-spotted newt, *Notophthalmus viridescens rafinesque* (Amphibia, Urodela, Salamandridae) in waters exceeding 12 meters in Lake George, New York: Journal of Herpetology, v. 11, no. 1, p. 87–90.

Giardini, M., 2003, Note sulla biologia, l'ecologia e le modalità di controllo di *Salvinia molesta* D.S. Mitchell (Salviniaceae), specie infestante nuova per il Lazio: Rivista di Idrobiologia, v. 42, no. 1–3, p. 263–282.

Giardini, M., 2004, *Salvinia molesta* D.S. Mitchell (Salviniaceae): seconda segnalazione per l'Italia (Lazio) e considerazioni sul controllo di questa specie infestante: Webbia, v. 59, no. 2, p. 457–467.

Weber, A., Amphibia, *in* Gunn, J., ed., Encyclopedia of Caves and Karst Science: New York, Fitzroy Dearborn, p. 61–62.

Iannilli, V., and Vigna Taglianti, A., 2005, New data on genus *Niphargus* (Amphipoda, Niphargidae) in Italy, with the description of a new species of the *Orcinus* group: Crustaceana, v. 77, no. 10 (2004), p. 1253–1261. doi:10.1163/1568540043166029.

Joly, P., 1987, Le régime alimentaire des amphibians: méthodes d'étude: Alytes, v. 6, no. 1–2, p. 11–17.

Köhler, J., Vences, M., D'Cruze, N., and Glaw, F., 2010, Giant dwarfs: discovery of a radiation of large-bodied 'stump-toed frogs' from karstic cave environments of northern Madagascar: Journal of Zoology, v. 282, no. 1, p. 21–38. doi:10.1111/j.1469-7998.2010.00708.x.

Lewin, J., and Woodward, J.C., 2007, Karst geomorphology and environmental change, *in* Woodward, J., ed., The Physical Geography of the Mediterranean: Oxford, Oxford University Press, p. 287–317.

Magurran, A.E., 2004, Measuring Biological Diversity: Malden, Massachusetts, Blackwell Publishing, 256 p.

Palozzi, R., Caramanna, G., Albertano, P., Congestri, R., Bruno, L., Romano, A., Giganti, M.G., Zenobi, R., Costanzo, C., Valente, G., Polani, D., Vecchio, M., Vinci, M., and Sbordoni, V., 2010, The underwater exploration of the Merro sinkhole and the associated diving physiological and psychological effects: Underwater Technology, v. 29, no. 3, p. 125–134. doi:10.3723/ut.29.125.

Racca, L., Bressi, N., Dolce, S., and Giacoma, C., 2002, Studio etologico del comportamento alimentare di *Proteus anguinus anguinus* (Amphibia, Urodela) in cattività: Atti Museo Civico di Storia Naturale di Trieste, v. 49, p. 157–167.

Romanazzi, E., and Bonato, L., 2011, Anfibi sul Montello: Distribuzione dei siti riproduttivi in un territorio carsico prealpino, *in* Bon, M., Mezzavilla, F., and Scarton, F., eds., Atti del 6° Convegno dei Faunisti Veneti: Bollettino del Museo civico di Storia Naturale, Venezia, suppl. to, v. 61, p. 88–95.

Romano, A., Ventre, N., De Riso, L., Pignataro, C., and Spilinga, C., 2010, Amphibians of the "Cilento e Vallo di Diano" National Park (Campania, Southern Italy): updated check list, distribution and conservation notes. Acta Herpetologica, v. 5, no. 2, p. 233–244.

Salvidio, S., 1992, Diet and food utilization in a rockface population of *Speleomantes ambrosii* (Amphibia, Caudata, Plethodontidae): Vie et Milieu, v. 42, no. 1, p. 35–39.

Schabetsberger, R., and Jersabek, C.D., 1995, Alpine newts (*Triturus alpestris*) as top predators in a high-altitude karst lake: daily food consumption and impact on the copepod *Arctodiaptomus alpinus*: Freshwater Biology, v. 33, p. 47–61. doi:10.1111/j.1365-2427.1995.tb00385.x.

Schabetsberger, R., Jersabek, C.D., and Brozek, S., 1995, The impact of Alpine newts (*Triturus alpestris*) and minnows (*Phoxinus phoxinus*) on the microcrustacean communities of two high altitude karst lakes: Alytes, v. 12, no. 4, p. 183–189.

Schmitter-Soto, J.J., Comin, F.A., Escobar-Briones, E., Herrera-Silveira, J., Alcocer, J., Suárez-Morales, E., Elias-Gutiérrez, M., Díaz-Arce, V., Marín, L.E., and Steinich, B., 2002, Hydrogeochemical and biological characteristics of cenotes in the Yucatan Peninsula (SE Mexico): Hydrobiologia, v. 467, no. 1–3, p. 215–228. doi:10.1023/A:1014923217206.

Sket, B., 1997, Distribution of *Proteus* (Amphibia: Urodela: Proteidae) and its possible explanation: Journal of Biogeography, v. 24, no. 3, p. 263–280. doi:10.1046/j.1365-2699.1997.00103.x.

Stoch, F., and Dolce, S., 1984, Alimentazione e rapporti alimentari di *Triturus alpestris alpestris* (Laur.), *Triturus cristatus carnifex* (Laur.) e *Triturus vulgaris meridionalis* (Boul.). (Osservazioni sull'alimentazione degli Anfibi: III): Quaderni ETP, Rivista di Limnologia, Udine, v. 9, p. 17–28.

Vanni, S., Andreone, F., and Tripepi, S., 2007, *Triturus carnifex* (Laurenti, 1768), *in* Lanza, B., Andreone, F., Bologna, M., Corti, C., and Razzetti, E., eds., Fauna d'Italia XLII: Amphibia, Bologna, Edizioni Calderini, p. 265–272.

Vignoli, L., Bombi, P., D'Amen, M., and Bologna, M.A., 2007, Seasonal variation in the trophic niche in a heterochronic population of *Mesotriton alpestris apuanus* (Amphibia, Salamandridae) from the south-western Alps: Herpetological Journal, v. 17, p. 183–191.

Vignoli, L., Luiselli, L., and Bologna, M.A., 2009, Dietary patterns and overlap in an amphibian assemblage at a pond in Mediterranean central Italy: Vie et Milieu / Life and Environment, v. 59, no. 1, p. 47–57.

Wilson, K., and Hardy, I.C.W., 2002, Statistical analysis of sex ratios: an introduction, *in* Hardy, I.C.W., ed., Sex Ratios – Concepts and Research Methods: Cambridge, Cambridge University Press, p. 48–92.

M.D. Johnston, B.A. Muench, E.D. Banks, and H.A. Barton – Human urine in Lechuguilla Cave: the microbiological impact and potential for bioremediation. *Journal of Cave and Karst Studies,* v. 74, no. 3, p. 278–291. DOI: 10.4311/2011MB0227

HUMAN URINE IN LECHUGUILLA CAVE: THE MICROBIOLOGICAL IMPACT AND POTENTIAL FOR BIOREMEDIATION

Michael D. Johnston, Brittany A. Muench, Eric D. Banks, and Hazel A. Barton*
Department of Biology, University of Akron, Akron, OH 44325

Abstract: During extended exploration trips in caves, it is sometimes not possible to remove all excreted urine due to its volume and weight. Excess urine can be particularly problematic in dry caves where, without dilution, urine introduces a significant source of nitrogen into these otherwise nitrogen-limited environments. It was the aim of this study to determine the impact that human urine could have on cave microbiota over an extended period of time. To do this, we examined the microbial community structure of a heavily impacted site in Lechuguilla Cave, USA. Using a molecular phylogenetic approach we generated a 136-member 16S rRNA clone library that demonstrated representatives of the *Alpha-* *Beta-* and *Gammaproteobacteria*, the *Bacteroidetes*, *Firmicutes*, *Actinobacteria* and *Deinococcus-Thermus* group at this site. The structure of the microbial community at the impacted site suggests that it is colonized by endemic cave species rather than human commensal organisms, while metabolic inference suggests that these organisms are taking advantage of both the nitrogenous and organic compounds in urine for growth. The intrinsic nature of such metabolic activity in the cave environment was confirmed by examining non-impacted sites using cultivation, which demonstrated that endemic species express both the capacity to degrade urine and to reduce urea to nitrogen gas. Our results differ from those of previous studies by implying a more resilient nature of the microbial ecosystem in caves to invasion by exogenous (commensal) species, while suggesting that endemic microbial species may be able to mitigate the impact of excess nitrogen in the cave through bioremediation.

Introduction

Cave environments become more energy- and nutrient-limited as you travel farther from surface inputs (Barr, 1967; Hardin and Hassell, 1970; Raesly and Gates, 1987; Culver and Sket, 2000; Lavoie et al., 2007), and the environment becomes increasingly difficult for troglobitic species to subsist. As a result, the biome becomes increasingly dominated by microorganisms (Barr, 1967; Culver and Sket, 2000; Barton and Jurado, 2007). Yet in these nutrient-limited environments, even microorganisms are dependent on the availability of both energy and nutrients such as nitrogen, sulfur, and phosphorus for growth. The presence of these nutrients, in both endogenous (autochthonous) and exogenous (allochthonous) form, can have a profound impact on microbial growth and community structure (Ikner et al., 2007; Summers Engel et al., 2010; Iker et al., 2010). Depending on local geochemistry, sulfur and phosphorus may be present within the mineral matrix of the rock; however, there is rarely any intrinsic source of nitrogen in caves (Klimchouk, 2000). As a result, the availability of nitrogen becomes critical for microbial subsistence, as demonstrated by the abundance of nitrogen-fixing bacterial species in cave environments (Northup et al., 2003; Barton et al., 2007; Ikner et al., 2007; Spear et al., 2007). The introduction of allochthonous nitrogen can have a dramatic impact on the microbial community structure in such ecosystems, created by an excess of this normally limited nutrient (Ikner et al., 2007; Iker et al., 2010).

In order to understand caves, humans must enter and explore them (Kambesis, 2007); however, the human exploration of caves has the potential to impact microbial ecosystems through the introduction of nutrients (Northup et al., 1997; Lavoie and Northup, 2005; Ikner et al., 2007). To minimize such impacts, speleologists use a number of techniques, including staying on designated trails, wearing non-marking footwear, avoiding leaving food crumbs, and removing all waste (Northup et al., 1997; Elliott 2006). Some caves are sufficiently large and deep that exploration requires extended periods underground, sometimes exceeding thirty days (Reames et al., 1999; Stone et al., 2002; Tabor, 2010), and the removal of human waste becomes impractical due to weight constraints. If removing all liquid waste is mandated, there is a danger that speleologists will undergo self-induced dehydration to minimize waste and weight. Dehydration, compounded by exercise, can adversely affect judgment and motor skills, increasing the likelihood of an accident (Lieberman, 2007). To avoid the large-scale impact that a rescue would have, it is therefore

* Corresponding Author: bartonh@uakron.edu

sometimes more reasonable to leave human waste in the cave.

Due to the high protein content of the human diet, excess nitrogen is produced in the form of ammonia (NH_3) from the catabolism of amino acids (Wright, 1995). This ammonia is excreted as urea [$(NH_2)_2CO$], the major component of urine in mammals. In the environment, microbial hydrolysis can convert this urea back into ammonia (Fig. 1A), which can be assimilated by plants or microorganisms back into amino acids. Ammonia and other nitrogenous species (NO_2^-, NO_3^-, NO, N_2O) contain nitrogen in a number of valency states, allowing these compounds to function in biological redox reactions (Fig. 1B). Microorganisms, therefore, have the capacity to use ammonia for dissimilatory (energy generating) metabolic processes (Fig. 1A), with the resulting products (NO_2^-, NO_3^-, and N_2O) serving in additional (denitrifying) redox reactions (Francis et al., 2007; Fig. 1B). Excess ammonia in a nitrogen-limited environment can impact both microbial nitrogen assimilatory (nitrogen uptake) and dissimilatory (energy generating) processes, with the potential to dramatically change both nitrogen scavenging activities and ecosystem energetics (Iker et al., 2010).

Lechuguilla Cave, New Mexico, is an extensive cave system over 200 km in length and 500 meters in depth (S. Allison, personal communication, 2010). Exploration of this large system has required extended underground camping trips lasting up to eight days (Reames et al., 1999). Due to the long duration of these trips, urine has been deposited at campsites throughout the cave (Northup et al., 1997; Reames et al., 1999). Because of the potential impact of this urine on microbial-ecosystem dynamics, we examined how microorganisms in Lechuguilla Cave respond to this nutrient at both impacted and non-impacted sites using a combination of cultivation and molecular phylogenetics. Our results demonstrate a dramatic change in the microbial community in response to urine deposition and suggest the potential for bioremediation strategies to minimize future impacts.

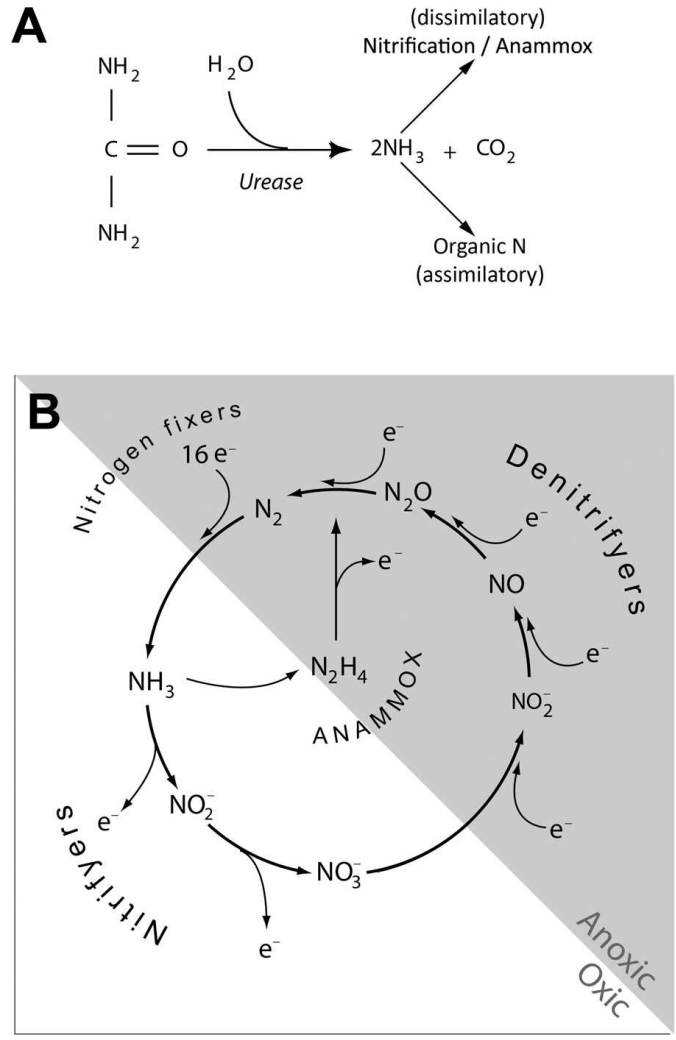

Figure 1. The degradation of urea and the nitrogen cycle. A. A simplification of the breakdown of urea by urease into ammonia. B. The nitrogen cycle not only provides nitrogen in a bioavailable form for plants and bacteria (NO_3^-), but the valency of the nitrogen species also allows them to serve as electron donors or electron acceptors in bacterial energy-generating processes. Ammonia is oxidized by nitrifying bacteria into nitrite and nitrate, while nitrate can be reduced by denitrifying bacteria to generate nitrous oxide and nitrogen gas. Under anaerobic conditions, ammonia can be directly oxidized to nitrogen gas by anaerobic ammonia-oxidizing (ANAMMOX) bacteria. In either case, either nitrogen gas from the nitrogen cycle or directly from the air can be made bioavailable by nitrogen-fixing bacteria in the form of ammonia.

Methods

Cave Description and Geology

Lechuguilla Cave is located in Carlsbad Caverns National Park, Eddy County, New Mexico. The cave is located in a desert region and does not connect to any known surface streams, limiting allochthonous nutrient input (Davis, 2000). The cave was formed primarily in the Capitan Formation of the Delaware Basin by hypogenic sulfuric acid speleogenesis with a postulated biogenic origin (Hill, 2000; Palmer and Palmer, 2000; Barton, 2013). Due to the complex geology of the cave, with both back-reef and fore-reef facies, numerous secondary elements can be found within the limestone, including iron, manganese, titanium, silica, and other constituents of sedimentary minerals (Scholle et al., 1992; Northup et al., 2003).

Sample Collection and Molecular Techniques

At the Big Sky campsite, a small depression off the main corridor has served as the urine deposition site for more than twenty years (Fig. 2). The gypsum where the urine was poured has acquired a black patina, similar to that seen at other urine deposit sites within the cave.

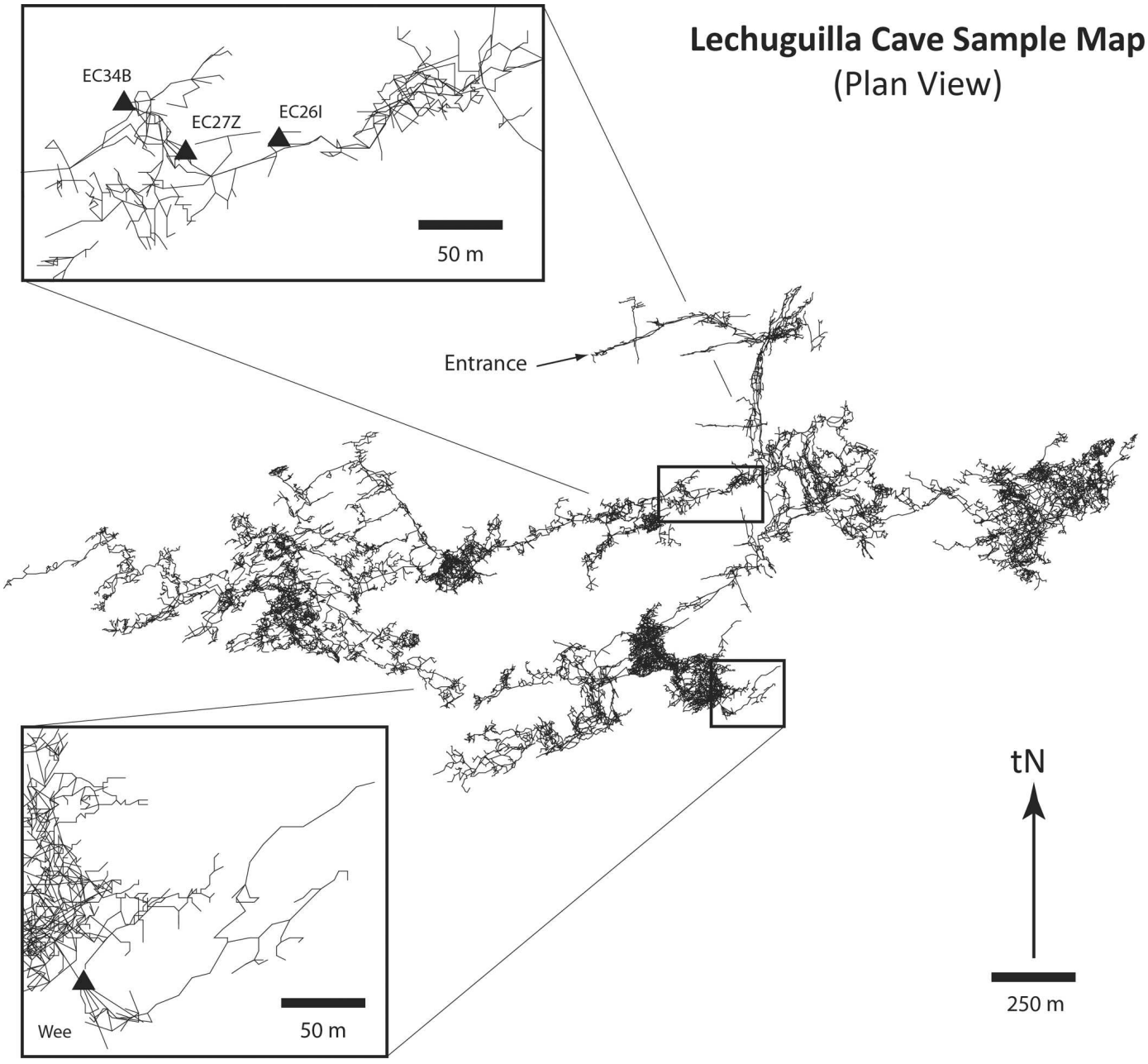

Figure 2. Map of Lechuguilla Cave, showing the relative locations of the sample sites. The sample for molecular phylogenetic analysis was collected at the Big Sky Camp urine site (Wee), while samples collected for cultivation were collected at EC34B, EC27Z, and EC26I in the Western Borehole region.

Approximately one month following the most recent use of this urine site, a 2 cm^3 sample of the black patina (designated Wee) was obtained for molecular phylogenetic analysis by breaking off a piece of protruding gypsum using a sterile spatula. A similarly-sized piece of gypsum was collected approximately 40 m away at a non-impacted site to serve as a control (designated CTL). When collected, the samples were placed in 70% ethanol for transport out of the cave and stored at −80 °C prior to analysis in the lab.

All DNA protocols were carried out in a laminar-flow hood using aerosol-resistant pipette tips to reduce the likelihood of contamination. Negative control isolations were carried out in parallel to measure any contamination of the final samples. DNA was extracted from either 0.5 mL of liquid culture or 0.5 g of sediment using our previously described protocol (Barton et al., 2006). Community 16S ribosomal RNA gene sequence libraries for Bacteria were prepared from extracted DNA by amplification using the universal forward primer 8F (5′ - AGA GTT TGA TCC

TGG CTC AG - 3′) and bacterial-specific reverse primer 1391R (5′ - GAC GGG CGG TGW GTR CA - 3′) at an annealing temperature of 58 °C. For an Archaeal library, the archaeal-specific primers 333Fa (5′ – TCC AGG CCC TAC GGG – 3′) and 1100Ar (5′ – TGG GTC TCG CTC GTT G – 3′) were used across a range of annealing temperatures (55 to 65 °C) (Hales et al., 1996). Purified PCR products were cloned into a pTOPO-TA Cloning Vector (Invitrogen Corp., Carlsbad, California) according to the manufacturer's recommended protocol. Representative clones were sequenced at the University of Kentucky Advanced Genetic Technologies Center (UK-AGTC; http://www.uky.edu/Centers/AGTC). Partial sequences of each 16S rRNA gene were compiled using DNA Baser Sequence Assembler (Heracle Software Co., Germany) and compared to the NCBI database by BLAST (http://www.ncbi.nlm.nih.gov) (Altschul et al., 1997). The compiled sequences were screened for removal of potential chimeric sequences using Bellerophone software (http://comp-bio.anu.edu.au/bellerophon/bellerophon.pl) (Huber et al., 2004). Remaining sequences were deposited in the NCBI GenBank database (accession numbers JN032353–JN032396). DNA alignments were carried out using a NAST aligner (DeSantis et al., 2006) with manual corrections in the ARB Software Package (http://www.arb-home.de), with additional sequences from the Ribosomal Database Project (RDP; Cole et al., 2009) and Rainey et al. (2005). For evolutionary distance calculations, a maximum-likelihood algorithm using a general time-reversal (GTR) substitution model was carried out in RAxML 7.2.7 with 1000 bootstrap replicates to test the robustness of the inferred topologies (Stamatakis et al., 2008). In all cases, *Bacillus pumulis* was used as the outgroup (AB195283).

Sample Collection for Cultivation and Metabolic Activity

Samples for cultivation were collected from three pristine locations within Lechuguilla Cave, including two 5 mL water samples from shallow pool sites (EC26I and EC27Z) and 1 g of floor sediment (EC34B) collected with sterile syringes and spatulas, respectively (Fig. 2). These samples were used to immediately inoculate 20 mL of filter-sterilized urine (from a healthy 24 yr old male, no medications) under oxic and anoxic conditions in septated vials (Wheaton Scientific, Millville, New Jersey). The anoxic conditions were generated by removing the oxygen from 250 mL of air using ascorbic acid, with the anaerobic nature of the resultant gas confirmed using an anaerobic test strip. This deoxygenated air was then used to degas each 20 mL of urine by replacing the headspace gas three times over a twenty-four-hour period. Half of the urine within the vials was treated with 40 µL of urease (1 mg mL^{-1}). The result was four culture conditions (urine under oxic and anoxic conditions, and urine plus urease under oxic and anoxic conditions) for each sample site (Fig. 3). An uninoculated sample was used as a control to verify the sterility of the urine under each condition. All cultures were incubated in the cave (20 °C) for forty-eight hours and transported to the lab at 4 °C to prevent cell damage from the high temperature variations from shipping during the summer. The primary cultures generated in the cave were sub-cultured two weeks later in the laboratory at 20 °C. Sub-cultures were prepared from 1 mL samples of the primary cultures, which were used to inoculate 20 mL of urine media under the described conditions. To determine whether a carbon and energy source was necessary for growth, 40 mg mL^{-1} of filter-sterilized glucose was included in one set of the sub-cultures, resulting in eight varieties of sub-culture, oxic or anoxic, with or without urease, and with or without glucose (Fig. 3). Three replicate samples from each of the oxic cultures were analyzed for the presence of ammonia, nitrate, and nitrite via spectroscopy with ammonia (TNT 831) and nitrate (TNT 839) test kits (Hach, Loveland, Colorado). Very little variation was observed in the anoxic cultures, and these measurements were not repeated.

For comparative nitrate reduction assays, *Pseudomonas* strains previously isolated from Lechuguilla Cave (Johnston et al., 2011) were grown in sterile nitrate broth to test for denitrification according to the manufacturer's guidelines (Difco™ Nitrate Broth, Becton Dickinson, Franklin Lakes, New Jersey) and incubated at room temperature for 48 hrs. The presence of gas bubbles was recorded as positive for nitrogenous gas production. Samples were then evaluated for nitrate and nitrite reduction following the manufacturer's recommended protocol.

Results

To assess the impact of human urine on microorganisms over extended periods in Lechuguilla Cave, we conducted a comparative analysis of the microbial-community profile at the Big Sky urine site (Fig. 2). This area of Lechuguilla Cave was discovered in 1989 and has served as a permanent campsite, averaging two to three six-person expeditions per year. At the end of each expedition, urine is poured into a shallow depression off of the main trail, flowing over rock and gypsum deposits. Over time, this has caused a black patina to develop, as is seen at all the urine sites throughout the cave. The chemistry of this patina is unknown, but the amorphous nature of the residue suggests that it is organic in nature; it closely resembles amberat. A small sample (~ 2 cm^3) of patina-covered gypsum was collected (designated Wee) and examined using molecular phylogenetic techniques to describe the microbial species present following extended exposure to urine. A similar piece of gypsum was collected from an un-impacted area in the general region of the Big Sky site to serve as a negative control (CTL).

We attempted to extract DNA from both the Wee and CTL gypsum samples. While DNA was readily obtained

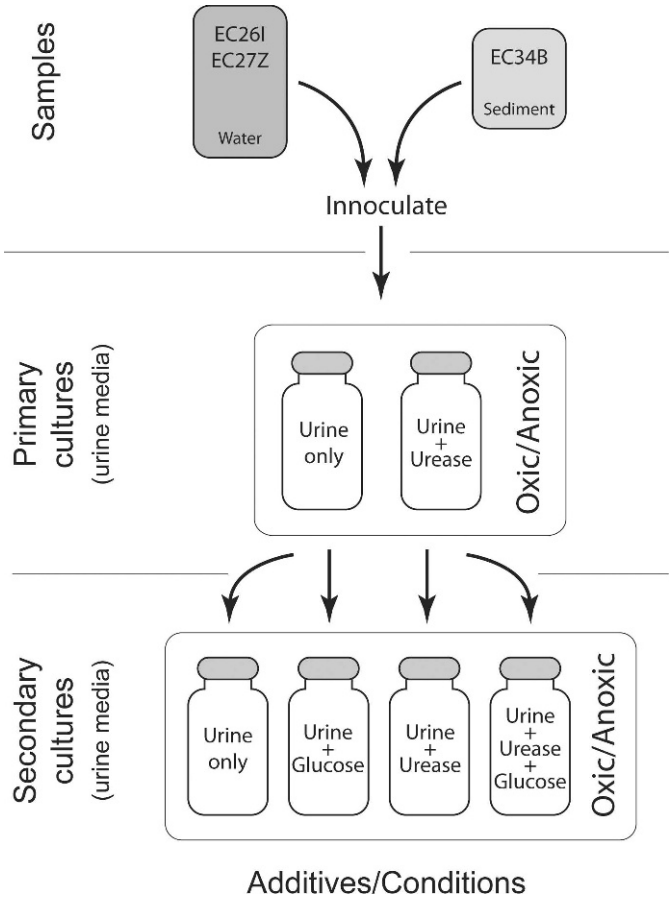

Figure 3. Diagram of described culture conditions. Liquid or sediment samples were inoculated in the cave under four growth conditions to generate the primary cultures: urine under oxic or anoxic conditions, and urine + urease under oxic or anoxic conditions. The secondary cultures were inoculated in the laboratory to create eight growth conditions: urine under oxic or anoxic conditions, urine + glucose under oxic or anoxic conditions, urine + urease under oxic or anoxic conditions, and urine + glucose + urease under oxic or anoxic conditions.

from the Wee samples, three independent attempts were unable to isolate DNA from the CTL sample. This suggests that the total number of microorganisms in the CTL sample was below the detection limit of this assay ($\sim 10^4$ cells g^{-1}; Barton et al., 2006). A clone library of 136 bacterial phylotypes was generated from the Wee sample DNA via PCR amplification; however, no amplifiable PCR products were obtained using archaeal-specific primers after numerous attempts (data not shown). A comparative BLAST of the bacterial library at the Wee site (Table 1) demonstrated that a significant proportion of the phylotypes (42%) had a low level of similarity (≤95%) to previously identified bacterial species. This low level of identity was unexpected due to the amount of human urine that had been deposited at this site and the presumed presence of human commensal species (Hunter et al., 2004; Lavoie and Northup 2005). A small percentage (9%) of the 136 phylotypes did have distant similarity to species that have been associated with human populations (WeeA_H02, 92% identity to a pulmonary infection; WeeA_C08, 97% identity to a *Bacillus* isolated from a patient's blood), but the vast majority of the phylotypes identified (78%) were related to soil species (Table 1), demonstrating a broad diversity within the Bacteria, including the *Alpha-, Beta- and Gammaproteobacteria*, the *Actinobacteria*, *Firmicutes*, *Deinococci-Thermus*, and *Bacteriodetes.* Of interest was the presence of representative phylotypes from the Order *Deinococcales,* which are not normally associated with cave environments (Cox and Battista, 2005). The *Deinococcales* identified in the Wee clone library demonstrated a comparatively low 16S identity with previously identified representatives of the *Deinococci* (92 to 95%) and the cultivated *Truepera* (91%) (Table 1). To determine whether these *Deinoccales* phylotypes represent a previously undescribed group within this phyla, we generated a phylogenetic tree that included the closest cultured and un-cultured representatives of the *Deinococcale* from the NCBI and RDP databases (Rainey et al., 2005). Using a maximum likelihood tree-building algorithm, the dendogram suggests that these phylotypes represent a new, previously unrecognized clade within the *Deinococci-Thermus* (Fig. 4). It is interesting to note that the other representative phylotypes within this clade (HQ727579-81) were found in nitrate- and ammonia-rich environments.

The lack of recognized human commensal species at the Wee site suggested that endemic microbial species, rather than exogenous species, might be subsisting long-term to utilize the urine in situ. To determine if endemic species are capable of utilizing human urine, we attempted to culture bacteria from pristine locations in Lechuguilla Cave using human urine as a culture medium. No carbon or energy sources were added to this urine, allowing us to select for species capable of utilizing organic molecules present in urine as a carbon and energy source (Kusano et al., 2011). The three sample sites, EC26I, EC27Z, and EC34B, were chosen due to their distance from impacted urine sites (Deep Seas, Red Seas, Rusticles, Big Sky, and Far-East camps) and sites of limited human activity (away from major survey junctions or main trails) (Fig. 2). Given that urine is a liquid, pools were sampled at EC26I and EC27Z for planktonic species, while EC34B was a representative sediment sample. The samples were inoculated into 20 mL of sterile urine (Fig. 3) under oxic (20% O_2) and anoxic (0% O_2) conditions. Anoxic conditions were included due to the dependence on anaerobic conditions for urease production by a number of bacterial species (Mobley and Hausinger, 1989; McCarty and Bremmer, 1991), while other species can only use ammonia as an energy source under anaerobic conditions (Kowalchuk and Stephen, 2001). Without knowing whether endemic cave species possess the urease activity

Table 1. Phylogenetic affinities of phylotypes identified at the wee sample site.

Phylum	Clone	No. Clones[a]	Closest Identified Sequence[b]	Origin of Closest Identified Sequence[b]	16S ID[c]	NCBI Accession No.[d]
Actinobacteria	WeeA_H02	5/6	*Microbacterium senuense*	Symptomatic pulmonary infection patient	92%	DQ536408
	WeeA_F10	1/6	Uncultured *Mycobacterium sp.*	Microbial composition associated with trembling aspen	91%	EF019585
Deinococcus-Thermus	WeeA_E02	18/31	Uncultured Deinococci bacterium	Microbial composition from five Hawaiian lakes	87%	AF513964
	WeeA_B08	10/31	Uncultured bacterium	Soil composition from Cape Evans, Mcmurdo Dry Valley, Antarctica.	90%	AY676482
	WeeA_G07	2/31	Uncultured *Deinococcus sp.*	Soils of Marble Point and Wright Valley, Victoria Land, Antarctica	88%	DQ366016
	WeeA_E01	1/31	Uncultured Deinococci bacterium BC_COM473	Bioremediation of petroleum-contaminated soil with composting	92%	HQ727578
Firmicutes	WeeA_A07	18/56	*Bacillus sp.*	Soils from The Netherlands, Bulgaria, Russia, Pakistan, and Portugal	98%	AY289499
	WeeA_B04	25/56	*Sporosarcina soli*	Microbe composition of upland soils isolated from Korea	98%	DQ073394
	WeeA_C08	7/56	*Bacillus hackensackii*	Bacillus isolated from a patient's blood culture	97%	AY148429
	WeeA_F02	2/56	*Bacillus sp.*IDA3504	Soil isolates for novel *Bacillus*-related lineages	98%	AJ544784
	WeeA_E03	1/56	*Bacillus clausii* KSM-K16	Alkaline protease activity of *Bacillus sp.* KSM-K16, isolated from soil	92%	AP006627
	WeeA_E10	1/56	*Sporosarcina aquimarina*	Bacterium isolated from seawater in Korea	95%	NR_025049
	WeeA_D04	1/56	*Sporosarcina luteola*	Isolated from soy sauce production equipment from Japan	94%	AB473560
	WeeA_D01	1/56	Uncultured *Bacillus sp.*	Microbial composition associated with trembling aspen	91%	EF019702
Alphaproteobacteria	WeeA_H07	5/10	*Sphingomonas koreensis*	Yellow-pigmented bacteria isolated from natural mineral water	94%	NR_024998
	WeeA_D08	2/10	Uncultured *Bradyrhizobiaceae* bacterium	Microbial composition associated with trembling aspen	90%	EF018691
	WeeA_E07	2/10	Uncultured *Rickettsiales* bacterium	Microbiota associated with phylogenetically ancient epithelia	90%	EF667896
	WeeA_A04	1/10	*Alphaproteobacterium*	Heterotrophic N2-fixing bacterioplankton in the Baltic Sea	90%	AY972871
Betaproteobacteria	WeeA_H06	1/2	*Thiobacillus denitrificans* [ATCC® 25259]	*Thiobacillus denitrificans* ATCC 25259	89%	CP000116
	WeeA_D07	1/2	Uncultured *Betaproteobacterium*	Radionuclide-contaminated subsurface sediments	93%	EU236233
Gammaproteobacteria	WeeA_B02	14/29	*Rhodanobacter fulvus*	Korean soil sample mixed with rotten rice straw	97%	AB100608

Table 1. Continued.

Phylum	Clone	No. Clones[a]	Closest Identified Sequence[b]	Origin of Closest Identified Sequence[b]	16S ID[c]	NCBI Accession No.[d]
	WeeB_A08	9/29	Uncultured *Xanthomonadaceae* bacterium	Clone isolated from biofilters treating dimethyl sulphide	98%	FJ536874
	WeeA_H12	2/29	*Stenotrophomonas humi*	Nitrate-reducing bacteria isolated from soil	99%	AM403587
	WeeA_F12	2/29	*Frateuria sp.*EC-K130	Rhizomicrofloral composers isolated from soil	94%	AB264175
	WeeA_D06	1/29	*Rhodanobacter lindaniclasticus*	Isolate from Korean granule sludge	90%	AB244763
	WeeA_E12	1/29	*Uncultured Xanthomonadaceae bacterium*	Biofilters treating dimethyl sulphide: with/ without methanol	95%	FJ536874
Bacteroidetes	WeeA_E04	2/2	*Flavobacterium sp.* MH51	Cultivable bacteria associated with the soil fungistasis	98%	EU182879

[a] Number of phylotypes identified/total number of phylotypes in phylum.
[b] Via a BLAST search of the NCBI database (Altschul et al. 1997).
[c] To nearest sequence in the NCBI database.
[d] NCBI accession number of sequence with highest identity in NCBI database.

necessary for the first step in urine breakdown, we also included urease pre-treated urine as a medium (Fig. 3).

The cultures were grown at cave temperature (20 °C), and after two weeks significant growth was seen under both oxic and anoxic conditions, with and without the presence of urease. No growth was observed in the uninoculated control. Subcultures of these primary cultures were then established in the laboratory to determine if nitrogen redox-cycling was occurring in terms of nitrifying ($NH_3^+ \rightarrow NO_2^-$) or denitrifying ($NO_2^- \rightarrow N_2O \rightarrow N_2$) activity (Fig. 1B). The one modification to these secondary cultures was the addition of a glucose (40 mg L^{-1}) to determine whether the organic molecules present in urine were sufficient to serve as a carbon and energy source for growth of heterotrophic species, or if additional sources were necessary (Fig. 3).

After five days of growth in the laboratory, the secondary cultures were tested for ammonia, nitrite, and nitrate production. All sterile, uninoculated urine controls were below the level of detection for each of these compounds (data not shown). The data (Fig. 5) demonstrate that ammonia was produced in all cultures regardless of urease addition, although ammonia concentrations were generally higher under anoxic conditions. In all the urine cultures, nitrite was only detected at trace levels (<0.1 mg L^{-1}; data not shown); this low concentration is presumably due to the rapid conversion of nitrite to nitrate by the microbial species present (Roman et al., 1991). The addition of glucose did not appear to significantly increase the production of ammonia or nitrate under the conditions tested. Interestingly, the addition of urease appeared to greatly reduce variability in the amount of ammonia produced in these cultures. This suggests that the variation observed in the EC27Z planktonic culture under aerobic conditions may be due to the production of this enzyme. Nonetheless, the levels of ammonia only had a minimal impact on the resultant nitrate levels in the cultures, and no correlation between ammonia and nitrate concentration was observed.

To account for the comparatively low level of nitrate to ammonia in the samples, we wanted to determine if nitrate was being removed from the culture by reduction to gaseous nitrogen (NO, N_2O, or N_2). To test this, we added 1 mL of each secondary culture (Fig. 3) into 3 mL of fresh urine media containing a Durham tube. After forty-eight hours of growth, no bubbles were observed in the Durham tubes, suggesting that no gas was produced and hence no nitrate reduction was occurring during growth (data not shown). Nonetheless, it was possible that the absence of gas in these assays was due to limitations in the media used, rather than the absence of nitrate reduction. We therefore inoculated a traditional nitrate broth (Difco) containing Durham tubes from the secondary cultures. Again, no bubbles were observed after forty-eight hours of growth, and testing of the nitrate broth for the presence of nitrite suggested that nitrate reduction was not being carried out in these cultures.

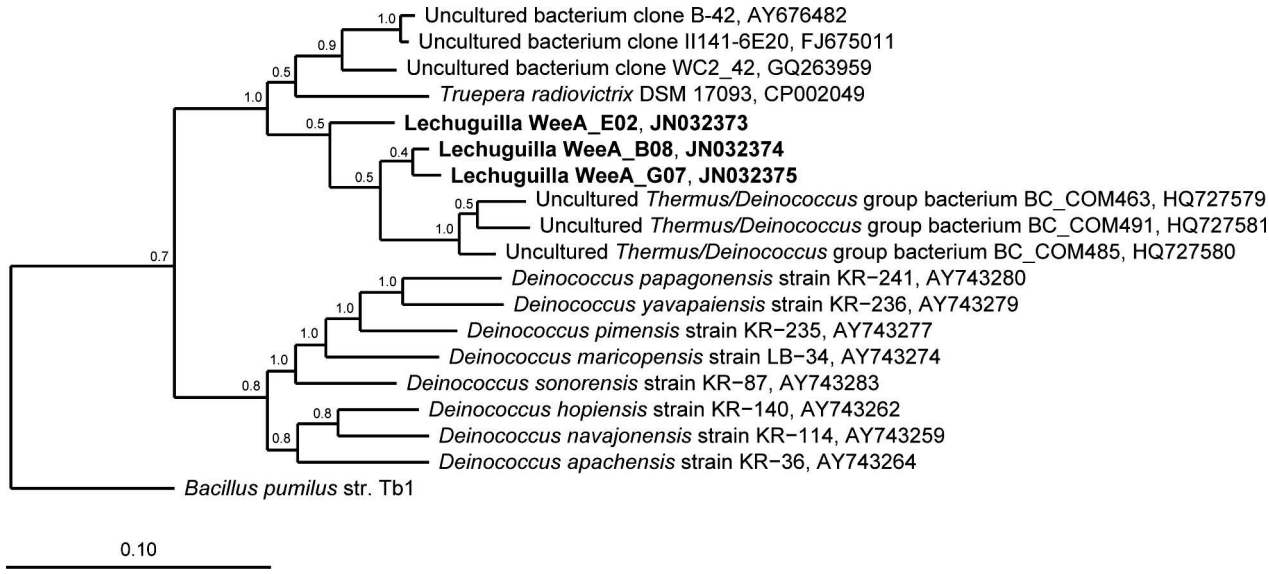

Figure 4. Phylogenetic tree of cultured and uncultured representatives of the *Deinococci*, demonstrating the unique clade of uncultured *Deinococci* in which the Wee site phylotypes are found. The dendrogram was constructed using a Maximum-likelihood algorithm. The robustness of the inferred topologies was tested with 1,000 bootstrap replicates, with the likelihood of generating the inferred topology at each node shown. The outgroup used was *Bacillus pumulis* (AB195283).

Even though complete reduction of ammonia to nitrogen gas was not occurring in the urine cultures, the presence of a trace concentration of nitrite indicates that nitrifying and denitrifying reactions are occurring. To identify the species in these cultures that may be involved in such reactions, we examined the oxic secondary cultures of EC26I, EC27Z and EC34B (without amendment) using a molecular phylogenetic approach. Clone libraries containing twenty-four, twenty-two, and twenty-three bacterial phylotypes were obtained for the EC26I, EC27Z, and EC34B oxic samples, respectively (Table 2). No archaea were identified in these cultures using a PCR-based approach. The pool samples EC26I and EC27Z showed the lowest diversity, while the sediment sample EC34B showed the greatest diversity (Table 2). It is notable that the species identified using this technique demonstrated a high percentage similarity (99 to 100%) to previously cultured bacteria, including five with potential similarity to human commensal populations (EC26ID10, EC34BG06, EC34BH08, EC34BE02 and EC34BD06; Table 2), even though all samples came from pristine locations within the cave. One potential explanation of this finding is that filter-sterilized, urine was used as a culture medium. It is therefore possible that these genera represented commensal contaminants obtained during urine collection. Nonetheless, our uninoculated controls did not contain microbial growth, and these genera are not known to produce ultra-small cells capable of passing through a 0.22 mm filter (Bakken and Olsen, 1987; Rappé et al., 2002; Hahn et al., 2003; Godoy et al., 2005; Miteva and Brenchley, 2005). A number of the identified genera are also known to produce urease or tolerate urea, including representatives of the genera *Bacillus, Corynebacteria, Micrococcus, Pseudomonas,* and *Ochromobactrum* (Brenner et al., 2005). Additionally, members of the *Bacilli, Corynebacteriaceae, Pseudomonads,* and *Ochrobactraceae* are known to carry out denitrification reactions (Brenner et al., 2005).

Despite the presence of denitrifying species in the cultures, the absence of nitrate reduction to gaseous nitrogen suggests that this final step in the nitrogen cycle is not occurring. In a separate study (Johnston et al., 2011), we have cultured a number of *Pseudomonas* species from Lechuguilla Cave, a genus that is known to possess this denitrification phenotype (Brenner et al., 2005). To determine if *Pseudomonas* strains endemic to the cave are capable of complete nitrate reduction (Fig. 1), we carried out a nitrate reduction test on twenty-three *Pseudomonas* strains, representing five different species (Table 3). Of these isolates, three species, *Pseudomonas abientaniphila, Pseudomonas graminis,* and *Pseudomonas resinovorans,* were able to reduce nitrate to nitrite, while *Pseudomonas stutzeri* was able to completely reduce nitrate to nitrogen gas. This result demonstrates the potential for endogenous cave species to completely oxidize urea to nitrogen gas.

Discussion

Human exploration allows the systematic documentation of caves and provides a critical component in the scientific understanding of these systems (Kambesis, 2007). Such work has allowed us to build a picture of the geological and hydrological processes that lead to the formation of caves and allowed significant advances in our understanding of speleogenesis, secondary mineral deposi-

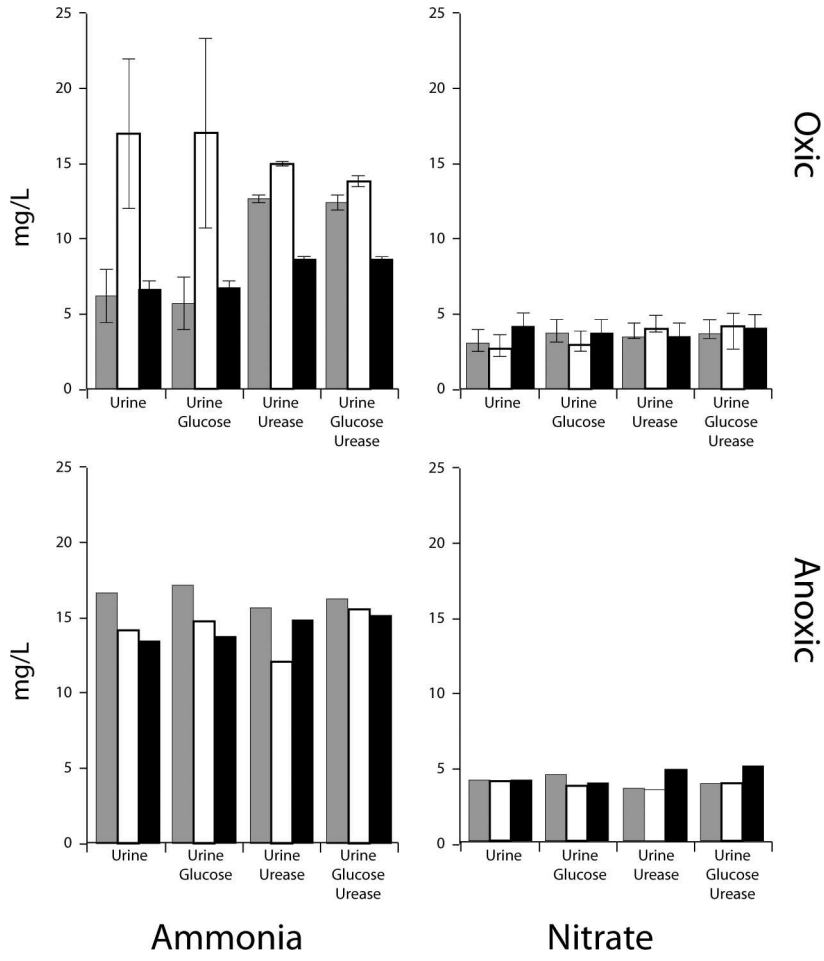

Figure 5. Production of ammonia, nitrite, and nitrate from urine in culture. Bacterial cultures were inoculated from non-impacted sites in Lechuguilla Cave, EC26I (gray, water), EC27Z (white, water), and EC34B (black, sediment). The average of ammonia and nitrate produced from the breakdown of urea after five days in culture are shown under aerobic and anaerobic conditions. For the oxic cultures, the averages and standard deviations (error bars) of three replicate samples are shown. Nitrite was only detected at trace levels and is not shown.

tion, and cave-ecosystem structure and dynamics. While hydrologically active systems can withstand a higher level of human impact, the consequences of human exploration on environmentally sensitive systems are not known or fully understood (Lavoie, 1995; Lavoie and Northup, 2005). Nonetheless, the limited surface water input into Lechuguilla Cave and the static nature of the environment suggests that this cave may be particularly sensitive to such impacts (Cunningham et al., 1995; Northup et al., 2003).

To examine human impact on the microbial flora of Lechuguilla Cave, Hunter et al. (2004) and Lavoie and Northup (2005) examined the cave system for the presence of bacterial species that could serve as a marker for human contamination. These investigators examined the cave for the presence of fecal (*Escherichia coli*), skin (*Staphylococcus aureus*), or soil (*Bacilli* spp.) bacterial species using chromogenic tests. Hunter et al. (2004) suggested that fecal *E. coli* could be found in pools throughout the cave, while Lavoie and Northup (2005) did not find *E. coli* in pools, but in pristine sites and active urine dumps. The discrepancy in the findings between studies was attributed by the authors to the short residence time of *E. coli* in cave sediments and its rapid entry into a viable but non-culturable state, making detection difficult using the cultivation-based techniques used in these studies (Lavoie and Northup, 2005). In this study, we use a culture-independent approach that is not subject to the limitations of cultivation (Pace, 1997).

It was our initial aim to carry out a comparative analysis between the endemic microbial population in a geochemically similar, unimpacted site in the cave and the urine-impacted site; however, the unimpacted control did not contain a sufficient microbial population to allow DNA extraction. The extraction techniques used have a detection limit of about 10^4 cells g^{-1} of sediment, suggesting that the microbial population of the control site contained very few cells, likely due to the osmotic stress of growth on gypsum. The ease of obtaining DNA from the impacted Wee site suggests a much higher biomass at

Table 2. Identity of cultured bacteria grown on urine media from pristine sites.

Sample Site	Clone	No. Clones[a]	Closest Identified Sequence[b]	Origin of Closest Identified Sequence[b]	16S ID[c]	NCBI Accession No.[d]
EC26I (water)						
Actinobacteria	EC26IB10	10/22	*Micrococcus luteus*	Medieval wall painting	99%	AJ409096
	EC26IB04	7/22	*Micrococcus sp.*JL-76	Marine environment	99%	AY745846
	EC26ID10	5/22	*Cellulomonas parahominis*	Clinical isolates of *Coryneform* group	99%	AY655729
Firmicutes	EC26IA02	2/2	*Paenibacillus borealis*	Humus bacteria of Norway spruce	90%	NR_025299
EC27A (water)						
Firmicutes	EC27ZB01	12/12	*Bacillus pumilus* SAFR-032	Soil polluted with chromium	99%	DQ416781
Alphaproteobacteria	EC27ZA05	10/10	*Ochrobactrum sp.* TK14	Soil and wheat roots samples	99%	AJ550273
EC34B (sediment)						
Actinobacteria	EC34BG06	1/3	*Corynebacterium jeikeium K411*	Nosocomial pathogen	99%	CR931997
	EC34BH03	1/3	*Rhodococcus erythropolis*	Rocks of an ancient gold mine	99%	EF491951
	EC34BH08	1/3	*Propionibacterium acnes JCM6473*	16S rRNA gene sequence of JCM strain	100%	AB573714
Firmicutes	EC34BB05	4/5	Uncultured bacterium KSC2-41	Spacecraft clean room	99%	DQ532287
	EC34BE10	1/5	*Bacillus weihenstephanensis KBAB4*	Root-associated bacteria	99%	CP000903
Alphaproteobacteria	EC34BA04	5/5	*Bradyrhizobium elkanii*	Commercial rhizobial strains	99%	FJ025139
Betaproteobacteria	EC34BC01	2/2	*Ralstonia sp. C1*	Biofilm in spent nuclear fuel pool	99%	AY479983
Gammaproteobacteria	EC34BD05	2/6	*Acinetobacter sp.*	Bovine products and soil	99%	Z93442
	EC34BE02	2/6	Clone nbt97q09 *(Pseudomonas)*	Human skin microbiota	99%	EU539061
	EC34BA02	1/6	*Pseudomonas fluorescens* Pf0-1	Corn plant, greenhouse conditions	99%	AY958233
	EC34BG09	1/6	*Serratia proteamaculans*	Lau Basin hydrothermal vents	99%	CP000826
Bacteroidetes	EC34BD06	2/2	Uncultured bacterium rRNA082	Human vaginal epithelium	99%	AY958855

[a] Number of phylotypes identified/total number of phylotypes in phylum.
[b] Via a BLAST search of the NCBI database (Altschul et al. 1997).
[c] To nearest sequence in the NCBI database.
[d] NCBI accession number of sequence with highest identity in NCBI database.

this location, which corresponds to the findings of Lavoie (1995), who demonstrated that urine amendment of sediments from Lechuguilla Cave led to a dramatic increase in cell number, from less than 10^4 to 10^7 cells g^{-1}. This suggests that the urine deposition at the Wee site led to a dramatic increase in population size. This increase in numbers also matches the detection limits of our assay (Barton et al., 2006; Lavoie, 1995).

Using a molecular phylogenetic analysis of this increased population at the Big Sky urine site, we found twelve phylotypes that demonstrated some similarity to human isolates, including similarity to a bacterium from human pulmonary (WeeA_H02) and blood (WeeA_C08) infections, but these phylotypes show only a weak similarity (92 and 97%, respectively) to these pathogens. Such low 16S similarity suggests that these phylotypes do

Table 3. Nitrogen reduction in Lechuguilla Cave *Pseudomonad* cultures.

Strains			Metabolic Test		
Bacteria	% ID[a]	No.[b]	N_2	NO_2^-	NO_3^-
Pseudomonas stutzeri	99	16	+	−	+
Pseudomonas abietaniphila	99	1	−	+	ND[c]
Pseudomonas graminis	98	1	−	+	ND[c]
Pseudomonas resinovorans	99	2	−	+	ND[c]
Pseudomonas gingeri	99	3	−	−	−

[a] To type strain (*P. stutzeri* ATCC 17587, *P. abietaniphila* ATCC 700689, *P. graminis* ATCC 700544, *P. resinovorans* ATCC 14235, *P. gingeri* NCPPB 3146).
[b] The total number of strains in the Lechuguilla Culture Collection.
[c] ND = not done (nitrate positive tests can not be tested for nitrate reduction using this assay).

not belong to the same species (or in the case of 92% identity, the same genera) as these potential human pathogens (Gevers et al., 2005). Further, these phylotypes are also members of genera commonly found in cave environments (*Microbacterium* and *Bacillus;* Johnston et al., 2011), supporting an endemic origin for these species. In this study, we did not find *E. coli* in our Wee sample site or cultures using the more sensitive and specific molecular approach. The cultivation-based chromogenic techniques of Hunter et al. (2004) and Lavoie and Northup (2005) measure a single phenotypic characteristic to identify *E. coli*, in this case lactose fermentation. Yet a number of the cultured species identified in this study also ferment lactose, including members of the *Cellulomonaceae, Micrococci, Paenibacilli,* and *Bacilli* (Tables 1 and 2). Thus, the identification of bacteria based exclusively on lactose fermentation would give a false-positive for fecal coliforms. As such, the presence of *E. coli* within the cave requires supporting evidence (Barton and Pace, 2005). Such evidence could come in the form of confirmatory tests, including culture (mTEC), morphological (Gram stain), and molecular (16S ribotyping) assays (Barton and Pace, 2005), but no such confirmatory tests were carried out in these previous studies (Hunter et al., 2004; Lavoie and Northup, 2005).

Our phylogenetic analysis does not demonstrate the presence of *E. coli* or other fecal bacterial species at the sample site. This does not indicate that they are not being deposited, but that the commensals may not be able to compete or subsist under the conditions of the cave. The loss of commensal species from an environment contaminated by human waste (German toilets) has previously been described (Egert et al., 2010). There the source of the endemic species was determined to be from the environment (from flushing) and this may be the case here; the environmental source is the cave itself.

The presence of a number of phylotypes potentially involved in nitrogen-cycling activities at the Wee site (specifically denitrification; Table 1) suggests that the bacterial species at the urine site may be taking advantage of nitrogenous compounds derived from the urine for energy generation. The presence of numerous phylotypes with similarity to heterotrophic soil species also suggests that the species present could be taking advantage of the organic compounds found in urine for growth (Kusano et al., 2011). The identification of members of the *Deinococcales* group is much harder to reconcile at this location. The *Deinococci-Thermus* group represent a heterotrophic, deeply branching lineage within the Bacteria (Alburquerque et al., 2005; Dworkin et al., 2006) that are known for their high level of resistance to ionizing (X-, α-, β- and γ-rays) and non-ionizing (UV) radiation (Cox and Battista, 2005). It is unlikely that Lechuguilla Cave provides selective pressure from radiation, particularly from UV radiation, but the mechanisms of DNA repair that provide radiation resistance for these species also allow resistance to dehydration (Mattimore and Battista, 1996). *Truepera radiovictrix*, which shows closer homology to the phylotypes in our phylogenetic analysis than other cultured members of the *Deinococci,* has been shown to use nitrate as an electron acceptor (Alburquerque et al., 2005). This suggests that nitrate within the environment may be providing an additional selection pressure. It is interesting to note that the *Deinococcales* are readily cultured on heterotrophic media, such as that used in previous studies (Hunter et al., 2004; Lavoie and Northup, 2005), and display lactose fermentation capabilities (Rainey et al., 2005; Alburquerque et al., 2005).

Our phylogenetic results suggested that the breaking down of human urine at the Wee site may be being facilitated by endemic cave species. To test whether endemic species demonstrate this capacity, we established cultures from cave sites that had not been impacted by human urine (Fig. 2). Even though these cultures were established with microorganisms from pristine sites, the bacteria identified had similar 16S rDNA identity to human commensal species, including members of the *Cellulomonas, Corynebacterium, Propionibacterium,* and *Pseudomonas* genera (EC26ID10, EC34BG06, EC34BH08, EC34BE02, and EC34BD06). Rather than being indicative of contamination at these sites, it is likely that the urine in our culture medium enriches for the growth of bacterial species able to utilize urea, resist the high levels of urea encountered, or catabolize the organic molecules found

in the urine (Kusano et al., 2011). Indeed, the genera represented by these isolates have been associated with human urinary-tract infections, increasing the likelihood of their cultivation using this approach (Sellin et al., 1975; Carpenter and Dicks, 1982; Mobley and Hausinger, 1989; Kunin, 1994; Kesserü et al., 2002; Walter et al., 2007; Zhao et al., 2010). Similar phylotypes have also been found in other caves and subsurface environments, including gold mines and the soil (Table 2), suggesting that the origin of these species was the cave environment.

Given an endemic origin of the species found associated with urine in this study, it is interesting to note that among the samples from pristine sites, the water samples EC26I and EC27Z showed the lowest species diversity (four and two phylotypes, respectively), while the sediment sample EC34D demonstrated the highest (thirteen phylotypes in six divisions). The EC26I culture is dominated by heterotrophic species (Table 2), including members of the *Micrococci*, *Cellulomonaceae,* and *Paenibacilli*. While *Micrococci* are potential human commensals, we have previously isolated members of this genus within caves (Johnston et al., 2011). Indeed, the isolate cultured in this study (EC26IB10) shared the highest identity to a bacterium isolated from the wall-painting of a medieval church (Table 2), arguing for an organism better adapted to nutrient limitation than human skin (Wieser et al., 2002). The pool culture EC27Z contained near-equal phylotypes of *Bacillus pumilus* and a representative of the *Ochrobactrum* (Table 2). Both have previously been isolated from cave environments (Johnston et al., 2011) and are capable of heterotrophic nitrification and aerobic denitrification (Zhao et al., 2010). The urine culture from the sediment (EC34B) sample contained the greatest diversity of heterotrophic species and reflects a more complex ecosystem involved in nitrogen cycling, including representatives of the *Rhodococci, Bradyrhizobia,* and *Ralstonia* (Dworkin et al., 2006). Members of the *Cellulomonas, Micrococci,* and *Paenibacilli* are also lactose-fermenting species, suggesting that cultivation from pristine sites can also generate false positives for the presence of *E. coli* (Hunter et al., 2004; Lavoie and Northup, 2005).

In all the established cultures, the microorganisms present seem capable of breaking down urine without the addition of an exogenous carbon source or urease. Under anaerobic conditions, the conversion of urea to ammonia via urease appeared to occur at high levels (Fig. 5), an observation consistent with the increased urease activity of soil species under anaerobic conditions (McCarty and Bremmer, 1991). Although none of our established cultures demonstrated the complete reduction of urea to N_2, *Pseudomonas* species previously isolated from Lechuguilla Cave were able to reduce accumulated NO_3^- to N_2. Collectively, this suggests that it might be possible to engineer a collection of endemic cave species that could completely oxidize urea to N_2 gas, without supplementation with additional nutrients (an energy source or urease). These species could then to be added to the urine before it is dumped in the cave. By reducing the total amount of nitrogen in the urine, it might be possible to limit the introduction of nitrogen compounds in urine using an ecosystem-neutral method of in situ bioremediation.

Our data demonstrate that even under the pressure of allochthonous nitrogen and exogenous bacterial species, the microbial community at the Big Sky urine site still appears to be dominated by indigenous cave species. The data suggest that the native microbial community remains resistant to invasion from human commensal species. Factors that could make the microbial ecosystem resistant to such xenobiotic invasion may be the uniquely oligotrophic nature of the cave environment that limits the establishment of copiotrophic species (Barton and Jurado, 2007), the impact of host-rock geochemistry on growth (Barton et al., 2007), or even the selection pressure of the gypsum present at this site. High species diversity can also play a role in community resistance to environmental perturbations, allowing metabolic flexibility and community adaptation under ever-changing conditions (Girvan et al., 2005). To determine what factors control the diversity and speciation of the microbial community at the Wee and other urine sites will require additional experiments, including additional cultivation and in-depth biogeochemistry of the urine sites within Lechuguilla Cave.

The dramatic change in the structure of the microbial community at the Wee site supports the established caving principles: it is important to limit human impact in cave environments, particularly from the introduction of waste. While the microbial community at the Wee site remains dominated by endemic species, it is clearly different from a nearby un-impacted site in the cave (CTL). Without knowing the long-term impact of such a dramatic change on the entire microbial ecosystem, such impacts must be limited by employing sound management practices to balance the delicate nature of the ecosystem with our need to understand and protect these critical habitats.

Acknowledgements

The authors would like to thank Bradley Lubbers, David Bunnell, and Elizabeth Rosseau for assistance with sample collection, three anonymous reviewers for comments that improved the manuscript, and Dr. Kathleen Lavoie for critical comments and valuable references. The authors would also like to thank Paul Burger and Stan Allison of Carlsbad Caverns National Park for access and in-cave assistance. Funding was provided by the NSF KY EPSCoR Program to HAB.

References

Albuquerque, L., Simões, C., Fernando Nobre, M., Pino, M.N., Battista, J.R., Silva, M.T., Rainey, F.A., and da Costa, M.S., 2005, *Truepera radiovictrix* gen. nov., sp. nov., a new radiation resistant species and the proposal of *Trueperaceae* fam. nov.: FEMS Microbiology Letters, v. 247, p. 161–169. doi:10.1016/j.femsle.2005.05.003.

Altschul, S.F., Madden, T.L., Schäffer, A.A., Zhang, J., Zhang, Z., Miller, W., and Lipman, D.J., 1997, Gapped BLAST and PSI-BLAST: a new generation of protein database search programs: Nucleic Acids Research, v. 25, p. 3389–3402. doi:10.1093/nar/25.17.3389.

Bakken, L., and Olsen, R., 1987, The relationship between cell size and viability of soil bacteria: Microbial Ecology, v. 13, p. 103–114. doi:10.1007/BF02011247.

Barr, T.C. Jr., 1967, Observations on the ecology of caves: American Naturalist, v. 101, p. 475–491.

Barton, H.A., 2013, Biospeleogenesis: Biogenetic Processes and Microbial Impact on Speleogenesis, Frumkin, A., ed., Treatise on Geomorphology: Atlanta, GA, Elsevier, (in press).

Barton, H.A., and Jurado, V., 2007, What's up down there? Microbial diversity in caves: Microbe, v. 2, p. 132–138.

Barton, H.A., and Pace, N.R., 2005, Discussion: Persistent coliform contamination in Lechuguilla Cave pools: Journal of Cave and Karst Studies, v. 67, p. 55–57.

Barton, H.A., Taylor, N.M., Kreate, M.P., Springer, A.C., Oehrle, S.A., and Bertog, J.L., 2007, The impact of host rock geochemisry on bacterial community structure in oligotrophic cave environments: International Journal of Speleology, v. 36, p. 93–104.

Barton, H.A., Taylor, N.M., Lubbers, B.R., and Pemberton, A.C., 2006, DNA extraction from low-biomass carbonate rock: an improved method with reduced contamination and the low-biomass contaminant database: Journal of Microbiology Methods, v. 66, p. 21–31. doi.org/10.1016/j.mimet.2005.10.005.

Brenner, D.J., Krieg, N.R., and Staley, J.T., 2005, eds., Bergey's Manual of Systematic Bacteriology, Volume 2: The Proteobacteria, Part C: The *Alpha-, Beta-, Delta-* and *Gammaproteobacteria*, second edition: New York, Springer, 1392 p.

Carpenter, E.M., and Dicks, D., 1982, Isolation of *Pseudomonas fluorescens* after suprapubic catheterisation: Journal of Clinical Pathology, v. 35, 581 p.

Cole, J.R., Wang, Q., Cardenas, E., Fish, J., Chai, B., Farris, R.J., Kulam-Syed-Mohideen, A.S., McGarrlll, D.M., Marsh, T., Garrity, G.M., and Tiedje, J.M., 2009, The Ribosomal Database Project: improved alignments and new tools for rRNA analysis: Nucleic Acids Research, v. 37, supplement 1, p. D141–145. doi:10.1093/nar/gkn879.

Cox, M.M., and Battista, J.R., 2005, *Deinococcus radiodurans* — The consummate survivor: Nature Reviews Microbiology, v. 3, p. 882–892. doi:10.1038/nrmicro1264.

Culver, D.C., and Sket, B., 2000, Hotspots of subterranean biodiversity in caves and wells: Journal of Cave and Karst Studies, v. 62, p. 11–17.

Cunningham, K.I., Northup, D.E., Pollastro, R.M., Wright, W.G., and LaRock, E.J., 1995, Bacteria, fungi and biokarst in Lechuguilla Cave, Carlsbad Caverns National Park, New Mexico: Environmental Geology, v. 25, p. 2–8. doi:10.1007/BF01061824.

Davis, D.G., 2000, Extraordinary features of Lechuguilla Cave, Guadalupe Mountains, New Mexico: Journal of Cave and Karst Studies, v. 62, p. 147–157.

DeSantis, T.Z. Jr., Hugenholtz, P., Keller, K., Brodie, E.L., Larsen, N., Piceno, Y.M., Phan, R., and Andersen, G.L., 2006, NAST: a multiple sequence alignment server for comparative analysis of 16S rRNA genes: Nucleic Acids Reseach, v. 34, supplement 2, p. W394–399. doi:10.1093/nar/gkl244.

Dworkin, M., Falkow, S., Rosenberg, E., Schleifer, K.H., and Stackebrandt, E., 2006, The Prokaryotes: A Handbook of the Biology of Bacteria, third edition: New York, Springer, 7 volumes.

Egert, M., Schmidt, I., Bussey, K., and Breves, R., 2010, A glimpse under the rim — the composition of microbial biofilm communities in domestic toilets: Journal of Applied Microbiology, v. 108, p. 1167–1174. doi:10.1111/j.1365-2672.2009.04510.x.

Elliott, W.R., 2006, Biological dos and don'ts for cave conservation and restoration, *in* Hildreth-Werker, V., and Werker, J.C., eds., Cave Conservation and Restoration: Huntsville, National Speleological Society, p. 33–46.

Francis, C.A., Beman, M.J., and Kuypers, M.M.M., 2007, New processes and players in the nitrogen cycle: The microbial ecology of anaerobic and archaeal ammonia oxidation: The ISME Journal, v. 1, p. 19–27. doi:10.1038/ismej.2007.8.

Gevers, D., Cohan, F.M., Lawrence, J.G., Spratt, B.G., Coenye, T., Feil, E.J., Stackebrandt, E., Van de Peer, Y., Vandamme, P., Thompson, F.L., and Swings, J., 2005, Re-evaluating prokaryotic species: Nature Reviews Microbiology, v. 3, p. 733–739. doi:10.1038/nrmicro1236.

Girvan, M.S., Campbell, C.D., Killham, K., Prosser, J.I., and Glover, L.A., 2005, Bacterial diversity promotes community stability and functional resilience after perturbation: Environmental Microbiology, v. 7, p. 301–313. doi:10.1111/j.1462-2920.2005.00695.x.

Godoy, F., Vancanneyt, M., Martínez, M., Steinbüchel, A., Swings, J., and Rehm, B.H., 2003, *Sphingopyxis chilensis* sp. nov., a chlorophenol-degrading bacterium that accumulates polyhydroxyalkanoate, and transfer of *Sphingomonas alaskensis* to *Sphingopyxis alaskensis* comb. nov.: International Journal of Systematic and Evolutionary Microbiology, v. 53, p. 473–477.

Hahn, M.W., Lunsdorf, H., Wu, Q., Schauer, M., and Hofle, M.G., 2003, Isolation of novel ultramicrobacteria classified as Actinobacteria from five freshwater habitats in Europe and Asia: Applied and Environmental Microbiology, v. 69, p. 1442–1451. doi:10.1128/AEM.69.3.1442-1451.2003.

Hales, B.A., Edwards, C., Ritchie, D.A., Hall, G., Pickup, R.W., and Saunders, J.R., 1996, Isolation and identification of methanogen-specific DNA from blanket bog peat by PCR amplification and sequence analysis: Applied and Environmental Microbiology, v. 62, p. 668–675.

Hardin, J.W., and Hassell, M.D., 1970, Observation on waking periods and movements of *Myotis sodalis* during hibernation: Journal of Mammalogy, v. 51, p. 829–831.

Hill, C.A., 2000, Sulfuric acid, hypogene karst in the Guadalupe Mountains of New Mexico and West Texas (U.S.A.), *in* Klimchouk, A.B., Ford, D.C., Palmer, A.N., and Dreybrodt, W., eds., Speleogenesis: Evolution of Karst Aquifers: Huntsville, National Speleological Society, p. 309–316.

Huber, T., Faulkner, G., and Hugenholtz, P., 2004, Bellerophon; a program to detect chimeric sequences in multiple sequence alignments: Bioinformatics, v. 20, p. 2317–2319. doi:10.1093/bioinformatics/bth226.

Hunter, A.J., Northup, D.E., Dahm, C.N., and Boston, P.J., 2004, Persistent coliform contamination in Lechuguilla cave pools: Journal of Cave and Karst Studies, v. 66, p. 102–110.

Iker, B.C., Kambesis, P., Oehrle, S.A., Groves, C., and Barton, H.A., 2010, Microbial atrazine breakdown in a karst groundwater system and its effect on ecosystem energetics: Journal of Environmental Quality, v. 39, p. 509–518. doi:10.2134/jeq2009.0048.

Ikner, L.A., Toomey, R.S., Nolan, G., Neilson, J.W., Pryor, B.M., and Maier, R.M., 2007, Culturable microbial diversity and the impact of tourism in Kartchner Caverns, Arizona: Microbial Ecology, v. 53, p. 30–42. doi:10.1007/s00248-006-9135-8.

Johnston, M., Millette, J., Banks, E.D., Jurado, V., and Barton, H.A., 2011, The culturable diversity of oligotrophic heterotrophs: The lechuguilla cave culture library, *in* Proceedings of the American Society for Microbiology General Meeting. New Orleans, LA: Washington, D.C., American Society for Microbiology, N1795 p.

Kambesis, P., 2007, The importance of cave exploration to scientific research: Journal of Cave and Karst Studies, v. 69, p. 46–58.

Kesserü, P., Kiss, I., Bihari, Z., and Polyák, B., 2002, The effects of NaCl and some heavy metals on the denitrification activity of *Ochrobactrum anthropi*: Journal of Basic Microbiology, v. 42, p. 268–276. doi:10.1002/1521-4028(200208)42:4<268::AID-JOBM268>3.0.CO;2-E.

Klimchouk, A.B., Ford, D.C., Palmer, A.N., and Dreybrodt, W., eds., 2000, Speleogenesis, Evolution of Karst Aquifers: Huntsville, National Speleological Society, 527 p.

Kowalchuk, G.A., and Stephen, J.R., 2001, Ammonia-oxidizing bacteria: A model for molecular microbial ecology: Annual Review of Microbiology, v. 55, p. 485–529. doi:10.1146/annurev.micro.55.1.485.

Kunin, C.M., 1994, Urinary tract infections in females: Clinical Infectious Diseases, v. 18, p. 1–12. doi:doi:10.1093/clinids/18.1.1.

Kusano, M., Mendez, E., and Furton, K.G., 2011, Development of headspace SPME method for analysis of volatile organic compounds present in human biological specimens: Analytical and Bioanalytical Chemistry, v. 400, p. 1817–1826. doi:10.1007/s00216-011-4950-2.

Lavoie, K.H., 1995, The effects of urine deposition on microbes in cave soils, *in* Proceedings of the 1993 National Cave Management Symposium Proceedings, Carlsbad, NM,: Huntsville, AL, National Speleological Society, p. 302–312.

Lavoie, K.H., Helf, K.L., and Poulson, T.L., 2007, The biology and ecology of North American cave crickets: Journal of Cave and Karst Studies, v. 69, p. 114–134.

Lavoie, K.H., and Northup, D.E., 2005, Bacteria as indicators of human impact in caves, *in* Rea, G.T., ed., Proceedings of the 17th National Cave and Karst Management Symposium Proceedings: October 31–November 4, 2005, Albany, New York, p. 40–47.

Lieberman, H.R., 2007, Hydration and cognition: A critical review and recommendations for future research: Journal of the American College of Nutrition, v. 26, supplement 5, p. 555S–561S.

Mattimore, V., and Battista, J.R., 1996, Radioresistance of *Deinococcus radiodurans:* Functions necessary to survive ionizing radiation are also necessary to survive desiccation: Journal of Bacteriology, v. 178, p. 633–637.

McCarty, G.W., and Bremmer, J.M., 1991, Production of urease by microbial activity in soils under aerobic and anaerobic conditions: Biology of Fertile Soils, v. 11, p. 228–230. doi:10.1007/BF00335772.

Miteva, V.I., and Brenchley, J.E., 2005, Detection and isolation of ultrasmall microorganisms from a 120,000-year-old Greenland glacier ice core: Applied and Environmental Microbiology, v. 71, p. 7806–7818. doi:10.1128/AEM.71.12.7806-7818.2005.

Mobley, H.L.T., and Hausinger, R.P., 1989, Microbial ureases: Significance, regulation, and molecular characterization: Microbiology Reviews, v. 53, p. 85–108.

Northup, D.E., Barns, S.M., Yu, L.E., Spilde, M.N., Schelble, R.T., Dano, K.E., Crossey, L.J., Connolly, C.A., Boston, P.J., Natvig, D.O., and Dahm, C.N., 2003, Diverse microbial communities inhabiting ferromanganese deposits in Lechuguilla and Spider Caves: Environmental Microbiology, v. 5, p. 1071–1086. doi:10.1046/j.1462-2920.2003.00500.x.

Northup, D.E., Beck, K.M., and Mallory, L.M., 1997, Human impact on the microbial communities of Lechuguilla Cave: Is protection possible during active exploration? [abstract]: Journal of Cave and Karst Studies, v. 59, 166 p.

Pace, N.R., 1997, A molecular view of microbial diversity and the biosphere: Science, v. 276, p. 734–740. doi:10.1046/j.1462-2920.2003.00500.x.

Palmer, A.N., and Palmer, M.V., 2000, Hydrochemical interpretation of cave patterns in the Guadalupe Mountains, New Mexico: *Journal of Cave and Karst Studies*, v. 62, p. 91–108.

Raesly, R.L., and Gates, J.E., 1987, Winter habitat selection by north temperate cave bats: American Midland Naturalist, v. 118, p. 15–31.

Rainey, F.A., Ray, K., Ferreira, M., Gatz, B.Z., Fernanda Nobre, M., Bagaley, D., Rash, B.A., Park, M.-J., Earl, A.M., Shank, N.C., Small, A.M., Henk, M.C., Battista, J.R., Kämpfer, P., and da Costa, M.S., 2005, Extensive diversity of ionizing-radiation-resistant bacteria recovered from Sonoran Desert soil and description of nine new species of the genus *Deinococcus* obtained from a single soil sample: Applied and Environmental Microbiology, v. 71, p. 5225–5235. doi:10.1128/AEM.71.9.5225-5235.2005.

Rappé, M.S., Connon, S.A., Vergin, K.L., and Giovannoni, S.J., 2002, Cultivation of the ubiquitous SAR11 marine bacterioplancton clade: Nature, v. 418, p. 630–633. doi:10.1038/nature00917.

Reames, S., Fish, L., Burger, P., and Kambesis, P., 1999, Deep Secrets: The Discovery and Exploration of Lechuguilla Cave: Dayton, Cave Books, 381 p.

Roman, M., Dovi, R., Yoder, R., Dias, F., and Warden, B., 1991, Determination by ion chromatography and spectrophotometry of the effects of preservation on nitrite and nitrate: Journal of Chromatography A, v. 546, p. 341–346. 10.1016/S0021-9673(01)93032-8.

Scholle, P.A., Ulmer, D.S., and Melim, L.A., 1992, Late-stage calcites in the Permian Capitan Formation and its equivalents, Delaware Basin margin, west Texas and New Mexico: evidence for replacement of precursor evaporites: Sedimentology, v. 39, p. 207–234. doi:10.1111/j.1365-3091.1992.tb01035.x.

Sellin, M., Gillespie, W.A., Cooke, D.I., Sylvester, D.G.H., and Anderson, J.D., 1975, Micrococcal urinary-tract infections in young women: The Lancet, v. 2, p. 570–572. 10.1016/S0140-6736(75)90166-X.

Spear, J.R., Barton, H.A., Robertson, C.E., Francis, C.A., and Pace, N.R., 2007, Microbial community biofabrics in a geothermal mine adit: Applied and Environmental Microbiology, v. 73, p. 6172–6180. doi:10.1128/AEM.00393-07.

Stamatakis, A., Hoover, P., and Rougemont, J., 2008, A fast bootstrapping algorithm for the RAxML web-servers: Systematic Biology, v. 57, p. 758–771. doi:10.1080/10635150802429642.

Stone, W., am Ende, B., and Paulsen, M., 2002, Beyond the Deep: The Deadly Descent into the World's Most Treacherous Cave: New York, Time Warner Books, 351 p.

Summers Engel, A., Meisinger, D.B., Porter, M.L., Payn, R.A., Schmid, M., Stern, L.A., Schleifer, K.H., and Lee, N.M., 2010, Linking phylogenetic and functional diversity to nutrient spiraling in microbial mats from Lower Kane Cave (USA): The ISME Journal, v. 4, p. 98–110. doi:10.1038/ismej.2009.91.

Tabor, J.M., 2010, Blind Descent: The Quest to Discover the Deepest Place on Earth: New York, Random House, 286 p.

Walter, B., Hänssler, E., Kalinowski, J., and Burkovski, A., 2007, Nitrogen metabolism and nitrogen control in corynebacteria: Variations of a common theme: Journal of Molecular and Microbiology Biotechnology, v. 12, p. 131–138. doi:10.1159/000096468.

Wieser, M., Denner, E.B., Kämpfer, P., Schumann, P., Tindall, B., Steiner, U., Vybiral, D., Lubitz, W., Maszenan, A.M., Patel, B.K., Seviour, R.J., Radax, C., and Busse, H.J., 2002, Emended descriptions of the genus *Micrococcus, Micrococcus luteus* (Cohn 1872) and *Micrococcus lylae* (Kloos et al. 1974): International Journal of Systematic and Evolutionary Microbiology, v. 52, p. 629–637.

Wright, P.A., 1995, Nitrogen excretion: Three end products, many physiological roles: Journal of Experimental Biology, v. 198, p. 273–281.

Zhao Bin, He Yi Liang, and Zhang Xiao Fan, 2010, Nitrogen removal capability through simultaneous heterotrophic nitrification and aerobic denitrification by *Bacillus* sp. LY: Environmental Technology, v. 31, p. 409–416. doi:10.1080/09593330903508922.

J.C. Currens, R.L. Paylor, E.G. Beck, and B. Davidson – A method to determine cover-collapse frequency in the Western Pennyroyal karst of Kentucky. *Journal of Cave and Karst Studies,* v. 74, no. 3, p. 292–299. DOI: 10.4311/2011ES0247

A METHOD TO DETERMINE COVER-COLLAPSE FREQUENCY IN THE WESTERN PENNYROYAL KARST OF KENTUCKY

James C. Currens*, Randall L. Paylor, E. Glynn Beck, and Bart Davidson
Kentucky Geological Survey, University of Kentucky, 228 Mining and Mineral Resources Building, Lexington, KY 40506-0107

Abstract: To determine the rate of cover-collapse sinkhole formation in Christian County, Kentucky, we used large scale aerial photographs taken nearly twenty years apart. The negatives were enlarged and printed to 1:3,000 scale and examined for collapses. The photographs constrained the time period within which the collapse could have occurred, and the large scale of the prints provided a means to identify, locate, and field-verify the cover collapses. All features noted on the photographs were checked in the field. Sinkholes seen on the later photographs, but not the earlier ones, were recorded. The rate of formation calculated was 0.2 cover-collapse km^{-2} yr^{-1}.

Introduction

Cover collapse is the phenomena of apparently sudden collapse of soil or other unconsolidated cover over karstic bedrock. In Kentucky, cover collapse frequently damages buildings, roads, utility lines, and farm equipment. It has killed livestock, including some thoroughbred horses, and has injured people. The Kentucky Geological Survey estimates a total economic cost of $20 million annually in Kentucky from karst-generated geologic hazards (Dinger et al., 2007). The survey records an average of two dozen cover collapses per year and has developed a case history file spanning some thirty years. In this paper, we report a site-specific study of collapse frequency in a small area of the Western Pennyroyal sinkhole plain east of Hopkinsville in Christian County, Kentucky (Fig. 1).

Cover-Collapse Process

The development of voids in unconsolidated cover overlying karstic bedrock has been studied for decades (Beck, 1991; White and White, 1992). Small voids in soil at depths of a few meters are comparatively stable because of the lateral distribution of the overburden-induced stress by the arched roof of the void. The voids are enlarged by a loss of cohesion and loading of the arch-forming material caused by either a wetting front of soil water from infiltrating precipitation or by rapid draining of an inundated void. The saturated pores in the unconsolidated cover cannot drain as quickly as the conduit-connected void. The wetting and increased pore pressure result in an incremental loss of strength of the regolith arch (Tharp, 1999) and the underside of the arch sloughing into the soil void. Ultimately, the repeated sloughing from wetting and drying of the unconsolidated cover propagates the arched-over void to near the land surface (Hyatt and Jacobs, 1996; Waltham et al., 2005). The sudden appearance of a cover-collapse sinkhole is initiated when the arch becomes too thin to support its own weight and shears the remaining soil in a nearly circular pattern (Fig. 2). If sufficient volume is not available in the underlying bedrock cavity to store the collapsed soil, the loose material is transported away by groundwater flow through the bedrock conduit. Although the genesis of cover collapse is well understood, precisely predicting the time and place at which a collapse will occur is not yet possible (Hyatt et al., 2001).

Study Area

The study area is 4.04 km^2 in east-central Christian County, Kentucky (Fig. 3). The topography within the study area is karst plain and a single low hill, giving 23.5 m of local relief, formed by resistance to dissolution of the basal part of the Bethel Sandstone. Land use at the time of the study (2004) was largely pasture and row-cropped fields with scattered farmsteads, a retail agriculture supply store, a cement plant, and a restaurant. The boundaries were defined by the overlapping area of stereo aerial photograph pairs. The study area was selected without any prior knowledge of existing cover collapses in the area.

The exposed Mississippian section, in ascending order, is Ste. Genevieve Limestone, Renault Limestone, and Bethel Sandstone (Klemic, 1967). The bedrock at the base of the stratigraphic column is predominantly oobiosparites and micritic limestones, medium- to thick-bedded, and is greater than 95 percent calcium carbonate. Interbedded thin shale and argillaceous carbonates are a minor interruption to the otherwise very pure carbonate section. The residual 10 m of Bethel is a calcite-cemented, argillaceous quartzarenite that weathers into a friable, porous, sandy residuum that readily slumps into underlying sinkholes (Klemic, 1967). The Lost River Chert is exposed near the base of the Ste. Genevieve in local quarries, but is below the depth of karst development in the study area. The exposed Ste. Genevieve Limestone is

* Corresponding Author: currens@uky.edu

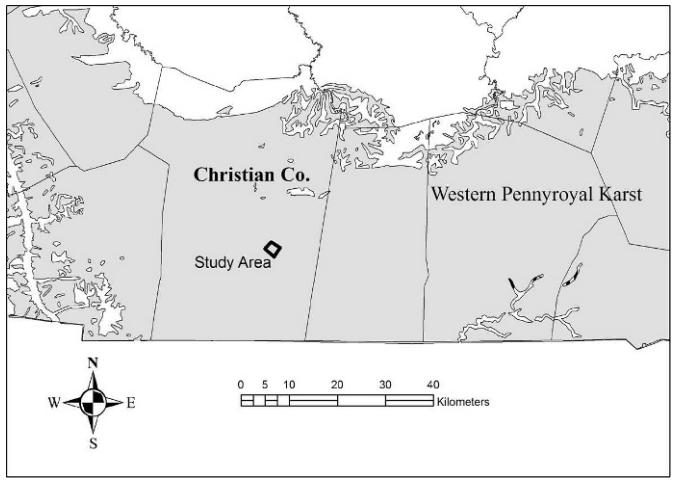

Figure 1. The black polygon is the study area in Christian County, east of Hopkinsville, Western Pennyroyal region in Kentucky. The gray shaded area is underlain by karstic carbonates.

over 52 m thick, while the Renault Limestone is some 15 to 29 m thick. The regional gentle dip of 3 m km^{-1} to the north is the only structure in the otherwise flat-lying bedrock at the study site.

The cover collapses inventoried were mostly in the outcrop area of the Renault. Because of the purity and thickness of the carbonates, the presence of topographically mapped dolines, and the moderate total relief of 60 m within the study area, we expected the rate of occurrence of cover collapse to be comparatively high. The conditions in the study area are nearly ideal for cover-collapse development.

Methods

We used a simple and inexpensive method to locate sinkholes and constrain the time of cover collapse. Because we did not have access to a magnifying stereoscope, the Kentucky Geological Survey purchased prints of black-and-white, low-altitude, large-scale, visible-light, aerial photography at an imaged scale of 1:12,000 (1 cm = 120 m; 1 in. = 1,000 ft) from the Tennessee Valley Authority. The photographs were taken March 9, 1971, and January 31, 1991. Although we also obtained stereo sets of contact prints, the most useful images were enlargements of the central image from the sets. The enlargements were printed at a scale of 1:3,000 (1 cm = 30 m; 1 in = 250 ft), four times the scale of the negative. Using 2-power magnifying glasses, we visually scanned the enlargements systematically for features appearing to be sinkholes. The emulsion grains on the print were sufficiently small in comparison with the typical cover-collapse that shadows cast on the interior of a collapse less than a meter in diameter could be discerned from those cast by small cedar trees, for example. Further, labeling devices could be attached to the enlargement print to preserve the interpretive data.

Figure 2. A classic example of a cover collapse in the study area.

We also searched for cover-collapse features on the stereo-pair contact prints and the digital images made at the KGS from scans of the enlargements. Most of the features identified on the 1:3,000-scale enlargements could not be relocated with confidence on the 1:12,000-scale contact prints. Scanned enlargements were saved as 16-bit gray-scale TIFF files at 1,200 dpi, giving a pixel size of roughly 0.5 m at ground level. The file size was large (428,853 kb) and prevented viewing the scan with image viewers on most of the available computers. We did view the images with GIS software, but could not relocate any cover-collapse locations on the digital images due to pixilation.

Fifty potential cover-collapse sites were selected for field inspection from the enlarged prints (Table 1). KGS staff field-checked all of the sites and determined if they were, in fact, cover collapses. Those sites that had developed within

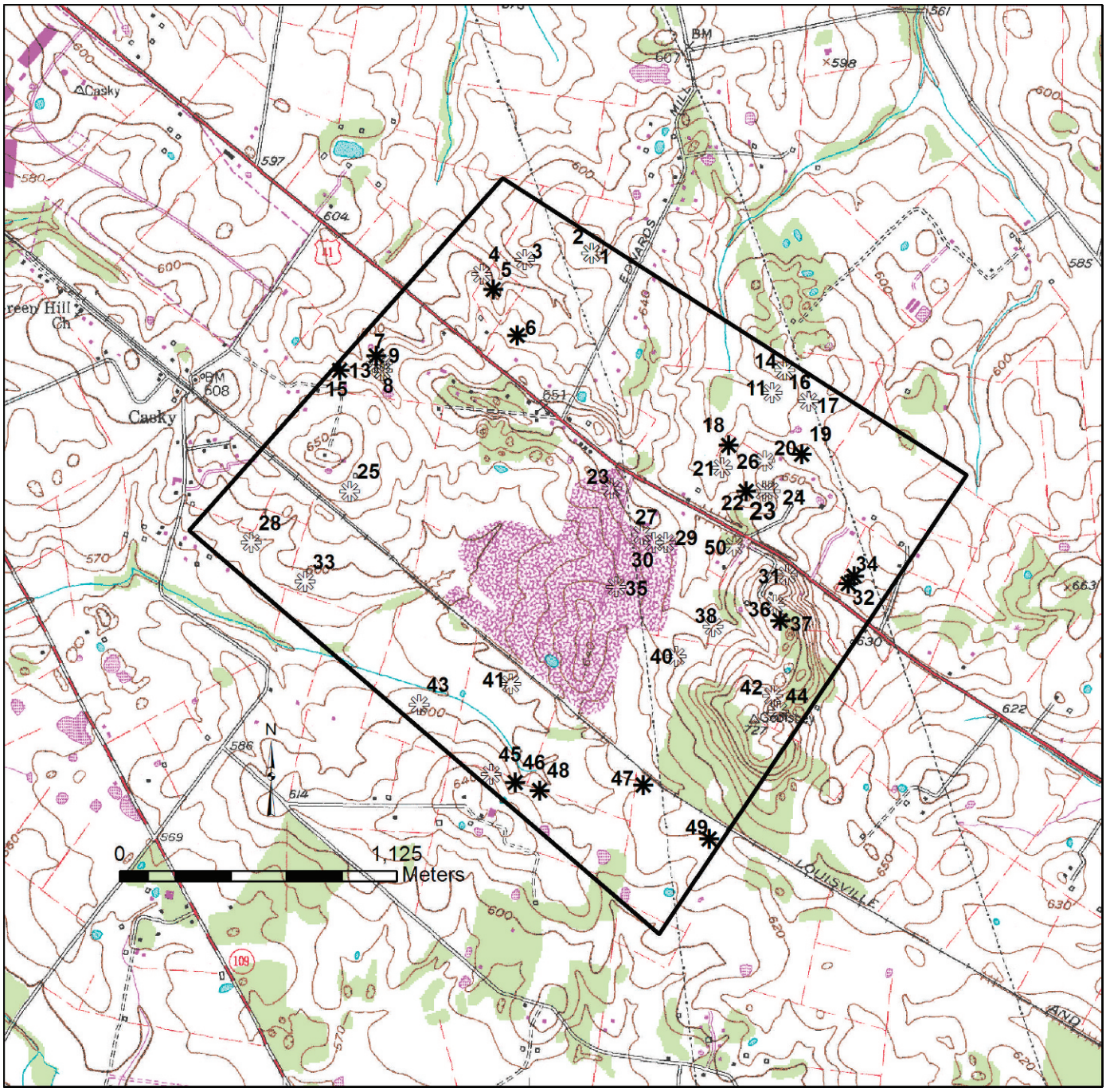

Figure 3. The cover-collapse inventory area in the Hopkinsville 7.5-minute quadrangle is inside the black line. The disrupted textured area enclosed by a gray line is the property of a limestone quarry, which was excluded from the inventory. Solid asterisks are cover-collapse sinkholes identified on the 1991 aerial photograph and verified in the field. Hollow asterisks are other features from the same images determined not to be cover-collapse.

the twenty-year period bracketed by the photographs were identified. We also found a small number of cover collapses that did not appear until after the 1991 photography. These were too recent to include in the calculation of the rate, but were documented for future reference. Some features that were visible on the earlier photographs, but not on the later ones, were also noted. We also received a limited number of reports that a collapse had occurred and had been filled and graded during the period between the aerial photography. Such cover collapses were included in the rate calculation only if we found field evidence that the report was correct. Field evidence for a filled sinkhole included a circular variation in texture and color of vegetation, buried trash exposed at the surface, subsidence due to soil compaction, or

Table 1. Features identified on aerial photographs and field verified as possible cover collapses since 1971.

Field and Map ID	Location		Present on 1971 Aerial Photograph	Present on 1991 Aerial Photograph	Correctly Identified on Photo as Cover Collapse?	Stratigraphic Unit	Comments and Notes
	Long., °W	Lat., °N					
5[c]	−87.4189	36.82111	N	Y	Y	Renault	PA[a]
6[c]	−87.4178	36.81944	N	Y	Y	Renault	SH[b] –Suspect
7[c]	−87.4242	36.81861	N	Y	Y	Renault	SH/PA Group
11	−87.4056	36.81833	N	Y	N	Renault	PA
14	−87.4056	36.81833	Y	Y	N	Renault	PA/SH – Omitted from rate computation. On both photographs.
15[c]	−87.4258	36.81806	N	Y	Y	Renault	SH - Obvious
19[c]	−87.4047	36.81528	Possibly	Y	Y	Renault	SH
22[c]	−87.4072	36.81389	N	Y	Y	Renault	SH - Suspect; photographed
32[c]	−87.4022	36.81083	N	Y	Y	Renault	SH - Near existing sink on US71
34[c]	−87.4025	36.81056	N	Y	Y	Renault	SH - Near existing sink on US71
37	−87.4056	36.80917	N	Y	Y	Bethel Sandstone	SH - May be others here.
41	−87.4178	36.80667	N	Y	N	Ste. Genevieve	PA
46[c]	−87.4175	36.80306	N	Y	Y	Ste. Genevieve	SH - photograph
47[c]	−87.4117	36.80306	A hint?	Y	Y	Ste. Genevieve	PA - another PA to the SE
48[c]	−87.4164	36.80278	Y	Y	Y	Ste. Genevieve	SH - Seems to have moved
49[c]	−87.4086	36.80111	A hint?	Y	Y	Renault	PA - has been filled in
50[c]	−87.4079	36.81183	N	N	N	Renault	Owner says formed between 1975 and 1980
1	−87.4144	36.8225	N	Y	N	Renault	PA
2	−87.4144	36.8225	N	Y	N	Renault	PA
3	−87.4175	36.82222	N	Y	N	Renault	SH/PA
4	−87.4194	36.82167	A hint?	Y	N	Renault	PA
8	−87.4242	36.81833	N	Y	N	Renault	SH/PA - Group
9	−87.4239	36.81833	N	Y	N	Renault	SH/PA - Group
10	−87.4239	36.81806	N	Y	N	Renault	SH/PA - Group
12	−87.4239	36.81806	N	Y	N	Renault	SH/PA - Group
13	−87.4239	36.81806	N	Y	N	Renault	SH/PA - Group
16	−87.4061	36.8175	N	Y	N	Renault	PA
17	−87.4044	36.81722	N	Y	N	Renault	PA - Suspect
18[c]	−87.4081	36.81556	N	Y	Y	Renault	SH
20	−87.4064	36.815	N	Y	N	Renault	PA?
21	−87.4083	36.81472	N	Y	N	Renault	SH - Suspect
24[c]	−87.4061	36.81389	N	Y	N	Renault	SH
25	−87.4253	36.81361	N	Y	N	Renault	PA
26[c]	−87.4064	36.81389	N	Y	N	Renault	SH - Has been filled.
27	−87.4119	36.81222	N	Y	N	Renault	SH - Suspect

Table 1. Continued.

Field and Map ID	Location		Present on 1971 Aerial Photograph	Present on 1991 Aerial Photograph	Correctly Identified on Photo as Cover Collapse?	Stratigraphic Unit	Comments and Notes
	Long., °W	Lat., °N					
28	−87.4297	36.81167	N	Y	N	Ste. Genevieve	SH - Suspect - possibly another to southwest
29[c]	−87.4108	36.81194	N	Y	N	Renault	SH
30	−87.4114	36.81194	N	Y	N	Renault	SH - Suspect
33	−87.4272	36.81028	N	Y	N	Ste. Genevieve	SH/PA - Possible berm?
36	−87.4058	36.80972	N	Y	N	Bethel Sandstone	SH
38	−87.4086	36.80889	N	Y	N	Renault	PA- In area now occupied by quarry
39	−87.4056	36.80889	N		N	Bethel Sandstone	Old pond site. In area now occupied by quarry.
40	−87.4103	36.80778	N	Y	N	Renault	SH – Suspect feature in area now occupied by quarry
42	−87.4058	36.80639	N	Y	N	Bethel Sandstone	SH
43	−87.4219	36.80583	N	Y	N	Ste. Genevieve	PA
44	−87.4056	36.80583	N	Y	N	Bethel Sandstone	SH
45[c]	−87.4186	36.80333	N	Y	N	Ste. Genevieve	SH – Two others possible a few feet to southwest
23	−87.4133	36.81389	N	Y	?	Renault	SH - Near existing US 71 sink destroyed by road infilling.
31	−87.4053	36.81083	N	Y	?	Renault	SH? -
35	−87.4131	36.81028	N	Y	?	Renault	SH (quarried away)

[a] PA– An obstacle in a crop field that was driven around during tillage of the ground.
[b] SH– Afield verified sinkhole.
[c] Used to calculate rate of occurrence.

Figure 4. The 1991 aerial photograph of the study area in the Hopkinsville East 7.5-minute quadrangle, Christian County, Ky. The dark area in the center is the now-flooded limestone quarry that was excluded from the analysis. North is at the top the photograph. The scale of the negative is 1:12,000.

a local change in soil color if the soil was bare. After comparing recent sinkholes to sinkholes that are clearly old, we think that insufficient time has passed in the 35 years between the earlier photography and our study for any recent cover collapses to have been naturally obscured by slumping and erosion. Finally, our method does not work in wooded areas, although woodlands can still be field-checked, which we did. No cover collapse was found in the small wooded area.

Limitations on Data Analysis

The primary goal of this study was the demonstration of the technique, and we anticipated several limitations on

the accuracy of the cover-collapse rate. The aerial coverage obtained from TVA has one of the largest scales available, and it is only available in Kentucky for the Tennessee River Valley. The limited area of photography restricted the selection of study areas. Although the area was well suited for cover collapse, we had some concern that none would be identifiable on the images or that no collapses had actually occurred in the study area. This proved unfounded. Third, the size of the study area was limited by the budget, which resulted in it being too small for a statistically significant sampling (Beck, 1991) that would be representative of the larger region. Ideally, an area of 10 or more square miles should be used, or several smaller sampling sites scattered over the region.

Large-scale photographic prints are not commonly used because of the increased cost of processing the prints necessary to cover the same area on the ground when compared to contact prints. It may become increasingly difficult to obtain contact prints and enlargements of traditional analog photography because of the closure of processing facilities. As of February 2010, the Tennessee Valley Authority still offered the enlargement service that KGS utilized (https://maps.tva.com/Scripts/MetaWeb/map_aerial.asp).

More problematic was a misunderstanding between the Kentucky Geological Survey and the Tennessee Valley Authority about the area to be covered. The KGS intended the quarry (the large dark area in the center of Fig. 4) to be a reference landmark outside of the photograph frame, not the object of the exercise. We did not realize the photographs encompassed the stone quarry until we received them. It was not possible to replace the prints. The staff of the stone quarry was contacted, and they stated that the quarry opened shortly after 1971 and operated less than ten years. They were not aware of any history of cover-collapse sinkholes induced by dewatering the quarry. The quarry occupies 0.88 km^2 or 18 percent of the study area. Only one probable cover collapse was found within the quarry area on the 1971 image, and it could not be verified in the field because its location had been mined by 1991. We could not find any obvious pattern that suggested induced sinkhole clustering near the quarry, either in the field or on the photographs. We think the effect of the quarry and the study was negligible beyond the obvious loss of study area.

Two of the features of the area, quarry dewatering and highly favorable geology, potentially inflate the population of cover-collapse features and one of the others, uncounted sinkholes that occurred and then were filled between photographs, possibly deflates the count. Further, if cover collapses occurred during the period between the two photos that we did not find, these would lead us to underestimate the rate of formation. Because of the pure, thick limestone and 60 m of relief within the study area, we think our rate of sinkhole formation should be considered a maximum for application to other areas.

Results

We identified fifty cover-collapse like features that occurred between 1971 and 1991 from the aerial photograph and reports from local residents. The photographic enlargements made possible the identification of the features and their location in the field. The detail of the photographic enlargement was an important factor in the success of the technique.

Also, we physically examined an estimated 90 percent of the study area. Of the fifty possible sites identified on the photographs, thirteen could not be found in the field and there was no evidence of collapse in the vicinity of the feature seen on the photograph. Of the remaining thirty-seven sites, sixteen (43 percent) were correctly identified on the photographs as to origin (whether cover-collapse or not) when located in the field. Fifteen of the cover-collapse sinkholes were accurately identified on the photographs and verified in the field, the remaining collapses were thought some other feature until field checked (Table 1). One cover collapse identified on the 1991 enlargement was also on the 1971 image and was not counted (Table 1). Ultimately, a total of eighteen sites were determined to be cover collapses that occurred within the time frame of the two images.

The primary benefit of the photographic enlargements was they directed us where to focus our field work. The total cover collapses correctly identified from the photographs (36 percent of the total features and 43 percent of the features that could be found in the field) is a useful success rate, but could be expected to improve with experience.

Calculation of the rate of formation of the cover-collapse is subject to the limitations cited above. We excluded the area of the quarry as defined by the property line (Fig. 3) from the rate calculation. The rate of cover-collapse events for the study area is 0.2 km^{-2} yr^{-1}

Table 2. Results of inventory and field-verified cover-collapse events between aerial photographs by TVA in 1971 and 1991 (19.9 years).

Area if Quarry Included/Excluded	Count, Cover-Collapse Sites	Inventory Area, km^2	Cover Collapse per Unit Area, km^2	Cover Collapse/Unit Area/Year, km^{-2} yr^{-1}
Included	18	4.92	3.7	0.18
Excluded	18	4.04	4.5	0.22

(0.6 mi^{-2} yr^{-1}; Table 2), which is consistent with some previous studies. Hyatt et al. (1996) reported more than 312 cover collapses in the vicinity of Albany, Georgia, that developed within a 25 km^2 study area within a week following a tropical storm in July 1994. The density of the features ranged from 0.09 km^{-2} to 5.3 km^{-2} (0.21 mi^{-2} to 13.7 mi^{-2}). A follow-up study by Hyatt et al. (1999) is perhaps the most complete descriptive study of cover-collapse sinkholes in the United States to date. We used their data to calculate the occurrence of cover-collapse at 12.5 events per square kilometer over the one week observation period. The minimum annual rate based on the 1994 data would be 0.2 km^{-2} yr^{-1}. Beck (1991) reported 0.11 km^{-2} yr^{-1} (0.29 mi^{-2} yr^{-1}) in Florida, and Ketelle et al. (1988) reported a range of 0.04 to 0.64 km^{-2} yr^{-1} (0.1 to 1.69 mi^{-2} yr^{-1}) in eastern Tennessee. Wilson et al. (1987) reported 0.01 km^{-2} yr^{-1} (0.04 mi^{-2} yr^{-1}), also in Florida.

Conclusions

The use of enlargements of conventional aerial photography to both locate and constrain the date of formation of cover-collapse sinkholes proved practical, inexpensive, and reasonably robust for the sinkhole plain of the Western Kentucky Pennyroyal. Although ground inspection is still needed, field work, regardless of how thorough, can only grossly estimate when an unobserved collapse occurred. The photography-based field inventory was possible because the land use of the study area was dominated by pasture and crop fields. Except for any undiscovered cover-collapse sinkholes that occurred and were filled in the interim between photographs, the method can be categorized as exhaustive.

In the study area, cover collapse occurs at 0.2 km^{-2} yr^{-1} (0.58 mi^{-2} yr^{-1}), consistent with most previous studies. Because of the favorable geology of thick, pure carbonates, the rate calculated here should be considered a maximum if applied to other karst areas in Kentucky.

References

Beck, B.F., 1991, On calculating the risk of sinkhole collapse, *in* Kasting, E.H., and Kasting, K.M., eds., Appalachian Karst, Proceedings of the Appalachian Karst Symposium, Radford, Virgina, March 23–26, 1991: National Speleological Society, Huntsville, p. 231–236.

Dinger, J.S., Zourarakis, D.P., and Currens, J.C., 2007, Spectral enhancement and automated extraction of potential sinkhole features from NAIP imagery — initial investigations: Journal of Environmental Informatics, v. 10, no. 1, p. 22–29. doi:10.3808/jei.200700096.

Hyatt, J.A., and Jacobs, P.M., 1996, Distribution and morphology of sinkholes triggered by flooding following Tropical Storm Alberto at Albany, Georgia, USA: Geomorphology, v. 17, p. 305–316. doi:10.1016/0169-555X(96)00014-1.

Hyatt, J.A., Wilkes, H.P., and Jacobs, P.M., 1999, Spatial relationships between new and old sinkholes in covered karst, Albany, Georgia, USA, *in* Beck, B.F., Pettit, A.J., and Herring, J.G., eds., Hydrogeology and Engineering Geology of Sinkholes and Karst: Rotterdam, Balkema, p. 37–44.

Hyatt, J.A., Wilson, R., Givens, J.S., and Jacobs, P.M., 2001, Topographic, geologic, and hydrogeologic controls on dimensions and locations of sinkholes in thick covered karst, Lowndes County, Georgia, *in* Beck, B.F., and Herring, J.G., eds., Proceedings of Geotechnical and Environmental Applications of Karst Geology and Hydrology, Rotterdam, Balkema, p. 37–45.

Ketelle, R.H., Newton, J.G., and Tanner, J.M., 1988, Karst subsidence in East Tennessee, *in* Proceedings 2nd Conference on Environmental Problems in Karst Terranes and Their Solutions: Dublin, Ohio, National Water Well Association, p. 51–65.

Klemic, H., 1967, Geologic map of the Hopkinsville quadrangle, Christian County, Kentucky: U.S. Geological Survey, Geologic Quadrangle Map GQ-651, scale 1:24,000.

Tharp, T.M., 1999, Mechanics of upward propagation of cover-collapse sinkholes: Engineering Geology, v. 52, p. 23–33. doi.org/10.1016/S0013-7952(98)00051-9.

Waltham, T., Bell, F., and Culshaw, M., 2005, Sinkholes and Subsidence: Karst and Cavernous Rocks in Engineering and Construction: New York, Springer-Praxis Books in Geophysical Sciences, 382 p.

White, W.B., and White, E.L., 1992, Sinkholes and sinkhole collapses *in* Majundar, S.K., Forbes, G.S., Miller, E.W., and Schmalz, R.F., eds., Natural and Technological Disasters: Causes, Effects and Preventative Measures, Pennsylvania Academy of Science, p. 280–293.

Wilson, W.L., McDonald, K.M., Barfus, B.L., and Beck, B.F., 1987. Hydrogeologic Factors Associated with Recent Sinkhole Development in the Orlando Area, Florida; Florida Sinkhole Research Institute, University of Central Florida, Report No. 87-88-4, 109 p.